Topological Objects in Gauge Theories

Changhai Lu

Submitted in partial fulfillment of the

requirements for the degree

of Doctor of Philosophy

in the Graduate School of Arts and Sciences

COLUMBIA UNIVERSITY

2000

©2000

Changhai Lu

All rights reserved

ABSTRACT

Topological Objects in Gauge Theories

Changhai Lu

In this thesis we study topological objects in gauge theories using Nahm's formalism.

On the first topic, we explore a BPS state made of two massive and one massless monopoles in Sp(4) theory with gauge symmetry broken to SU(2)×U(1). This monopole system carries a purely Abelian total magnetic charge. We construct the field configurations with axial symmetry and compute the exact moduli space metric of this monopole system using Nahm's formalism. We also analyze the properties of various submanifolds of the moduli space.

On the second topic, we study the two-monopole system in SU(3) and Sp(4) theories. We compute the exact energy density of both systems, check several special limits, and go through the massless limit in detail. We perform a numerical study on the formation of non-Abelian cloud based on these computations. As a byproduct of the work, the coefficient of the internal part of the moduli space metric of the Sp(4) system is computed using the

analytic result of energy density.

On the third topic, we investigate a single SU(2) caloron (finite temperature instanton) with non-trivial Higgs expectation value at spatial infinity. This work generalizes the previous results by considering gauge symmetry breaking. We construct the explicit field configuration of the caloron and study various limits using Nahm's formalism. From the analysis, we explore the constituent monopole picture of the caloron in detail. As an application of the constituent monopole picture, the moduli space metric of the caloron is computed.

Contents

1 Introduction **1**

2 Monopoles, Instantons, Nahm's Formalism and All That **6**

2.1 BPS Monopoles 6

2.1.1 Introduction 6

2.1.2 Monopoles as topological objects 10

2.1.3 Bogomol'nyi condition and self-duality 14

2.1.4 Monopoles in arbitrary gauge theories 19

2.1.5 Moduli space metrics 26

2.2 Instantons and Calorons 31

2.2.1 Instantons 31

2.2.2 Calorons 37

2.3 Nahm's Formalism 39

2.3.1 Nahm data 39

2.3.2 ADHMN construction 45

2.3.3 Nahm's formalism for the moduli space metric 48
2.3.4 Energy density 50

3 Two Massive and One Massless Sp(4) Monopoles 54

3.1 Introduction 54
3.2 Nahm Data in the Sp(4) Case 59
3.2.1 The embedding procedure 59
3.2.2 Sp(4) Nahm data and the symmetries and submanifolds of their moduli space 61
3.3 Higgs Configurations 69
3.3.1 Spherically symmetric case 71
3.3.2 Hyperbolic case 72
3.3.3 Trigonometric case 74
3.3.4 Non-Abelian cloud and the physical meaning of moduli space parameters 77
3.4 The Moduli Space Metric 79
3.4.1 The moduli space metric on M^8 79
3.4.2 Submanifolds of moduli space and special limits of the metric 84

4 Two-Monopole Systems and the Formation of Non-Abelian Clouds 97

4.1 Introduction 97
4.2 Two Fundamental Monopoles in SU(3) Theory 99
4.2.1 Energy density 99
4.2.2 Various limits of the energy density 104
4.3 Two Fundamental Monopoles in Sp(4) Theory 106
4.3.1 Energy density 107
4.3.2 Various limits of the energy density 110
4.3.3 From the moment of inertia to the moduli space metric at massless limit 116
4.4 Interaction Energy Density and the Formation of Non-Abelian Clouds 118

5 SU(2) Calorons and Magnetic Monopoles 125

5.1 Introduction 125
5.2 ADHMN Construction of a Single SU(2) Caloron 127
5.2.1 Fundamental SU(2) monopoles on $R^3 \times S^1$ 127
5.2.2 ADHMN construction 131
5.3 Various Limits of the Configuration 135
5.3.1 Near each monopole 136
5.3.2 Near singularity 138
5.3.3 Massless monopole limit 138

5.3.4 Zero temperature limit 140
5.4 Moduli Space Metric 141

6 Conclusion **144**

A Mathematics Appendix **152**

A.1 Simple Facts about Lie Algebras 152
A.2 HyperKähler Quotient 155
A.3 Derivation of (3.38) 160

B Single SU(2) Monopole **163**

B.1 Field Configuration 163
B.2 Moduli Space and Its Metric 165
B.3 ADHMN Construction 167

C Quantization of Charges **169**

C.1 Dirac's Monopole 169
C.2 Quantization Conditions 171

List of Figures

2.1 Nahm data and monopole solutions 41

3.1 Root diagram of Sp(4) theory 59

3.2 Submanifolds of the Sp(4) monopole moduli space 69

3.3 $k - D$ space of Sp(4) monopoles 79

3.4 $D - E$ space of Sp(4) monopoles 86

3.5 Principal axes and the configurations of Sp(4) monopoles . . . 89

3.6 Parameters of the asymptotic Sp(4) metric 93

4.1 Root diagram of SU(3) theory 99

4.2 Energy density of two SU(3) monopoles 103

4.3 Root diagram of Sp(4) theory 107

4.4 Energy density of two Sp(4) monopoles 111

4.5 Contour diagrams of $\rho_{\rm int} = 0$ in the SU(3) theory 120

4.6 Contour diagrams of $\rho_{\rm int} = 0$ in the Sp(4) theory 121

4.7 $\rho_{\rm int}$ for the SU(3) and the Sp(4) theories at massless limit . . . 122

5.1 Positions of the constituent monopoles of an SU(2) caloron . . 132

5.2 General calorons and their relation with other solutions 136

ACKNOWLEDGMENTS

Firstly I would like to thank sincerely my advisor Professor Kimyeong Lee for his guidance throughout the period of my work at Columbia. His consistent stimulation and encouragement is invaluable to me. Sharing his creative way of doing physics is one of the most precious experience I have had at Columbia. Without his extensive discussions during every stage of the works, this thesis would not be possible to accomplish.

I am also grateful to Professor Erick Weinberg for helpful discussions and guidance. Since Kimyeong has left for a professorship in Korea, he is effectively my advisor and his advises on the thesis and my future career is tremendously helpful to me.

I would like to thank all the professors who have taught me physics and helped me in various occasions, including Allen Blaer, Miklos Gyulassy, Brian Greene, Malvin Ruderman. I also wish to thank Lalla Grimes and other stuff members in Department Office for their administrative assistance and help.

Many thanks to my fellow graduate students at the Physics Department, especially to Ping Chen, Xuelei Chen, Zhang Chen and Bin Zhang. Their friendship have made my life at Columbia a joyful experience.

To my parents

Hongyi Lu and Baochen Zhang

Chapter 1

Introduction

Today, it is strongly believed that all the known fundamental interactions in the nature are described by gauge theories. At the present energy scale, some of the gauge symmetries are broken, but at higher energy, or equivalently earlier in the history of the universe, these gauge symmetries are believed to be exact. The breaking of the gauge symmetries can be triggered by various mechanisms. A dominant picture is provided by the so-called Higgs mechanism in which certain scalar fields acquire non-zero expectation values that break the gauge symmetries.

It has been realized since the 1970's that topological objects, such as magnetic monopoles[1] and instantons play a crucial role in various aspects of gauge theories. The effects of those objects are not in the perturbative regime, they opened a completely new field of research in modern physics.

[1] in this thesis, we will only discuss the so called BPS monopoles, which will be introduced in chapter 2.

It is known that magnetic monopoles will naturally arise in Grand Unification Theories (GUTs). They have serious consequences in cosmology in which the monopole abundance is one of the major puzzles that drove people to the so called inflationary models.

The introduction of magnetic monopoles also revived the old idea of electromagnetic duality in a modern context and in a much deeper form. This new form of electromagnetic duality relates the fundamental excitations (electrically charged fermions or gauge particles) of gauge theories to the solitonic states (magnetic monopoles) in the dual theories. and maps the weakly coupled theories into their strongly coupled dual theories. Such a duality has opened the door to understand strong coupling field theories by considering the weak coupling dual theories. Exploring the details of this duality has brought physicists lots of deep insights of gauge theories and has become a fruitful source of discoveries.

As a consequence of the electromagnetic duality, massless monopoles must enter the picture as the counterparts of massless gauge particles. For instance, in some sense, a meson with two massive quarks bound by a massless gluon might be treated as the dual object to a monopole system consisting of two massive and one massless monopoles. How to understand and describe massless monopoles is one of the most interesting questions raised by electromagnetic duality. Based on the recent research works, it is known that

massless monopoles arise when gauge symmetry has a non-Abelian unbroken sector. It is also known that the existence of massless monopoles relies on their interaction with massive monopoles. A physically non-pathological monopole system must carry Abelian total charge, similar to the well-known QCD result that physical states must be color neutral. In such a system, massless monopoles form a cloud structure which neutralizes the non-Abelian components of the magnetic field. A more detailed introduction will be given in chapter 2.

On the other hand, instantons, arising as the classical solutions of Euclidean field theories, describe the tunneling processes in Minkowski quantum field theories. These Euclidean field theories also provide a natural framework to study finite temperature quantum field theories. It is known that the QCD vacuum has a periodic structure which can be connected only by instanton effects. Such effects have led to a highly nontrivial structure called the θ-vacuum, and it is a major open question to explain the smallness of the θ parameter.

Down to a more phenomenological level, instantons and monopoles both play important roles in understanding the QCD vacuum and have recieved clear support from lattice computations. For instance, it is known that by assuming that QCD vacuum is made of an instanton gas one can qualitatively explain the chiral phase transition. On the other hand, instanton model

is known to be useless in another well-known feature of QCD: the color confinement. So far the best proposal for the confinement mechanism is the dual superconductor hypothesis which assumes that the QCD vacuum is a condensation of magnetic monopoles. Many numerical computations have been done and the results seem to support this model.

A natural question arises since we have only one QCD vacuum. What is the genuine content of the QCD vacuum? We have seen that both the instanton picture and the monopole picture play certain exclusive roles in the QCD vacuum. It is certainly not satisfactory that we need two distinct pictures of QCD vacuum. A nice resolution of the problem will be to find a relationship between instantons and magnetic monopoles which unifies the two pictures of QCD vacuum. We will see that this is indeed quite possible.

The outline of the thesis is as follows: Chapter 2 introduces the concepts and some fundamental facts about magnetic monopoles, instantons and calorons. It also contains a synthesized introduction of Nahm's formalism which is the method used for all the topics described in the other chapters. Nahm's formalism is based on a type of duality between gauge theories in d-dimensional space and $4-d$ dimensional space. It significantly reduces the complexity of the computation and is one of the major methods used in modern monopole and caloron (finite temperture instanton) studies. Chapter 3 discusses a monopole system made of two massive and one massless

monopoles in Sp(4) gauge theory [47]. This is a configuration that contains a non-Abelian cloud. We compute the Nahm data of the system and explore some of the Higgs configurations with strong spherical or axial symmetry. The exact moduli space metric of the monopole system is also derived which is one of the few exact results known in this field. Chapter 4 provides a numerical study on the formation of non-Abelian clouds [54]. In this chapter the explicit form of the energy density of the two systems is derived. Based on this result we try to explore the interaction between the massless monopole and the massive monopole by numerical computation and describe the formation of the non-Abelian cloud. Chapter 5 studies the structure of an SU(2) caloron in presence of symmetry breaking [48]. It gives rise to a clear and new picture connecting instantons and magnetic monopoles. Finally, in chapter 6, I conclude with some comments. Three appendices are added to address some supplementary topics. Appendix A contains a short introduction of some mathematics concepts and results used in the thesis. Appendix B describes several simple results of a single SU(2) monopole. Appendix C is devoted to charge quantization and its relation with magnetic monopoles.

Chapter 2

Monopoles, Instantons, Nahm's Formalism and All That

2.1 BPS Monopoles

2.1.1 Introduction

For quite a long time in the history of physics, electricity and magnetism have been studied parallelly. Although all magnets found in nature contain both a north pole and a south pole, the remarkable similarity of electricity and magnetism has stimulated the concept of a magnetic monopole (in what follows, we will often simply called it a monopole) as the source of magnetism and the analogue of electric charge. The mathematical foundation of classical electromagnetism was established in 19th century by J. C. Maxwell. Maxwell's theory elegantly describes all the known classical electromagnetic phenomena. To monopole physics, the role played by Maxwell's theory is two-fold: On one hand, it describes magnetism as a by-product of

electricity and therefore denies any fundamental role of magnetic monopoles, as was conceived in the old days. On the other hand, the form of Maxwell's equations itself (in proper units)

$$\begin{aligned} \nabla \cdot \mathbf{E} &= \rho \\ \nabla \times \mathbf{E} &= -\frac{\partial \mathbf{B}}{\partial t} \\ \nabla \cdot \mathbf{B} &= 0 \\ \nabla \times \mathbf{B} &= \frac{\partial \mathbf{E}}{\partial t} + \mathbf{J} \end{aligned} \tag{2.1}$$

strongly suggests that one might *add* magnetic sources into the theory. Once such sources are added, Maxwell's theory looks more beautiful and allows a new symmetry called electromagnetic duality. This extended Maxwell's theory forms the framework of classical monopole physics, but the classical theory of magnetic monopoles didn't go quite far.

The situation changed drastically in 1931 when P. A. M. Dirac incorporated classical monopole theory into quantum mechanics. What he found was that the existence of a *single* monopole quantizes *all* the electric charges in the universe, or more specifically

$$eg = 2\pi n\hbar, \tag{2.2}$$

where e, g are the electric and magnetic charges, $\hbar$ is the Planck constant, n is an integer. This result, called the Dirac quantization condition, is of

fundamental importance in monopole physics and is very attractive since "electric charges are known to be quantized and no reason for this has yet been proposed apart from the existence of magnetic poles"[18].

The proof of Dirac's quantization condition will be left to appendix C, but we would like to point out that it is not surprising to see such a restriction on magnetic monopoles. As was known for quite a long time, although formally Maxwell's equations are quite symmetric between electric and magnetic sides, they have very different natures. The magnetic part of the theory is actually two mathematical identities! They must be satisfied so long as the electromagnetic fields are to be derived from single-valued and non-singular potential functions. Therefore adding magnetic sources to the theory breaks the possibility of introducing such potential functions. At the classical level, potential functions have no direct physical meaning, therefore adding magnetic charge won't cause any problem (but because of this it also won't lead us any further). In quantum theory, however, the interaction of charged particles and electromagnetic fields is *necessarily* described by potential functions. Breaking the structure of the potential-based field strength would be a disaster at the quantum level. Fortunately, it turns out quantum mechanics *does not* require an unambiguous definition of the potential functions, rather it is only concerned with the loop integral $\oint A_\mu dx_\mu$[1]. It is this freedom that

[1]More precisely $\exp(\oint A_\mu dx_\mu)$.

allows the existence of magnetic monopoles, and it is the physical relevance of potential functions at the quantum level that leads to certain restrictions, namely the Dirac's quantization condition[2].

Dirac's paper encouraged people to consider magnetic monopole seriously, but until early 1970's, there was no significant further progress on Dirac's monopole theory. The reason is that Dirac's monopole is added into Maxwell equations *by hand*, therefore one can't predict any physical properties (except for its magnetic charge) of such an object. It can't be treated as a *prediction* of the existence of magnetic monopole.

Now imagine a theory which allows magnetically charged states that are stable, localized and have finite energies. That kind of theory, if it exists, will give a completely new framework for magnetic monopoles. String theorists have a famous statement: In string theory everything that looks true is true. A similar statement seems relevant to cosmology: In the early universe, everything that could exist must have been created! So if any *realistic* theory allows the existence of such magnetically charged states, then stable magnetic monopoles must have been created and we should in principle be able to see them somewhere in the universe. If they are not too massive, we could even create them in laboratories. So the questions are: Are there any such

[2]Briefly speaking: If physics only depends on $F_{\mu\nu}$, monopoles are allowed and not restricted at all. If physics depends on A_μ, monopoles are not allowed. If physics depends on $\oint A_\mu dx_\mu$, monoples are allowed but restricted by Dirac's quantization condition.

theories? Are there any such *realistic* theories? The research in the past quarter of a century has given a positive answer to the first question and strongly suggested a positive answer to the second.

2.1.2 Monopoles as topological objects

With the development of non-Abelian gauge theory in 1950's , we realized that in the general framework of gauge theories, electromagnetic theory is only a particular gauge theory whose gauge group is U(1). Furthermore, with the discovery of spontaneous symmetry breaking mechanism, namely the Higgs mechanism, we realized that electromagnetic theory is not the *only* U(1) gauge theory. U(1) theories or U(1) sectors of theories can arise from various underlying non-Abelian gauge theories through the Higgs mechanism. We have already known that in electromagnetic theory, magnetic sources are added by hand, but how about those other U(1) theories coming from the Higgs mechanism? The underlying non-Abelian gauge theories will determine all the aspects of the unbroken U(1) theories. In particular, one should be able to see whether there are any magnetic sources in the unbroken U(1) sectors and in case there are such sources, the properties of the sources. These considerations naturally lead us to modern monopole theories.

The simplest model to consider is the SU(2) gauge theory with gauge symmetry broken to U(1). This model was first discussed by 't Hooft and

Polyakov independently[3] [68, 74]. We choose the Minkowski metric to be $g_{\mu\nu} = \mathrm{diag}(1, -1, -1, -1)$. The Lagrangian under consideration is

$$\mathcal{L} = -\frac{1}{4}F^a_{\mu\nu}F^{a\mu\nu} + \frac{1}{2}D_\mu\Phi^a D^\mu\Phi^a - \frac{\lambda}{4}(\Phi^a\Phi^a - v^2)^2, \tag{2.3}$$

where A^a_μ and Φ^a are the components of the gauge field and the Higgs field. The field intensity and covariant derivative are defined as

$$F^a_{\mu\nu} = \partial_\mu A^a_\nu - \partial_\nu A^a_\mu + e\epsilon^{abc}A^b_\mu A^c_\nu, \tag{2.4}$$

$$D_\mu\Phi^a = \partial\Phi^a + e\epsilon^{abc}A^b_\mu\Phi^c. \tag{2.5}$$

We are going to use a flexible convention of summations: whether two common indexes (not necessarily one upper one lower) in an equation are summed up is determined by their appearance in the equation. If a pair of indexes does not appear in every term of the equation, they are summed, otherwise they are not summed.

For any solutions with finite energy, $\Phi^a\Phi^a$ must approach v^2 at spatial infinity. This non-zero vacuum expectation value of Φ breaks the SU(2) gauge symmetry. We introduce the vacuum manifold M_H of Higgs fields to describe all the gauge inequivalent (with respect to the unbroken gauge symmetry) Higgs values at spatial infinity. It is easy to see that

$$M_H = G/H, \tag{2.6}$$

[3]What 't Hooft really studied was the SO(3) monopole, but the SO(3) and SU(2) theories have the same monopole content (see appendix C for a brief explanation).

where G and H are the original gauge group and the unbroken gauge group, respectively.

An important property of the asymptotic Higgs configurations is that such configurations can be categorized by the homotopy class of the mappings from spatial infinity S_∞ to M_H, namely $\Pi_2(M_H)$. In our case $\Pi_2(M_H) = \Pi_2(\mathrm{SU}(2)/\mathrm{U}(1)) = \mathrm{Z}$. Thus the configurations are characterized by an integer n called the winding number which can be computed by

$$n = \frac{1}{8\pi} \int \epsilon_{ijk} \epsilon^{abc} \partial_i \hat{\Phi}^a \partial_j \hat{\Phi}^b \partial_k \hat{\Phi}^c d^3x, \tag{2.7}$$

where $\hat{\Phi} = \Phi/v$.

After symmetry breaking, the theory is effectively a U(1) gauge theory and therefore must have a U(1) field intensity $F_{\mu\nu}$. It is natural to require that $F_{\mu\nu}$ satisfy the following conditions:

1. It should lead to $\partial_\mu A^3_\nu - \partial_\nu A^3_\mu$ when $\hat{\Phi}$ points to a constant direction which we choose as $(0, 0, 1)$.

2. The definition of $F_{\mu\nu}$ must be gauge invariant.

Such a tensor was found by 't Hooft [74]:

$$F_{\mu\nu} = \hat{\Phi}^a F^a_{\mu\nu} - \frac{1}{e} \epsilon^{abc} \hat{\Phi}^a D_\mu \hat{\Phi}^b D_\nu \hat{\Phi}^c. \tag{2.8}$$

From Eq. (2.8) we can compute the derivative of the dual tensor $\tilde{F}^{\mu\nu} =$

$\frac{1}{2}\epsilon^{\mu\nu\rho\sigma}F_{\rho\sigma}$ which gives

$$\partial_\mu \tilde{F}^{\mu\nu} = \frac{4\pi}{e}k^\nu, \tag{2.9}$$

where k^ν is the magnetic current given by

$$k^\nu = \frac{1}{8\pi}\epsilon^{\nu\rho\sigma\delta}\epsilon^{abc}\partial_\rho\hat{\Phi}^a\partial_\sigma\hat{\Phi}^b\partial_\delta\hat{\Phi}^c, \tag{2.10}$$

where $\epsilon^{\mu\nu\rho\sigma}$ is defined so that $\epsilon^{0123} = 1$. The magnetic charge associated to this current is

$$g = \frac{4\pi}{e}\int k^0 d^3x = \frac{1}{2e}\int \epsilon_{ijk}\epsilon^{abc}\partial_i\hat{\Phi}^a\partial_j\hat{\Phi}^b\partial_k\hat{\Phi}^c d^3x = \frac{4\pi}{e}n, \tag{2.11}$$

where n is the winding number defined in Eq. (2.7). An analytic solution of the field configuration with unit magnetic charge (namely the $n = 1$ case) was found by M. K. Prasad and C. M. Sommerfeld in the limit $\lambda = 0$ (called the Prasad-Sommerfeld limit) [69]. (See appendix B for a brief introduction) From these results we can learn the following consequences:

1. The underlying SU(2) theory completely determines the structure of the unbroken U(1) theory. The existence of the magnetic current is no longer an arbitrary assumption of the theory. For the first time we have a theory that *predicts* the existence of magnetic monopoles.

2. The conservation of k^ν comes directly from the antisymmetricity of $\epsilon^{\nu\rho\sigma\delta}$, this distinguishes k^ν from the usual Noether current whose con-

servation comes from the dynamics of the system. k^ν is called a topological current.

3. Magnetic monopoles are topological objects. The topological property of magnetic charge (namely that it is proportional to the winding number of the Higgs configuration) preserves the stability of the monopoles with unit charge.

Another thing that one might have noticed is that Eq. (2.11) is quite similar, but not identical, to the Dirac quantization condition. Their relationship is analyzed in appendix C.

2.1.3 Bogomol'nyi condition and self-duality

In 1976, E. B. Bogomol'nyi studied the stability of magnetic monopoles (and of the dyons which we are not going to discuss) in the Prasad-Sommerfeld limit. He found that the total energy of a monopole or a monopole system is bounded from below by $v|g|$ (g is the total magnetic charge) and that the bound is saturated when the monopole configuration satisfies a set of first order equations. This set of equations is called the Bogomol'nyi condition (or Bogomol'nyi equations) and is the starting point of many modern discussions of magnetic monopoles.

To derive the Bogomol'nyi condition, we notice that from Lagrangian

(2.3), the potential energy (in the Prasad-Sommerfeld limit) of the Yang-Mills-Higgs system is

$$\begin{aligned} U &= \int d^3x \left(\frac{1}{4}F_{ij}^a F_{ij}^a + \frac{1}{2}D_k\Phi^a D_k\Phi^a\right) \\ &= \frac{1}{4}\int d^3x (F_{ij}^a \mp \epsilon_{ijk}D_k\Phi^a)^2 \pm \frac{1}{2}\int d^3x \epsilon_{ijk}F_{ij}^a D_k\Phi^a. \end{aligned} \tag{2.12}$$

The second term in Eq. (2.12) can be rewritten as

$$\begin{aligned} \frac{1}{2}\int d^3x \epsilon_{ijk}F_{ij}^a D_k\Phi^a &= \frac{1}{2}\int d^3x D_k(\epsilon_{ijk}F_{ij}^a\Phi^a) \\ &= \frac{1}{2}\int d^3x \partial_k(\epsilon_{ijk}F_{ij}^a\Phi^a) \\ &= \frac{1}{2}\int_{S_\infty} d^2S_k\ \epsilon_{ijk}F_{ij}^a\Phi_k^a \\ &= v\int_{S_\infty} d^2S_k\ B_k \\ &= vg, \end{aligned} \tag{2.13}$$

where we have used the fact that $\epsilon_{ijk}F_{ij}^a\Phi_k^a$ is a scalar in internal space (so that the covariant derivative can be replaced by an ordinary derivative) and the asymptotic behavior $F_{ij}^a\Phi^a \sim vF_{ij}$. Now the total energy can be written as

$$E \geq U = \frac{1}{4}\int d^3x (F_{ij}^a \mp \epsilon_{ijk}D_k\Phi^a)^2 \pm vg. \tag{2.14}$$

By choosing the proper sign, the total energy is bounded from below by $v|g|$ and the bound is saturated by static configurations satisfying

$$F_{ij}^a \mp \epsilon_{ijk}D_k\Phi^a = 0. \tag{2.15}$$

Eq. (2.15) is called the Bogomol'nyi condition (for positive charge the "–" sign applies, otherwise the "+" sign applies). Without losing generality, unless otherwisely stated, we will only consider positive charge in what follows, so the Bogomol'nyi condition has the form

$$F_{ij}^a - \epsilon_{ijk} D_k \Phi^a = 0, \tag{2.16}$$

or equivalently

$$B_k^a = D_k \Phi^a. \tag{2.17}$$

In the Prasad-Sommerfeld limit, a static monopole system satisfying the Bogomol'nyi condition has the lowest energy, and is therefore stable against small perturbations. Monopoles in such systems are called BPS monopoles.

This argument is one of the early pieces of evidence supporting the existence of static multi-monopole solutions, although no explicit solution has been found. Another way to understand the existence of such solutions is to notice that although the Coulomb magnetic forces between BPS monopoles are repulsive, the scalar forces (sometimes called dilatonic forces) mediated by the massless Higgs are attractive and also obey Coulomb's law. These always balance the magnetic forces as the dilatonic charge of each BPS monopole is equal to the magnetic charge of the monopole as shown in Eq. (B.6).

It is easy to check that the configuration of a single SU(2) monopole given in appendix B satisfies Bolgomol'nyi condition. This means that, due

to the clever choice of ansatz (B.1) and (B.2), the single SU(2) monopole solution found by Prasad and Sommerfeld is already a BPS monopole. In general, however, the Prasad-Sommerfeld limit simplifes the potential, while the Bogomol'nyi condition is about minimal energy, they are independent conditions.

The concept of BPS states can be generalized to supersymmetric theories. In supersymmetric theories BPS states are those states that are preserved by some (usually half) of the supersymmetries. These remaining supersymmetries give us non-perturbative control over the quantum behavior of the BPS states. A nice fact is that the non-supersymmetric monopole solutions turn out to be valid in supersymmetric theories. Therefore all the results on non-supersymmetric monopoles are relevant in supersymmetry content. To see this, we write the Langrangian of $N = 2$ super-Yang-Mills here [30][40]:

$$\begin{aligned} \mathcal{L}_{N=2} &= \mathrm{tr}\left\{-\frac{1}{2}F_{\mu\nu}F^{\mu\nu} - (D_\mu P)^2 - (D_\mu S)^2 - [S,P]^2 \right. \\ &\quad \left. -2i\overline{\psi}\gamma^\mu D_\mu \psi - 2\overline{\psi}[S,\psi] - 2\overline{\psi}\gamma_5[P,\psi]\right\}. \end{aligned} \tag{2.18}$$

All the fields (include the gaugino) are in the adjoint representation of the gauge group. The BPS monopole solution in this theory is realized by a parity-conserving vacuum $\langle S\rangle > 0$, $\langle P\rangle = 0$. It is easy to see that the bosonic BPS monopole configurations are exactly the same configuration as we considered before. It is also known (but less obvious) that such configura-

tions preserve half of the supersymmetry (namely the theory has a residual $N = 1$ supersymmetry).

For later applications, it is helpful to introduce an alternative form of the Bogomol'nyi condition. The monopole solutions we are considering are static and satisfy $A_0^a = 0$ (i.e. purely magnetic). We can combine A_i^a with Φ^a to form a Euclidean vector $A_m^a = (\mathbf{A}^a, \Phi^a)$. Then the Bogomol'nyi condition (2.16) can be rewritten as a set of self-dual equations (everything is assumed to be independent of x^4):

$$F_{mn}^a = \frac{1}{2}\epsilon_{mnrs}F_{rs}^a = \tilde{F}_{mn}^a, \tag{2.19}$$

where ϵ_{mnrs} is choosen such that $\epsilon_{1234} = 1$. For later convenience, it is also useful to notice that Gauss' law

$$D_i F^{ai0} = e[\Phi, D^0\Phi]^a \tag{2.20}$$

now becomes

$$D_m F_{0m}^a = 0, \tag{2.21}$$

where $D_m = \partial_m + [A_m, \quad]$. This equivalence between the Bogomol'nyi condition and self-duality opens the door for the relationship between BPS solutions on R^3 and self-dual solutions on R^4. As we will see, this relationship is helpful in understanding Nahm's formalism and the connection between magnetic monopoles and instantons.

2.1.4 Monopoles in arbitrary gauge theories

In this subsection, we are going to consider magnetic monopoles in arbitrary gauge theories with arbitrary symmetry breaking patterns. This is not only the natural way to generalize the previous discussions, but also a necessary step to revealing the physical relevance of magnetic monopoles since, so far as we know, SU(2) theory alone does not describe any physical interactions.

First, let's make some general consideration. As we mentioned in subsection 2.1.2, monopole configurations are categorized by $\Pi_2(G/H)$. Therefore any symmetry breaking pattern having nontrivial $\Pi_2(G/H)$ admits monopole solutions. The first physically relevant gauge theory with symmetry breaking is electroweak theory in which $\mathrm{SU}(2) \times \mathrm{U}(1)$ is broken to U(1). Unfortunately, $\Pi_2((\mathrm{SU}(2) \times \mathrm{U}(1))/\mathrm{U}(1)) = 0$, so there is no magnetic monopole in electroweak theory. Since the electroweak sector is the only part of standard model that contains symmetry breaking, we conclude that there is no magnetic monopole (in the content of our previous discussion) in the standard model. What, if we go beyond the standard model? Strongly positive news comes from GUT (Grand Unification Theory). Suppose that in a GUT, a simply connected grand gauge group G is broken to the standard model gauge group $\mathrm{SU}(3) \times \mathrm{SU}(2) \times \mathrm{U}(1)$. Using a well-known mathematical

theorem, $\Pi_2(G/H) = \Pi_1(H)$, we have

$$\Pi_2(G/(\mathrm{SU}(3) \times \mathrm{SU}(2) \times \mathrm{U}(1))) = \Pi_1(\mathrm{SU}(3) \times \mathrm{SU}(2) \times \mathrm{U}(1)) = Z. \quad (2.22)$$

This results says any such GUT will admit magnetic monopoles! Since monopole structure in a gauge theory is determined by the universal covering of the gauge group which is always simply connected. This argument strongly suggests that magnetic monopoles might exist at GUT scale.

Now, let's go to detailed discussions. The Higgs field is assumed to be in the adjoint representation of the gauge group. We choose the asymptotic Higgs field along the z-direction to be in the Cartan subalgebra, namely $\Phi_\infty = \mathbf{h} \cdot \mathbf{H}$ (see appendix A for a brief introduction to Lie algebras). For each root $\boldsymbol{\alpha}$, there is associated an SU(2) subalgebra (therefore an SU(2) subgroup) with generators:

$$\begin{aligned} t^1(\boldsymbol{\alpha}) &= \frac{1}{\sqrt{2|\boldsymbol{\alpha}|^2}}(E_{\boldsymbol{\alpha}} + E_{-\boldsymbol{\alpha}}) \\ t^2(\boldsymbol{\alpha}) &= \frac{-i}{\sqrt{2|\boldsymbol{\alpha}|^2}}(E_{\boldsymbol{\alpha}} - E_{-\boldsymbol{\alpha}}) \\ t^3(\boldsymbol{\alpha}) &= \boldsymbol{\alpha}^* \cdot \mathbf{H}. \end{aligned} \quad (2.23)$$

It is easy to see that for $\mathbf{h} \cdot \boldsymbol{\alpha} \neq 0$, this SU(2) subgroup doesn't leave Φ_∞ invariant, which means the SU(2) symmetry is broken by the Higgs field (however, a U(1) factor generated by $t^3(\boldsymbol{\alpha})$ is always unbroken which is a general property so long as the Higgs field is in the adjoint representation).

If $\mathbf{h} \cdot \boldsymbol{\gamma} \neq 0$ for all the root $\boldsymbol{\gamma}$, then the gauge symmetry is (maximally) broken to $\mathrm{U}(1)^r$ (where r is the rank of the original gauge group G), otherwise there is going to be a non-Abelian unbroken symmetry. We will call the two cases MSB (Maximal Symmetry Breaking) and NUS (Non-Abelian Unbroken Symmetry) cases for simplicity[4].

We consider the MSB case at first. In this case it turns out that one can choose a unique set of simple roots such that $\mathbf{h}$ has positive inner products with all the simple roots. In what follows we will always refer to this set of roots when we talk about simple roots.

The simplest monopole solution one can construct is the SU(2)-embedded solution associated to an arbitrary root $\boldsymbol{\alpha}$:

$$A_i = A_i^a(\mathbf{x}, |\mathbf{h} \cdot \boldsymbol{\alpha}|)t^a,$$

$$\Phi = \Phi^a(\mathbf{x}, |\mathbf{h} \cdot \boldsymbol{\alpha}|)t^a + (\mathbf{h} - \mathbf{h} \cdot \boldsymbol{\alpha}^* \boldsymbol{\alpha}) \cdot \mathbf{H}. \tag{2.24}$$

Where A_i and Φ are defined by B.1 and B.2. The mass of such an SU(2)-

[4]Another way to see the symmetry breaking pattern is to notice that the mass term for gauge particles is $-e^2\mathrm{tr}\{[A_\mu, \Phi_\infty][A^\mu, \Phi_\infty]\}$. Choosing a Cartan-Weyl basis for the generators, we see that there are always r massless gauge bosons (whose component fields are associated with the Cartan subalgebra corresponding to the $\mathrm{U}(1)^r$ unbroken symmetry). The masses of the other bosons are determined by the matrix $M_{\boldsymbol{\alpha}\boldsymbol{\beta}} = (\mathbf{h} \cdot \boldsymbol{\alpha})(\mathbf{h} \cdot \boldsymbol{\beta})\mathrm{tr}(E_{\boldsymbol{\alpha}} E_{\boldsymbol{\beta}})$. When $\mathbf{h} \cdot \boldsymbol{\gamma} \neq 0$ $(\forall \boldsymbol{\gamma})$, this matrix is in full rank, therefore all other gauge bosons are massive. This is certainly the MSB case. Otherwise, $M_{\boldsymbol{\alpha}\boldsymbol{\beta}}$ is not full rank and that is the NUS case.

embedded monopole is given by[5]

$$m_{\boldsymbol{\alpha}} = g|\mathbf{h}\cdot\boldsymbol{\alpha}^*|. \tag{2.25}$$

At the first glance, all such solutions are similar to each other, but actually those associated to simple roots turn out to be more *fundamental* than others in the sense that all the other monopoles are the superpositions of those monopoles. To see this let $\boldsymbol{\beta}_a$ $(a = 1, ..., r)$ be the simple roots. Without losing generality, let $\boldsymbol{\alpha}$ be an arbitrary positive root that is not simple, then $\boldsymbol{\alpha}^*$ can be expanded in terms of $\boldsymbol{\beta}_a^*$:

$$\boldsymbol{\alpha}^* = \sum_{a=1}^{r} n_a \boldsymbol{\beta}_a^*, \tag{2.26}$$

where all the coefficients are positive integers. According to (2.25) the mass of the SU(2) embedded monopole associated to $\boldsymbol{\alpha}$ is

$$m_{\boldsymbol{\alpha}} = \sum_{a=1}^{r} n_a m_{\boldsymbol{\beta}_a}. \tag{2.27}$$

This is an indication that the $\boldsymbol{\alpha}$ monopole is a composite object. A more convincing argument comes from the counting of zero modes of these SU(2)-embedded monopoles [77]. It was found that all the $\boldsymbol{\beta}_a$ monopoles have four zero modes, but the number of zero modes of the $\boldsymbol{\alpha}$ monopole is

$$N = 4\sum_{a=1}^{r} n_a. \tag{2.28}$$

[5]From the solution (2.24), $v = |\mathbf{h}\cdot\boldsymbol{\alpha}|$, the mass seems to be $g|\mathbf{h}\cdot\boldsymbol{\alpha}|$. However, the generators defined in Eq. (2.23) satisfy $\mathrm{tr}(t^a t^b) = \frac{1}{2}|\boldsymbol{\alpha}^*|^2\delta^{ab}$ which contribute a factor of $|\boldsymbol{\alpha}^*|^2$ to the mass.

This means that an $\boldsymbol{\alpha}$ monopole contains all the internal degrees of freedom of its constituent monopoles. So we conclude that it is reasonable to treat monopoles associated to simple roots as fundamental monopoles and others as composite monopoles (so some of the SU(2)-embedded solutions we wrote down are actually multi-monopole solutions).

Although the generalization from a single SU(2) monopole to multi-monopole systems in arbitrary gauge theories is conceptually straightforward, the explicit configurations of multi-monopole systems other than the SU(2)-embedded ones are hard to obtain. Asymptotically the magnetic field has the form

$$\mathbf{B} = \frac{\hat{\mathbf{r}}}{4\pi r^2} G(\Omega) + \mathcal{O}\left(\frac{1}{r^3}\right), \tag{2.29}$$

where $G(\Omega)$ is called the generalized magnetic charge (in contrast to the usual U(1) magnetic charge). $G(\Omega)$ is r-independent. The appearance of angular variable Ω indicates that G depends on spatial directions. It can be shown that[6]

$$[G(\Omega), \Phi_\infty(\Omega)] = 0, \tag{2.30}$$

and $G(\Omega)$ is a covariant constant, namely [7]

$$D_i G(\Omega) = 0. \tag{2.31}$$

[6]The argument goes as follows: $D_i\Phi = B_i \sim \mathcal{O}(1/r^2)$, so $[D_i, D_j]\Phi \sim \mathcal{O}(1/r^3)$. On the other hand $[D_i, D_j]\Phi \sim F_{ij}\Phi \sim \mathcal{O}(1/r^2)[G, \Phi]$, so $[G(\Omega), \Phi_\infty(\Omega)] = 0$.

[7]Since for large r, $D_i B_i = \frac{\hat{r}^i}{4\pi r^2} D_i G(\Omega)$ and $D_i B_i = \frac{4\pi}{e} k^0 = \mathcal{O}(1/r^3)$, therefore $D_i G(\Omega) = 0$.

Because of Eq. (2.30), one can choose $G(\Omega)$ along the z-direction to be in the Cartan subalgebra. Topological arguments [26] further determine $G(\hat{\mathbf{z}})$ to be

$$G(\hat{\mathbf{z}}) = g \sum_{a=1}^{r} n_a \boldsymbol{\beta}_a^* \cdot \mathbf{H}. \tag{2.32}$$

This is compatible with the picture that all monopole systems are made of fundamental monopoles (but unless $\sum_a n_a \boldsymbol{\beta}_a^*$ happens to be a co-root, we won't have the simple SU(2)-embedded solution).

Now let's consider the NUS case in which $\mathbf{h}$ is orthogonal to some root vectors. In the simplest case, assume $\mathbf{h}$ is orthogonal to a root, say $\boldsymbol{\alpha}$, so the SU(2) subgroup associated to $\boldsymbol{\alpha}$ leaves the Higgs field invariant, and there is an unbroken SU(2) symmetry. A couple of new issues arise in this case. For instance from the mass formula (2.25), the $\boldsymbol{\alpha}$ monopole becomes massless. An isolated massless monopole is meaningless in classical theory, but we will see that the presence of these massless monopoles in a monopole system turns out to be a rather nontrivial phenomenon.

Naively, it seems magnetic monopoles in the NUS case can carry non-Abelian magnetic charges, since the asymptotic magnetic field (2.29) transforms nontrivially under the unbroken non-Abelian gauge group. However, it is known that such configurations have topological pathologies [1, 2, 5, 65, 66] which prevent us from defining the non-Abelian charge globally. One sim-

ple way to understand those pathologies is to notice that once the total magnetic charge is non-Abelian, the unbroken non-Abelian gauge group acts non-trivally on $G(\Omega)$. The orbit of $G(\Omega)$ under these transformation is at least SU(2). Therefore Eq. (2.30) means that one has to find at least an SU(2) configuration on the sphere at spatial infinity such that

$$[\mathrm{SU}(2), \Phi_\infty] = 0 \tag{2.33}$$

is satisfied along any direction. This turns out to be impossible (in a similar sense as it is impossible to define a non-singular vector field on a sphere) since Φ_∞ winds nontrivially on the sphere.

On the other hand when the total magnetic charge is Abelian (namely $g\sum_{a=1}^{r} n_a \boldsymbol{\beta}_a^*$ in Eq. (2.32) is orthogonal to all roots of the unbroken non-Abelian gauge group), there is no topological obstacle, and the transition between the massive case and the massless case is smooth. Lots of research has been done to study this case [14, 47, 50, 78, 80]. It was found that when monopoles becomes massless, they lose their identities as distinct objects and form a non-Abelian cloud surrounding massive monopoles. Inside the non-Abelian cloud, the magnetic field has non-Abelian components. The cloud tends to neutralize these non-Ablelian components and leads to a purely Abelian magnetic field far away outside the cloud.

The degrees of freedom of these massless monopoles merge into the de-

grees of freedom of the cloud. For instance, in the SO(5) case with two distinct fundamental monopoles, when both monopoles are massive, the degrees of freedom are composed of six spatial coordinates, representing the positions of the two monopoles, and two U(1) phases. When one of the monopole becomes massless with the total magnetic charge kept Abelian, two spatial coordinates of the would-be massless monopoles turn into SU(2) gauge parameters. Symbolically, one may use $3+1 \to 1+3$ to represent this change of interpretation. We will discuss more about massless monopoles in chapter 4.

2.1.5 Moduli space metrics

So far we have only considered the static magnetic monopole solutions. The dynamical behavior of a monopole system is very complicated due to the nonlinearity of the theory. At low energy, however, it turns out that there exists a beautiful geometric description of monopole dynamics. This method, called the moduli space approximation, was first proposed by N. S. Manton [55].

It is known that all possible gauge-inequivalent configurations of a monopole system with a given energy are parameterized by several collective coordinates (also known as zero modes since they represent variations that don't cost energy). The abstract space spanned by these parameters is called the

moduli space of the monopole system. Different points in the moduli space represent different configurations of the monopole system that are not related by small gauge transformations[8]. Mathematically the moduli space is defined as

$$\mathcal{M} = \mathcal{A}/\mathcal{G} \tag{2.34}$$

where $\mathcal{A}$ is the BPS configuration space and $\mathcal{G}$ is the space of small gauge transformations.

What Manton showed is that there is a natural metric structure in the moduli space and that the low energy dynamics of a monopole system is simply described by the geodesic motions in the moduli space (equipped with that metric).

To see how this description arises, let's use the Euclidean formalism. The infinitesimal gauge transformations are given by

$$\delta A_m^a = D_m \Lambda^a \tag{2.35}$$

with $\Lambda^a(\mathbf{x}) = 0$ at spatial infinity. Let λ^α be the collective coordinates, and $\delta_\alpha A_m^a$ be the variations of A_m^a with respect to λ^α in the moduli space. To ensure that the variations are still in the moduli space, we further require

[8]Small gauge transformations are those gauge transformations that approach unity at spatial infinity.

$\delta_\alpha A_m^a$ to be orthogonal to small gauge transformations, namely

$$\begin{aligned} \langle \delta_\alpha A_m^a, D_m \Lambda^a \rangle &= \int d^3x (\delta_\alpha A_m^a D_m \Lambda^a) \\ &= -\int d^3x (D_m \delta_\alpha A_m^a) \Lambda^a \\ &= 0, \end{aligned} \tag{2.36}$$

where we have used the fact that $\Lambda^a(\mathbf{x}) = 0$ at spatial infinity. Eq. (2.36) is valid for all $\Lambda^a(\mathbf{x})$, therefore $\delta_\alpha A_m^a$ satisfies

$$D_m \delta_\alpha A_m^a = 0. \tag{2.37}$$

Furthermore, both A_m^a and $A_m^a + \delta_\alpha A_m^a$ are BPS solutions with the same energy, since they saturate the same Bogomol'nyi bound, so $\delta_\alpha A_m^a$ must satisfy the so called linearized Bogomol'nyi equations:

$$D_m \delta_\alpha A_n^a - D_n \delta_\alpha A_m^a = \frac{1}{2} \epsilon_{mnrs} (D_r \delta_\alpha A_s^a - D_s \delta_\alpha A_r^a). \tag{2.38}$$

Eqs. (2.37) and (2.38) form the definition of the tangent vectors of the moduli space.

A natural guess for the tangent vector $\delta_\alpha A_m^a$ would be the derivative of A_m^a with respect to λ^α, which is the usual way to obtain the tangent vector of a manifold. It is easy to check that such direct derivatives automatically satisfy the linearized Bogomol'nyi equation (2.38). But in general they will not satisfy condition (2.37), i.e, they will not be orthogonal to small gauge

transformations. This problem can be easily resolved by undoing the gauge part, and rewriting the tangent vector as

$$\delta_\alpha A_m^a = \frac{\partial A_m^a}{\partial \lambda_\alpha} - D_m \xi_\alpha^a, \tag{2.39}$$

where ξ_α^a is chosen to ensure the orthogonality condition (2.37).

Using an index theorem it was shown [77] from Eqs. (2.36) and (2.37) that the dimension of the moduli space of an arbitrary monopole system is $4n$ (n is the number of monopoles in the system). It can be proved that $\mathcal{M}$ is a hyperKähler space [4].

To study the dynamics of monopoles, we notice that any static monopole configuration can be written as

$$A_m^a = A_m^a(\mathbf{x}, \lambda^\alpha), \tag{2.40}$$

where λ^α are the collective coordinates. Now consider a trajectory $\lambda^\alpha(t)$ in moduli space. Certainly $A_m^a = A_m^a[\mathbf{x}, \lambda^\alpha(t)]$ describes an evolving configuration. Unfortunately, $A_m^a = A_m^a[\mathbf{x}, \lambda^\alpha(t)]$ usually does not satisfy the equations of motion and therefore does not describe the dynamics of the monopole system. This is not hard to understand, since at each instant $A_m^a = A_m^a[\mathbf{x}, \lambda^\alpha(t)]$ describes a static solutions with parameters $\lambda^\alpha(t)$, but a general dynamic configuration will not be identical to any static configuration at each moment. However, we can still reasonably hope that for sufficiently

slow evolution (quasi-static evolutions), $A_m^a = A_m^a[\mathbf{x}, \lambda^\alpha(t)]$ will give a good approximation of the dynamics. For such motions, monopole dynamics is completely determined by its trajectory $\lambda^a(t)$ in the moduli space.

The action of the monopole systems is

$$\begin{aligned} S &= \frac{1}{2}\int d^3x\, dt\, (F_{0i}^a F_{0i}^a + D_0\Phi^a D_0\Phi^a) - \int dt\, U \\ &= \int dt \left(\frac{1}{2}\int d^3x\, F_{0m}^a F_{0m}^a - U\right), \end{aligned} \tag{2.41}$$

where U is the potential energy given by Eq. (2.14). To compute the kinetic term, we notice that Gauss' law (2.21) and Eq. (2.37) have the same form, so F_{0m} can be solved as

$$F_{0m}^a = \dot{\lambda}^\alpha \delta_\alpha A_m^a, \tag{2.42}$$

which can also be obtained by choosing $A_0^a = \dot{\lambda}^\alpha \xi_\alpha^a$, where ξ_α^a was introduced in Eq. (2.39)[9]. With Eq. (2.42) in hand, one can rewrite Eq. (2.41) as

$$S = \int dt \left(\frac{1}{2} g_{\alpha\beta}\dot{\lambda}^\alpha \dot{\lambda}^\beta - U\right), \tag{2.43}$$

where

$$g_{\alpha\beta} = \int d^3x\, \delta_\alpha A_m^a \delta_\beta A_m^a \tag{2.44}$$

defines a metric $ds^2 = g_{\alpha\beta} d\lambda^\alpha d\lambda^\beta$ in the moduli space. Eq. (2.43) is a remarkable result. It has the form of particle dynamics in a curved manifold. One

[9]Once A_0 is chosen as this, $F_{0m}^a = \partial_0 A_m^a - D_m A_0^a = \dot{\lambda}^\alpha \partial_\alpha A_m^a - \dot{\lambda}^\alpha D_m \xi_\alpha^a = \dot{\lambda}_\alpha \delta_\alpha A_m$.

can further notice that for quasi-static motions, at each instant the Bogomol'nyi condition is satisfied, which means $U = v|g|$ is a constant. Therefore the dynamics of monopole system is solely described by the geodesic motion in the moduli space. This beautiful geometric picture of low energy monopole dynamics is called the moduli space approximation.

2.2 Instantons and Calorons

2.2.1 Instantons

One of the major techniques in path integral formalism is to analytically extend Minkowski space to Euclidean space, which greatly improves the convergenceness of the path integrals. By analytically extending to Euclidean space, usual field theories become Euclidean field theories.

Formally the analytical extension is realized by introducing a coordinate $x_4 = it = ix^0$, therefore the metric becomes Euclidean (the overall "–" sign will be factored out, so the Euclidean metric has the signature $(+, +, +, +)$) and consequently $\partial_0 = i\partial_4$ and $D_0 = iD_4$ (which implies $A_0 = iA_4$). The action of the field theory becomes

$$\begin{aligned} iS &\equiv i\int d^3x\, dt\, \mathcal{L}(t, \mathbf{x}) \\ &= \int d^4x_E\, \mathcal{L}(-ix_4, \mathbf{x}) \\ &= -\int d^4x_E\, \mathcal{L}_E(x_E) \end{aligned}$$

$$\equiv \quad -S_E, \tag{2.45}$$

where $\mathcal{L}_E(x_E) = -\mathcal{L}(-ix_4, \mathbf{x})$ defines the Euclidean Lagrangian density of the theory. In what follows we will drop the subscript "E" for simplicity. The quantum amplitude of a Euclidean field theory is given by the functional integral of $\exp(-S)$ over all the possible field configurations connecting the initial and final states. The local minima of the Euclidean action are of great importance to such an integral. In most cases (including Euclidean Yang-Mills theories) the minima of the Euclidean action are realized by configurations that are localized in Euclidean space. These configurations (and more generally any finite action solutions localized in Euclidean space) are called instantons.

In this thesis we are only interested in instantons in SU(2) gauge theory defined by the Euclidean action

$$S = \frac{1}{2}\int d^4x \ \mathrm{tr}(F_{mn}F_{mn}), \tag{2.46}$$

where m, n label Euclidean coordinates 1, 2, 3 and 4. To look for the configurations that minimize S we notice that S can be rewritten as (indices are omitted for simplicity)

$$\begin{aligned} S &= \frac{1}{2}\int d^4x \ \mathrm{tr}(F^2) \\ &= \frac{1}{4}\int d^4x \left[\mathrm{tr}(F^2) + \mathrm{tr}(\tilde{F}^2)\right] \end{aligned}$$

$$= \frac{1}{4}\int d^4x \ \mathrm{tr}\left[(F \pm \tilde{F})^2\right] \mp \frac{1}{2}\int d^4x \ \mathrm{tr}(F\tilde{F}), \tag{2.47}$$

where we have used $\mathrm{tr}(F^2) = \mathrm{tr}(\tilde{F}^2)$. Notice that

$$n = \frac{e^2}{16\pi^2}\int d^4x \ \mathrm{tr}(F\tilde{F}) \tag{2.48}$$

is the Pontryagin index of the gauge configuration. By properly choosing the sign in Eq. (2.47), one concludes that

$$S \geq \frac{8\pi^2}{e^2}|n|. \tag{2.49}$$

The equality is satisfied by

$$F_{mn} = \pm\tilde{F}_{mn}, \tag{2.50}$$

where "+" applies for positive n, "–" applies for negative n. Eq. (2.50) is called the self-duality (for "+" sign) or anti-self-duality (for "–" sign) equation depending on the sign. Field configurations satisfying Eq. (2.50) are called instantons (for "+" sign) or anti-instantons (for "–" sign) respectively.

Before writing down explicit instanton solutions, let's have a look at the physical meaning of the Pontryagin index n. It can be verified that

$$\mathrm{tr}(F_{mn}\tilde{F}_{mn}) = \partial_m J_m, \tag{2.51}$$

with

$$J_m = \epsilon_{mnrs}\mathrm{tr}\left(A_n F_{rs} + \frac{2i}{3}eA_nA_rA_s\right). \tag{2.52}$$

Therefore the Pontryagin index can be re-written as

$$n = \frac{e^2}{16\pi^2} \int d^3 S_m J_m + n_{\text{sing}}, \tag{2.53}$$

where n_{sing} denotes the possible contributions coming from the singularities of the configuration. Notice that $\int d^4x \ \text{tr}(F^2)$ should be finite, therefore the asymptotic behaviors of F_{mn} and A_m are

$$F_{mn} = \mathcal{O}\left(\frac{1}{r^3}\right), \tag{2.54}$$

$$A_m = \frac{i}{e} g \partial_m g^\dagger + \mathcal{O}\left(\frac{1}{r^2}\right). \tag{2.55}$$

which means the surface integral in Eq. (2.53) is dominated by

$$\frac{e^2}{16\pi^2} \int d^3 S_m J_m = \frac{1}{24\pi^2} \int d^3 S_m \epsilon_{mnrs} \text{tr}\left[(g\partial_n g^\dagger)(g\partial_r g^\dagger)(g\partial_s g^\dagger)\right]. \tag{2.56}$$

The quantity defined by this equation is the winding number of the mapping from S^3 to $\text{SU}(2) \cong S^3$, so for non-singular configurations, the Pontryagin index n is the winding number of the asymptotic gauge configuration. The index n is also called instanton number.

Now let's look at the simplest instanton solution with $n = 1$. Such a solution was first studied and found by Polyakov and collaborators [6] (they called it a pseudo-particle). In our notation, the solution of an instanton located at Euclidean coordinate a_m can be written as

$$A_m = \frac{2\Sigma_{mn}(x-a)_n}{(x-a)^2 + \rho^2}, \tag{2.57}$$

where $(x-a)^2 = (\mathbf{x}-\mathbf{a})^2 + (x_4 - a_4)^2$. The self-dual tensor Σ_{mn} in Eq. (2.57) is defined as

$$\Sigma_{mn} = -\frac{i}{2}(\sigma_m \overline{\sigma}_n - \delta_{mn}), \tag{2.58}$$

with $\sigma_m = (\boldsymbol{\sigma}, -i)$ and $\overline{\sigma}_m = (\boldsymbol{\sigma}, i)$. The parameter ρ in Eq. (2.57) is called the size of the instanton. With the help of the well-known SU(2) configuration with unit winding number:

$$g = \frac{i(x-a)_m \sigma_m}{|x-a|} = \frac{i(\mathbf{x}-\mathbf{a})\cdot\boldsymbol{\sigma} + (x_4 - a_4)}{|x-a|}, \tag{2.59}$$

Eq. (2.57) can be rewritten as

$$A_m = \frac{i}{e}\frac{(x-a)^2}{(x-a)^2+\rho^2} g \partial_m g^\dagger \tag{2.60}$$

Notice that Eq. (2.57) is non-singular and with the form given by Eq. (2.60) it is clear that the configuration approaches a pure gauge configuration with unit winding number, therefore the Pontryagin number n of this solution is one. Furthermore, it can be checked that the field tensor derived from Eq. (2.57) is

$$F_{mn} = -\frac{4}{e^2}\Sigma_{mn}\frac{\rho^2}{(x-a)^2+\rho^2}. \tag{2.61}$$

This field tensor is self-dual, therefore from the previous discussion the solution (2.57) minimizes Euclidean action and represents an instanton.

To consider the multi-instanton solutions it is useful to introduce a dif-

ferent formalism in which instanton solutions are given by a general form

$$A_m = -\frac{1}{e}\overline{\Sigma}_{mn}\partial_n \ln \phi, \tag{2.62}$$

where

$$\overline{\Sigma}_{mn} = -\frac{i}{2}(\overline{\sigma}_m \sigma_n - \delta_{mn}) \tag{2.63}$$

is an anti-self-dual tensor. Requiring that Eq. (2.62) leads to a self-dual field tensor restricts ϕ to be [70]

$$\phi = 1 + \sum_{i=1}^{n} \frac{\rho_i^2}{(x - a_i)^2}. \tag{2.64}$$

If all the a_i's are different, this gives a self-dual solution carrying instanton number n (namely an n-instanton solution). One should notice that this solution is singular, and the contribution to the instanton number comes from the n_{sing} term in Eq. (2.53). For $n = 1$ it is easy to verify that solutions (2.62) and (2.57) are related by a gauge transformation

$$A_m^{(2.57)} = g(A_m^{(2.62)} + \frac{i}{e}\partial_m)g^\dagger \tag{2.65}$$

with singular g given by Eq. (2.59).

It is known that a general n-instanton solution contains $8n$ parameters (in the case of $n = 1$, they are the four spatial coordinates, one size parameter and three SU(2) gauge degrees of freedom). The n-instanton solution we have introduced only contains $5n$ parameters plus three global gauge degrees

of freedom and is therefore only a special solution in which all the instantons have identical SU(2) phase. General explicit multi-instanton solutions are still not known.

2.2.2 Calorons

Euclidean field theory is not only a powerful tool for computing quantum amplitudes, but also proved to be the basic formalism of equilibrium finite temperature quantum field theory. In the latter case, the relevant space is $R^3 \times S^1$ equipped with Euclidean metric. The S^1 dimension goes from 0 to $\beta = 1/T$ (T is temperature). All the gauge and scalar fields are periodic on S^1.

The concept of instantons as local minima of the Euclidean action also applies to this case. Such instanton solutions were called "calorons" by Harrington and Shepard [29] because of their finite temperature nature ("calorie" $\rightarrow$ "caloron").

As in the case of multi-instanton solutions, the general explicit multi-caloron solutions are not known. In this section we only consider the single SU(2) caloron solution. To derive the solution, we notice that $S^1 = R^1/\mathrm{Z}$ (Z refers to the integer group), so that a periodic solution on S^1 can be thought of as the superposition of periodically placed identical instantons on R^1. Since these instantons have identical SU(2) phases, we can use formalism

(2.62)-(2.64) which exactly fits our demands. For the sake of simplicity, let's assume that the caloron is located at the origin, therefore we should superpose a series of instantons with identical SU(2) phases located at $x_4 = n\beta$ (the integer n runs from $-\infty$ to ∞). From (2.62)-(2.64) the caloron solution can be found as (our convention differs from [29] by a factor of i since we have chosen the gauge field to be Hermitian rather than anti-Hermitian)

$$A_m = -\frac{1}{e}\overline{\Sigma}_{mn}\partial_n \ln \phi, \tag{2.66}$$

with

$$\begin{aligned} \phi &= 1 + \sum_{n=-\infty}^{\infty} \frac{\rho^2}{|\mathbf{x}|^2 + (x_4 - n\beta)^2} \\ &= 1 + \frac{\pi\rho^2}{\beta|\mathbf{x}|} \frac{\sinh\left(\frac{2\pi}{\beta}|\mathbf{x}|\right)}{\cosh\left(\frac{2\pi}{\beta}|\mathbf{x}|\right) - \cos\left(\frac{2\pi}{\beta}x_4\right)}. \end{aligned} \tag{2.67}$$

As expected, when the temperature goes to zero ($\beta \to \infty$), Eq. (2.67) becomes Eq. (2.64). The instanton number of the caloron can also be evaluated to be one, because the contribution to instanton number comes from singularities and the fundamental zone $R^3 \times S^1$ only contains one singularity.

Finally, I want to mention that a relation between a single SU(2) caloron solution and a single SU(2) monopole solution is known. To see this, we go to the large size limit ($\rho \to \infty$) so the caloron configuration becomes

$$A_m = -\frac{1}{e}\overline{\Sigma}_{mn}\partial_n \ln \left\{ \frac{\sinh\left(\frac{2\pi}{\beta}|\mathbf{x}|\right)}{\frac{2\pi}{\beta}|\mathbf{x}| \left[\cosh\left(\frac{2\pi}{\beta}|\mathbf{x}|\right) - \cos\left(\frac{2\pi}{\beta}x_4\right)\right]} \right\}. \tag{2.68}$$

It can be verified [27] that

$$A_m^{\rm BPS}\left(\mathbf{x},\frac{2\pi}{\beta}\right)=g(A_m^{(2.68)}+\frac{i}{e}\partial_m)g^\dagger, \tag{2.69}$$

with

$$g=\exp\left\{-\frac{\hat{\mathbf{x}}\cdot\boldsymbol{\sigma}}{2}\tan^{-1}\left[\frac{\sinh\left(\frac{2\pi}{\beta}|\mathbf{x}|\right)\sin\left(\frac{2\pi}{\beta}x_4\right)}{\cosh\left(\frac{2\pi}{\beta}|\mathbf{x}|\right)\cos\left(\frac{2\pi}{\beta}x_4\right)-1}\right]\right\}. \tag{2.70}$$

Therefore the large size limit of a caloron is gauge equivalent to a BPS monopole with asymptotic Higgs value $v=\frac{2\pi}{\beta}$.

2.3 Nahm's Formalism

2.3.1 Nahm data

As mentioned in subsection 2.1.3, the Bogomol'nyi equations satisfied by BPS monopoles can be written as self-dual Yang-Mills equations (2.19) on R^4 with coordinates x_1,x_2,x_3,x_4. All the physical quantities of BPS monopoles depend only on x_1,x_2,x_3. It is easy to check that if everything only depends on the complementary variable x_4 (which will be denoted as t in what follows), then Eq. (2.19) becomes (we drop the coupling constant for simplicity)

$$\frac{dT_i}{dt}-i[T_4,T_i]-\frac{1}{2}i\epsilon_{ijk}[T_j,T_k]=0. \tag{2.71}$$

Equation (2.71) is called Nahm's equation. We have followed the convention of using T rather than A to denote the variables in Nahm's formalism. The

solutions of Nahm's equations satisfying certain boundary conditions (to be introduced below) are called Nahm data. We can always perform a gauge transformation to eliminate T_4, so usually T_4 is not included in Nahm's equations. Nahm's equations are much easier to solve than the original self-dual Yang-Mills equations as they are ordinary differential equations. The relationship between the Bogomol'nyi equations (depending on x_1, x_2, x_3) and Nahm's equations (depending on x_4) has been thoroughly investigated (especially in the SU(2) case) [19, 32, 57, 58, 59, 60, 61]. It is known that this is an example of a special kind of duality between self-dual theories in d and $4-d$ dimensions. This relationship enables us to construct monopole configurations from Nahm data and vice versa [13]. Furthermore, it is also conjectured that the moduli spaces of Nahm data and BPS monopoles are isometric to each other. This has been proven in the SU(2) case [62] and is believed to be true in general.

Another way to look at Nahm's equations is to treat the left hand side of Nahm's equations as a moment map (see appendix A for a brief description of moment map and related concepts) acting on an infinite dimensional flat (therefore trivially hyperKähler) space [31]. The moduli space of Nahm data is thus the (hyperKähler) quotient space of that infinite dimensional hyperKähler space, and therefore has a natural hyperKähler structure (see [33] or appendix A for more details). This hyperKählerity is evidence supporting

the conjecture that the moduli spaces of BPS monopoles and Nahm data are isometric.

Figure 2.1 describes the relationship between Nahm data and monopole solutions.

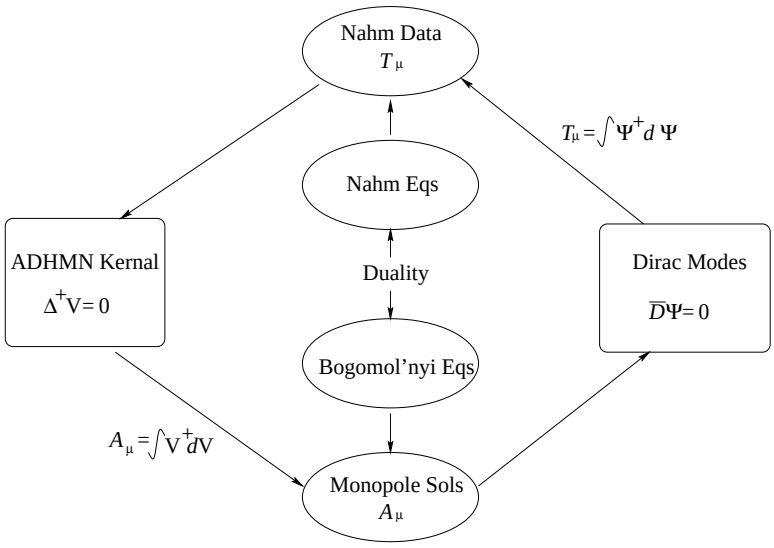

Figure 2.1: Nahm data and monopole solutions.

Let's begin the introduction of Nahm data with SU(2) case. The asymptotic Higgs field along the z-direction can be chosen as $\Phi_\infty = \mathrm{diag}(-1, 1)$. The Nahm data of an N-monopole solution are a triplet $\mathbf{T}$ satisfying the following conditions:

1. $\mathbf{T}$ is a triplet of analytic $u(N)$-valued functions satisfing Nahm's equations (2.71) in the interval $(-1, 1)$.

2. The residues of $\mathbf{T}$ at $t = \mp 1$ form an N-dimensional irreducible representation of $su(2)$.

3. $\mathbf{T}(-t)^T = \mathbf{T}(t)$.

The discussion on Nahm data of SU(2) monopoles has been generalized into gauge theories based on all types of classical groups [36, 37]. Let's first talk about the SU(N) case since all other groups will be treated by embedding them into SU(N). Assuming the asymptotic Higgs field along the z-direction is $\Phi_\infty = \mathrm{diag}(\mu_1, \cdots, \mu_N)$ with $\mu_1 < \cdots < \mu_N$, then the Nahm data for monopoles carrying charges $(m_1, \cdots, m_{N-1})$ are defined as $N-1$ triples ${}^l\mathbf{T} = ({}^lT_1, {}^lT_2, {}^lT_3)$ $(l = 1, \cdots, N-1)$ satisfying:

1. For each l, ${}^l\mathbf{T}$ are triplets of analytic $u(m_l)$-valued functions satisfying Nahm's equations in the interval (μ_l, μ_{l+1}), $l = 1, \cdots, N-1$.

2. The boundary conditions relating the Nahm data in two adjoint intervals are the following:

   (a) If $m_l < m_{l-1}$, then there exists a non-singular limit, $\lim_{t\to\mu_l^+} {}^l\mathbf{T} = {}^l\mathbf{S}$ and the structure of ${}^{l-1}\mathbf{T}$ near $t = \mu_l$ is

   $$\lim_{t\to\mu_l^-} {}^{l-1}\mathbf{T} = \begin{pmatrix} \frac{{}^{l-1}\mathbf{R}}{t-\mu_l} & * \\ * & {}^l\mathbf{S} \end{pmatrix}, \tag{2.72}$$

   where ${}^{l-1}\mathbf{R}$ form a triplet of $(m_{l-1} - m_l)$-dimensional irreducible representation of $su(2)$ (unless $m_{l-1} - m_l = 1$ in which case

${}^{l-1}\mathbf{R}/(t-\mu_l)$ has to be replaced by a non-singular expression), and "$*$" refers to the finite elements that are not restricted by boundary conditions.

(b) If $m_l > m_{l-1}$, the roles of (μ_{l-1}, μ_l) and (μ_l, μ_{l+1}) are reversed.

(c) If $m_l = m_{l-1}$, both limits $\lim_{t\to\mu_l^-} {}^{l-1}\mathbf{T}$ and $\lim_{t\to\mu_l^+} {}^{l}\mathbf{T}$ exist (and are non-singular). Let $\Delta\mathbf{T}$ be the difference of the two limits (the index l is omited for simplicity). Then the expression

$$S(\zeta) \equiv (\Delta T_2 + i\Delta T_3) + 2i\Delta T_1\zeta + (\Delta T_2 - i\Delta T_3)\zeta^2 \qquad (2.73)$$

is of rank at most one for all complex number ζ.

The way to embed the gauge groups $\mathrm{SO}(N)$ and $\mathrm{Sp}(N)$ into $\mathrm{SU}(N)$ are obtained by constraining the $\mathrm{SU}(N)$ generators further. The generators T of $\mathrm{Sp}(N)$ satisfy the condition $T^TJ + JT = 0$ with $JJ^* = -I$. The explicit form of J is representation dependent. A typical choice is

$$J = \begin{pmatrix} 0 & I \\ -I & 0 \end{pmatrix}. \qquad (2.74)$$

The generators T of $\mathrm{SO}(N)$ satisfy the condition $T^T + T = 0$.

The embedding procedures establish a relation between the $\mathrm{SO}(N)$, $\mathrm{Sp}(N)$ Nahm data with magnetic charge $(\rho_1, ..., \rho_{[N/2]})$ and the $\mathrm{SU}(N)$ Nahm data with asymptotic Higgs field $\Phi_\infty = \mathrm{diag}(\mu_1, ..., \mu_N)$ and magnetic charge $(m_1, ..., m_{N-1})$.

The embedding procedures are described in Table 1.

G	G-charge	ϕ_∞ in SU(N)	SU(N)-charge
Sp(N) $N = 2n$	$\rho_1, \cdots, \rho_n$	$\mu_l = -\mu_{2n+1-l}$ $l = 1, \cdots, n$	$m_l = m_{2n-l} = \rho_l$ $l = 1, \cdots, n$
SO(N) $N = 2n$	$\rho_1, \cdots, \rho_{n-2}$ ρ_+, ρ_-	$\mu_l = -\mu_{2n+1-l}$ $l = 1, \cdots, n$	$m_l = m_{2n-l} = \rho_l$ $l = 1, \cdots, n-2$ $m_{n-1} = m_{n+1} = \rho_+ + \rho_-$ $m_n = 2\rho_+$
SO(N) $N = 2n+1$	$\rho_1, \cdots, \rho_n$	$\mu_l = -\mu_{2n+2-l}$ $l = 1, \cdots, n+1$	$m_l = m_{2n+1-l} = \rho_l$ $l = 1, \cdots, n-1$ $m_n = m_{n+1} = 2\rho_n$

Table 1: The embedding of Sp(N), SO(N) in SU(N).

What is different is that we now have one more set of conditions connecting the Nahm data between different intervals:

3. There exist matrices ${}^lC$ $(l = 1, \cdots, N-1)$ satisfying

$$ {}^{N-l}\mathbf{T}(-t)^T = ({}^lC)\, {}^l\mathbf{T}(t)\, ({}^lC^{-1}), \tag{2.75} $$

and compatibility conditions:

(a) ${}^{N-l}C = {}^lC^T$ for Sp(N),

(b) ${}^{N-l}C = -{}^lC^T$ for SO(N).

These compatibility conditions reflect the fact that we are identifying certain SU(N) monopoles to get SO(N) and Sp(N) monopoles.

In the above discussions we have assumed $\mu_1 < \cdots < \mu_n$, which physically means that the gauge symmetry is maximally broken. We can also consider the cases with non-Abelian unbroken symmetry so that some μ_l's are equal. Geometrically, this is the case when some of the intervals shrink to zero length. Since the monopoles associated with the unbroken symmetry are massless, the shrunken intervals correspond to massless monopoles. All the procedures described above are applicable to this case.

In the following subsections, we will discuss various applications of Nahm data.

2.3.2 ADHMN construction

The ADHMN (Atiyah-Drinfeld-Hitchin-Mannin-Nahm) construction of self-dual configurations of Yang-Mills equations on R^3 is an analogy of the usual ADHM construction of instantons (which gives the self-dual configurations of Yang-Mills equations on R^4).

Let's first consider the case when $m_l \neq m_{l-1}$ is held for all the intervals. In each interval (μ_l, μ_{l+1}), given Nahm data ${}^l\mathbf{T}$, we can define a differential operator ${}^l\triangle^\dagger$

$$ {}^l\triangle^\dagger(\mathbf{x}) = i\frac{d}{dt} + (\mathbf{x} + {}^l\mathbf{T}) \otimes \mathbf{e} + x_4, \tag{2.76} $$

where $\mathbf{e} = (e_1, e_2, e_3)$ form a quaternion basis. We have included the fourth coordinate x_4 which will be used when we discuss calorons, for the rest part

of this thesis, x_4 can be chosen as zero. Let ${}^l v$ be a vector in the Kernal of ${}^l\triangle^\dagger$, namely

$$ {}^l \triangle^\dagger {}^l v = 0 \tag{2.77}$$

and satisfing the following boundary conditions between any two adjacent intervals:

1. If $m_l < m_{l-1}$, then the $2m_l$ components of $\lim_{t\to\mu_l^+} {}^l v$ are equal to $2m_l$ of the $2m_{l-1}$ components of $\lim_{t\to\mu_l^-} {}^{l-1} v$. Those $2m_l$ components of $\lim_{t\to\mu_l^-} {}^{l-1} v$ are called continuing components and are exactly those that correspond to the continuing block of $\lim_{t\to\mu_l^-} {}^{l-1}\mathbf{T}$ in Eq. (2.72). The other components of $\lim_{t\to\mu_l^-} {}^{l-1} v$ are called terminating components.

2. If $m_l > m_{l-1}$, the roles of (μ_{l-1}, μ_l) and (μ_l, μ_{l+1}) are reversed.

With these conditions imposed, it turns out that for SU(N) theory, there exist exactly N sets of solutions $\{{}^l v_i\}$ $(i = 1, ..., N)$. Let's combine all ${}^l v_i$ with fixed l to a $2m_l \times N$ matrix V_l, and normalize V_l by

$$\sum_{l=1}^{N-1} \int_{\mu_l}^{\mu_{l+1}} dt \;\; V_l^\dagger V_l = I. \tag{2.78}$$

Then the field configurations of the corresponding monopole solutions in R^3 are given by:

$$\Phi = -\sum_{l=1}^{N-1} \int_{\mu_l}^{\mu_{l+1}} dt \;\; t V_l^\dagger V_l, \tag{2.79}$$

$$A_j = i \sum_{l=1}^{N-1} \int_{\mu_l}^{\mu_{l+1}} dt \;\; V_l^\dagger \partial_j V_l. \tag{2.80}$$

This method is called ADHMN construction. It is sometimes convenient to replace V_l by $\exp(itx_4)V_l$. Eqs. (2.79) and (2.80) can then be combined as

$$A_m = i \sum_{l=1}^{N-1} \int_{\mu_l}^{\mu_{l+1}} dt \;\; V_l^\dagger \partial_m V_l. \tag{2.81}$$

Finally let's turn to the case when there are boundary points p on which $m_p = m_{p-1}$. As we mentioned in last subsection, the Nahm data will have a discontinuity $\Delta^p \mathbf{T}$ on such point, or equivalently Nahm's equations (2.71) will be modified as

$$\frac{dT_i}{dt} - i[T_4, T_i] - \frac{1}{2} i\epsilon_{ijk}[T_j, T_k] = \sum_p \Delta^p T_i \delta(t - t_p). \tag{2.82}$$

Because of condition 2(c) described in last subsection, it is proved that there exists a $2m_p$-component row vector a_p satisfying

$$a_p^\dagger a_p = i\Delta^p \mathbf{T} \cdot \mathbf{e} \;(\mathrm{mod}\; I), \tag{2.83}$$

where mod I means that the equality holds up to a term that is proportional to the identity. The boundary condition for V_p turns out to be

$$V_p - V_{p-1} = a_p^\dagger S_p, \tag{2.84}$$

where S_p is an N-component row vector. The normalization condition (2.78) is accordingly replaced by

$$\sum_{l=1}^{N-1} \int_{\mu_l}^{\mu_{l+1}} dt \;\; V_l^\dagger V_l + \sum_p S_p^\dagger S_p = I. \tag{2.85}$$

The field configuration in this case is given by (the factor $\exp(itx_4)$ is introduced to both V_l and S_p)

$$A_m = i\sum_{l=1}^{N-1}\int_{\mu_l}^{\mu_{l+1}} dt\ \ V_l^\dagger \partial_m V_l + i\sum_p S_p^\dagger \partial_m S_p, \tag{2.86}$$

or equivalently

$$\begin{aligned} A_m &= \frac{i}{2}\sum_{l=1}^{N-1}\int_{\mu_l}^{\mu_{l+1}} dt\ \left[V_l^\dagger \partial_m V_l - (\partial_m V_l^\dagger)V_l\right] \\ &\quad + \frac{i}{2}\sum_p \left[S_p^\dagger \partial_m S_p - (\partial_m S_p^\dagger)S_p\right]. \end{aligned} \tag{2.87}$$

2.3.3 Nahm's formalism for the moduli space metric

As was mentioned before, it is believed and in certain cases proved, that the moduli space of BPS monopoles and Nahm data are isometric, so that the metric of the monopole moduli space can be obtained by computing the metric of the moduli space of the corresponding Nahm data.

Since in this thesis we will only consider the moduli space metric of an Sp(4) system in which effectively only one interval [–1, 1] contributes, in what follows we will restrict our discussion to such situations. For more general cases, the idea is similar, but the boundary conditions concerning adjacent intervals make things significantly more difficult.

As in the case of the monopole moduli space, we need to define tangent vectors, which we call Y_m. These tangent vectors should satisfy the linearized

Nahm's equations

$$\dot{Y}_i - i[Y_4, T_i] - i[T_4, Y_i] - i\epsilon_{ijk}[T_j, Y_k] = 0, \tag{2.88}$$

and should be orthogonal to infinitesimal gauge transformations of Nahm data, namely

$$\langle Y_m, \delta_g T_m \rangle = 0, \tag{2.89}$$

where the natural inner product in the space of Nahm data is defined as

$$\langle T_m, T'_n \rangle \equiv \int dt \ \mathrm{tr}(T_m T'_n). \tag{2.90}$$

The infinitesimal gauge transformations of Nahm data are given by

$$\delta_g T_m = D_m \Lambda(t) \tag{2.91}$$

with $D_m = \partial_m - iT_m = (-i\mathbf{T}, \partial_t - iT_4)$ and Λ vanishes at the boundary points. Putting these into Eq. (2.89) one obtains

$$\dot{Y}_4 - i[T_m, Y_m] = 0. \tag{2.92}$$

We also need to remember that tangent vectors should also satisfy the symmetry condition (2.75). Once tangent vectors are solved from Eqs. (2.88) and (2.92), the metric can be evaluated as

$$ds^2(\mathbf{Y}, \mathbf{Y}) \equiv \langle Y_m, Y_m \rangle \tag{2.93}$$

2.3.4 Energy density

Recently Nahm's formalism has been generalized to deal with calorons [41, 42, 43, 46, 47]. In those works, a convenient method of computing the energy density of monopole systems was developed. We will use some of the results of those works.

Consider the SU(N) Yang-Mills-Higgs system with asymptotic Higgs field (or A_4 in Euclidean formalism) $\Phi_\infty = \mathrm{diag}(\mu_1, ..., \mu_N)$ (assume $\mu_1 \leq \cdots \leq \mu_N$). The Nahm data for the caloron that carries instanton number k are defined over intervals (μ_1, μ_2),..., (μ_{N-1}, μ_N), $(\mu_N, \mu_1 + 2\pi/\beta)$ (where β is the circumference along the S^1 direction in space $R^3 \times S^1$) with points μ_1 and $\mu_1 + 2\pi/\beta$ being identified. In each interval the Nahm data are a triplet of $k \times k$ Hermitian matrix functions $\mathbf{T}(t)$ determined by Nahm's equations and the boundary conditions. In this thesis we will only use the energy density formula in the case with $k = 1$ for which $-\mathbf{T}$ in each interval is a triplet of constants representing the positions of the corresponding constituent monopoles. It is known that the action density of instantons (in the usual ADHM method) is given by (the index "s" refers to the action S)

$$\rho_s = \mathrm{tr} F_{\mu\nu}^2 = \Box\Box \log\det f, \tag{2.94}$$

where f is the inverse operator (whose matrix elements form Green's function) of $\triangle^\dagger\triangle$ ($\triangle$ is the usual ADHM matrix), and $\Box$ refers to the four

dimensional Laplacian. This differs from [13, 67] by a sign since we choose $F_{\mu\nu}$ to be Hermitian rather than anti-Hermitian. For SU(N) calorons the same formula (2.94) has been established using a Fourier transformation of the original ADHM method and the following formula has been found for the Green's function $f(t,t') = \langle t|f|t'\rangle$ [41, 42, 43, 46, 47]:

$$\left[-\frac{d^2}{dt^2} + |\mathbf{x} + \mathbf{T}(t)|^2 + \sum_i |\mathbf{T}_i - \mathbf{T}_{i-1}|\delta(t-\mu_i)\right] f(t,t') = \delta(t-t'), \quad (2.95)$$

where the sum is taken over all the boundary points between adjacent intervals.

From these results it is not difficult to get the Green's function for magnetic monopoles instead of calorons. Notice that in the constituent monopole picture of calorons (see [46] and chapter 5 for details), an additional type of monopole has been introduced to neutralize the magnetic charge, so the usual multi-monopole Green's function can be obtained by moving that monopole to spatial infinity. This leads to the following natural boundary conditions

$$f(\mu_1, t') = f(\mu_N, t') = 0. \quad (2.96)$$

On the other hand, for purely magnetic configurations, $\mathbf{E} = 0$, the energy density is given by (a factor of $1/2$ is omitted for simplicity)

$$\rho = \rho_s = \Box\Box \log\det f. \quad (2.97)$$

For later convenience, it is useful to explore Eq. (2.97) a little bit further. Notice that for an operator f,

$$\log\det f = \mathrm{tr}\log f = -\mathrm{tr}\left[\sum_{n=1}^{\infty}\frac{(1-f)^n}{n}\right], \tag{2.98}$$

therefore $(i = 1, 2, 3)$

$$\partial_i \log\det f = \mathrm{tr}\left\{\left[\sum_{n=0}^{\infty}(1-f)^n\right]\partial_i f\right\} = \mathrm{tr}(f^{-1}\partial_i f). \tag{2.99}$$

Further notice that $f = (\triangle^\dagger\triangle)^{-1}$ with $\triangle^\dagger = i\partial_t - i(\mathbf{x} - \mathbf{T})\cdot\boldsymbol{\sigma}$ being the Nahm's construction operator (we choose the quaternion basis to be $\mathbf{e} = -i\boldsymbol{\sigma}$), so

$$\begin{aligned}
\mathrm{tr}(f^{-1}\partial_i f) &= \mathrm{tr}(\triangle^\dagger \triangle\, \partial_i f) \\
&= \mathrm{tr}[\partial_i(\triangle^\dagger \triangle\, f) - f\partial_i(\triangle^\dagger\triangle)] \\
&= -\sum_j\left[\int dt' f(t',t')\partial_i|\mathbf{x}+\mathbf{T}_j|^2\right] \\
&= -\sum_j\left[\partial_i|\mathbf{x}+\mathbf{T}_j|^2\int dt' f(t',t')\right]
\end{aligned} \tag{2.100}$$

So finally we obtain a formula that is more suitable for computations:

$$\partial_i \log\det f = -\sum_j\left[\partial_i|\mathbf{x}+\mathbf{T}_j|^2\int dt' f(t',t')\right] \tag{2.101}$$

where $\partial_i|\mathbf{x}+\mathbf{T}_j|^2$ has been moved out from the integration since in each interval it does not depend on t' (for the $k = 1$ case only). Equation (2.101) together with Eqs. (2.95) – (2.97) (in Eq. (2.97) use the three dimensional

Laplacian $\triangle$ in place of $\Box$) form a framework that will be used to compute the energy density of monopole systems considered in this paper.

Chapter 3

Two Massive and One Massless Sp(4) Monopoles

3.1 Introduction

In this chapter we will consider the Sp(4) ($\cong$ SO(5)) gauge theory with gauge symmetry broken to SU(2)×U(1). The asymptotic Higgs expectation value is chosen to be along one of the short roots (see Figure 3.1 in section 3.2). For the reasons discussed in chapter 2, we will investigate an Abelian configuration, i.e. the total magnetic charge of the configuration is Abelian. The simplest such configuration is made of two identical massive monopoles (associated to a long root) and one massless monopole (associated to a short root).

In this chapter we will use Nahm's formalism to study the Higgs configurations of such monopole systems with spherical and axial symmetries. The main result in this chapter will be the complete moduli space metric of the

system.

As was mentioned in chapter 2, both configurations and moduli space metrics of multi-monopole systems are very hard to obtain. So far, only a limited set of results are known. For instance (and for later reference) the major known moduli space metrics are the following:

1. Atiyah-Hitchin metric [4]:

$$ds^2 = (abc)^2 d\eta^2 + a^2\sigma_1^2 + b^2\sigma_2^2 + c^2\sigma_3^2, \tag{3.1}$$

where a, b, c are defined by

$$\begin{aligned} ab &= -2k(1-k^2)\mathrm{K}\frac{d\mathrm{K}}{dk} \\ bc &= ab - 2(1-k^2)\mathrm{K}^2 \\ ca &= ab + 2k^2\mathrm{K}^2 \end{aligned} \tag{3.2}$$

with

$$\mathrm{K}(k) = \int_0^{\pi/2} d\theta (1 - k^2\sin^2\theta)^{-1/2} \tag{3.3}$$

being the first complete elliptic integral. This is the exact metric for two (identical) SU(2) monopoles. It can be shown that $k \to 1$ is the large distance limit in which the distance between the two monopoles is roughly given by $r \sim -\ln\sqrt{1-k^2}$. The Atiyah-Hitchin metric is the first known nontrivial monopole moduli space metric.

2. Gibbons-Manton metric [25, 55]:

$$ds^2 = \frac{1}{2} M_{ab} d\mathbf{r}_a \cdot d\mathbf{r}_b + \frac{1}{2}(M^{-1})_{ab}(d\psi_a + \mathbf{W}_{ac} \cdot d\mathbf{r}_c)(d\psi_b + \mathbf{W}_{bd} \cdot d\mathbf{r}_d), \quad (3.4)$$

where $\mathbf{r}_a$ denotes the position of the a'th monopole (associated to root $\boldsymbol{\alpha}_a$), M_{ab} and $\mathbf{W}_{ab}$ are defined as follows ($r_{ab} = |\mathbf{r}_a - \mathbf{r}_b|$):

$$M_{aa} = m_a - \sum_{b \neq a} \frac{\boldsymbol{\alpha}_a^* \cdot \boldsymbol{\alpha}_b^*}{r_{ab}}, \quad (3.5)$$

$$M_{ab} = \frac{\boldsymbol{\alpha}_a^* \cdot \boldsymbol{\alpha}_b^*}{r_{ab}} \quad (a \neq b), \quad (3.6)$$

$$\mathbf{W}_{aa} = -\sum_{b \neq a} \boldsymbol{\alpha}_a^* \cdot \boldsymbol{\alpha}_b^* \, \mathbf{w}_{ab}, \quad (3.7)$$

$$\mathbf{W}_{ab} = \boldsymbol{\alpha}_a^* \cdot \boldsymbol{\alpha}_b^* \, \mathbf{w}_{ab} \quad (a \neq b), \quad (3.8)$$

with $\mathbf{w}_{ab}$, satisfying

$$\nabla_a \times \mathbf{w}_{ab}(\mathbf{r}_b - \mathbf{r}_a) = \frac{\mathbf{r}_b - \mathbf{r}_a}{r_{ab}}, \quad (3.9)$$

being the Dirac monopole potential. This is the approximate metric for widely separated monopoles of arbitrary types in arbitrary gauge theories. It is known that this metric can't be the exact form since it evolves singularities when monopoles approach each other. Although the Gibbons-Manton metric is not an exact metric, because of its generality, it is still one of the most important results of monopole moduli space metrics and is often used to test the asymptotic behavior of other metrics.

3. Dancer metric [14, 15, 16, 17, 38]: This is the exact metric for two massive and one massless monopoles in SU(3) gauge theory with symmetry breaking pattern SU(3)→SU(2)×U(1). Since this metric is fairly similar to what we will discuss, we won't bother writing it down here.

4. Lee-Weinberg-Yi metric [49, 51]: This exact moduli space metric is based on the observation that when applied to *distinct fundamental monopoles*, the Gibbons-Manton metric becomes smooth everywhere. Since Gibbons-Manton metric has the required hyperKähler structure, it was conjectured to be the exact metric for distinct fundamental monopoles. This conjecture was first proved for the SU(3) case with two fundamental monopoles [12, 22], and later on strongly supported by the computations based on Nahm's formalism for more general cases [9, 56].

We will extend this list by providing an exact metric of Dancer's type for Sp(4) gauge theory. We will then check various aspects of the metric and compare it with known metrics under various limits.

The moduli space of a monopole system containing a massless monopole was first studied in [50] for Sp(4) theory. What makes it different from the situation we are going to discuss is that in that case the asymptotic Higgs field lies along one of the long roots. Thus the simplest Abelian configuration

is made of one massive and one massless monopole. Since this is the massless limit of the case with two distinct fundamental Sp(4) monopoles, the metric can be obtained as the massless limit of the corresponding Lee-Weinberg-Yi metric. The configuration of such a monopole system is spherically symmetric and is also known [78]. This is actually one of the models on the basis of which the non-Abelian cloud picture of massless monopole was developed.

The next nontrivial purely Abelian configurations are made of two massive and one massless monopoles in an SU(4) theory with the symmetry breaking pattern $SU(4) \to U(1) \times SU(2) \times U(1)$. All the three monopoles are fundamental and distinct from each other. This is again the case where Lee-Weinberg-Yi metric can be directly applied. The metric for this case is sometimes called Taubian-Calabi metric [24, 71].

The real challenge comes when Lee-Weinberg-Yi metric is not applicable, namely when there are identical monopoles. The simplest such case arises in SU(3) (Dancer's case), Sp(4) (to be discussed in this chapter) and G_2 (yet to be explored) theories with gauge symmetries broken to $SU(2) \times U(1)$. The simplest Abelian configurations of these theories are all made of two (identical) massive monopoles and one massless monopole.

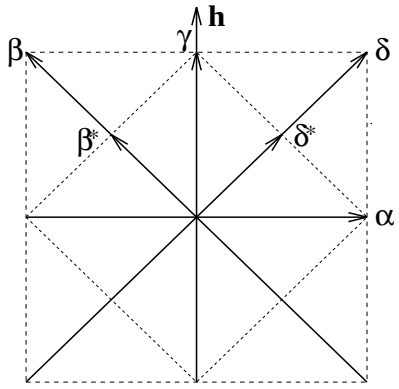

Figure 3.1: Root diagram of Sp(4) theory. $\boldsymbol{\beta}^*$ and $\boldsymbol{\delta}^*$ are co-roots, $\boldsymbol{\alpha}$ and $\boldsymbol{\gamma}$ are identical to their co-roots.

3.2 Nahm Data in the Sp(4) Case

3.2.1 The embedding procedure

The roots and co-roots of the Sp(4) group is shown in Figure 3.1. In our conventions the root $\boldsymbol{\alpha}$ has unit length, so $\boldsymbol{\alpha}^* = \boldsymbol{\alpha}$. The asymptotic Higgs field is given by $\Phi_\infty = \mathbf{h} \cdot \mathbf{H}$ which makes the $\boldsymbol{\alpha}$ monopole massless. The Abelian configuration carries total magnetic charge

$$\boldsymbol{\gamma}^* = 2\boldsymbol{\beta}^* + \boldsymbol{\alpha}^*, \tag{3.10}$$

which is orthogonal to the unbroken root $\boldsymbol{\alpha}$ and is invariant under the unbroken SU(2) symmetry generated by $\boldsymbol{\alpha}$.

As discussed in chapter 2, the Nahm data for the Sp(4) theory can be studied by embedding Sp(4) in SU(4). The Higgs field can be written as a 4×4 traceless Hermitian matrix. As shown in Table 1 in chapter 2, the Higgs

expectation value has the form $\Phi_\infty = \mathrm{diag}(-\mu_1, -\mu_2, \mu_2, \mu_1)$ with $\mu_1 \geq \mu_2 \geq 0$. Any generator T of the Sp(4) subgroup should be traceless, hermitian and satisfy

$$TJ + JT^T = 0, \tag{3.11}$$

where the Sp(4) invariant tensor J is chosen to be

$$J = \begin{pmatrix} 0 & 0 & 0 & 1 \\ 0 & 0 & 1 & 0 \\ 0 & -1 & 0 & 0 \\ -1 & 0 & 0 & 0 \end{pmatrix}. \tag{3.12}$$

This uniquely defines the Sp(4) embedding in SU(4) in consistent with Table 1. A consistent choice of the Cartan subalgebra of sp(4) can be found as $H_1 = \mathrm{diag}(-1, 1, -1, 1)/2$ and $H_2 = \mathrm{diag}(-1, -1, 1, 1)/2$. The symmetry breaking pattern for Sp(4)$\rightarrow$ SU(2)$\times$ U(1) shown in Figure 3.1 corresponds to $\mathbf{h}\cdot\mathbf{H} = 2H_2 = \mathrm{diag}(-1, -1, 1, 1)$ (an overall scale of Higgs field is irrelevant to us and is fixed by choosing $|\mathbf{h}| = 2$), namely $\mu_1 = \mu_2 = 1$. From the point of view of the SU(4) theory, this corresponds to the case where the SU(4) symmetry is broken to SU(2)$\times$U(1)$\times$SU(2).

From Table 1 in chapter 2, it can be found that the Sp(4) configuration given by (3.10) has the SU(4) magnetic charge $(1, 2, 1)$, that is, two identical massive monopoles and two distinct massless monopoles. It is clear that the two distinct massless SU(4) monopoles must be identified. This is realized by the compatibility condition (2.75), namely (we will keep T_4 for a while in

order to discuss the symmetries of Nahm data)

$$T_m(-t)^T = CT_mC^{-1} \tag{3.13}$$

with a symmetric matrix C for the middle interval (C will be computed soon). Since there are two shrunken intervals with charge 1 at $t = \pm 1$, the boundary conditions (2.72) requires the Nahm data to be analytic at $t = \pm 1$. The boundary condition (2.72) together with the compatibility condition (3.13) for the shunken intervals leads to

$$(T_m(-1))_{22} = (T_m(1))_{22}. \tag{3.14}$$

As we will see, this boundary value of the Nahm data is related to the position of the massless monopole in the center of mass frame.

3.2.2 Sp(4) Nahm data and the symmetries and submanifolds of their moduli space

The moduli space of Nahm data admits the following symmetries:

1. The local gauge transformations $G = \{g(t) \in U(2)\}$ whose actions on the Nahm data are defined as

$$T_i \rightarrow gT_ig^\dagger, \tag{3.15}$$

$$T_4 \rightarrow gT_4g^\dagger + ig\frac{d}{dt}g^\dagger \tag{3.16}$$

and are consistent with conditions (3.13) and (3.14). In order for the transformation to be non-trivial in moduli space, we should factor out the small gauge transformations, namely the subgroup $G_0^0 = \{g \in G : g(-1) = g(1) = 1\}$. Therefore the gauge symmetry in the moduli space of Nahm data is $G_0 = G/G_0^0 \cong U(2)$.

2. The spatial translation group R^3 with parameters λ_j whose actions on the Nahm data are defined as

$$T_j \to T_j - i\lambda_j I, \tag{3.17}$$

$$T_4 \to T_4. \tag{3.18}$$

3. The spatial rotation group SO(3)=$\{a_{ij} \in \mathrm{SO}(3)\}$ whose actions on the Nahm data are defined as

$$T_i \to \sum_j a_{ij} T_j, \tag{3.19}$$

$$T_4 \to T_4. \tag{3.20}$$

Notice that, unlike Dancer's case [15] in which spatial rotations are accompanied by gauge compensations , Eq. (3.19) is a pure rotation as there are no residues to be fixed at $t = \pm 1$.

To solve Nahm's equations together with the compatibility and boundary conditions, we choose the gauge such that $T_4 = 0$. We then apply a spatial

translation to make T_i traceless. These traceless Nahm data are called centered Nahm data. They describe monopole configurations in the center of mass frame. We will see in a moment that an equivalent way to introduce centered Nahm data is to perform a hyperKähler quotient based on the U(1) center of the gauge symmetry. We can further apply spatial rotations to eliminate the t-independent quantities $\mathrm{tr}(T_1T_2)$, $\mathrm{tr}(T_1T_3)$ and $\mathrm{tr}(T_2T_3)$. So finally we get that, for each $j = 1, 2, 3$

$$T_j = -\frac{i}{2} f_j e_j. \tag{3.21}$$

The e_j are quaternion units and will be chosen as

$$e_1 = i\sigma_1,\ e_2 = i\sigma_3,\ e_3 = i\sigma_2 \tag{3.22}$$

in order to keep a close notational similarity with Dancer's case. With the ansatz (3.21), Nahm's equations become the well-known Euler top equations:

$$\begin{aligned} \dot{f}_1 &= f_2 f_3, \\ \dot{f}_2 &= f_3 f_1, \\ \dot{f}_3 &= f_1 f_2. \end{aligned} \tag{3.23}$$

We note that $f_1^2 - f_2^2$ and $f_2^2 - f_3^2$ are independent of t. Without losing generality, we assume $f_1^2 \leq f_2^2 \leq f_3^2$. Then the solution to this set of equations is known in terms of Jacobi elliptic functions as

$$f_1 \quad = \quad -\frac{D\mathrm{cn}_k[D(t-t_0)]}{\mathrm{sn}_k[D(t-t_0)]},$$

$$\begin{aligned} f_2 &= -\frac{D\mathrm{dn}_k[D(t-t_0)]}{\mathrm{sn}_k[D(t-t_0)]}, \\ f_3 &= -\frac{D}{\mathrm{sn}_k[D(t-t_0)]}, \end{aligned} \tag{3.24}$$

where $k \in [0,1]$ is the elliptic modulus and D and t_0 are arbitrary constants. We can change the sign of any two of f_1, f_2 and f_3 by a spatial rotation by π which means that the Nahm data have $\mathrm{Z}_2 \times \mathrm{Z}_2$ isotropy group.

On the other hand, the compatibility condition (3.13) becomes

$$f_j(-t)e_j^T = f_j(t)Ce_jC^{-1} \tag{3.25}$$

with a symmetric matrix C. The boundary condition (3.14) becomes

$$f_2(-1) = f_2(1). \tag{3.26}$$

Among linear combinations of σ_1 and σ_3, the right choice of C with the Nahm data (3.21) turns out to be

$$C = \sigma_3. \tag{3.27}$$

This implies that f_1 is an odd function and f_2, f_3 are even functions, which requires that the parameter t_0 satisfies $\mathrm{cn}_k(Dt_0) = 0$. Taking into account all these conditions, the solution for Nahm's equations can now be re-written as

$$\begin{aligned} f_1 &= D\sqrt{1-k^2}\frac{\mathrm{sn}_k(Dt)}{\mathrm{cn}_k(Dt)}, \\ f_2 &= -D\sqrt{1-k^2}\frac{1}{\mathrm{cn}_k(Dt)}, \\ f_3 &= -D\frac{\mathrm{dn}_k(Dt)}{\mathrm{cn}_k(Dt)}. \end{aligned} \tag{3.28}$$

These Nahm data are regular for $t \in [-1, 1]$. The analyticity of the Nahm data requires that $0 \leq k \leq 1$ and $0 \leq D \leq \mathrm{K}(k)$, with $4\mathrm{K}(k)$ being the period of sn_k. $\mathrm{K}(k)$ is the first complete elliptic integral defined by Eq. (3.3). Eqs. (3.21) and (3.28) are the Nahm data we are looking for. More precisely, they are the Nahm data on a representative point of the $\mathrm{SO}(3)\times\mathrm{SO}(3)$ orbit[1]. Sometimes we will simply call Eq. (3.28) as Nahm data.

Another thing to notice is that there are eight equivalent copies of the above Nahm data: we can rotate f_1, f_2 and f_3 to be f_2, f_3 and f_1 (the 2nd function must be even as required by the boundary condition), or change the signs of any two of f_1, f_2 and f_3.

With Eq. (3.27) and the fact that f_1 is odd and f_2 and f_3 are even, the allowed gauge transformations of Eq. (3.15) that preserve the boundary and compatibility conditions are given by $g(t)$ such that

$$g(t) = e^{\epsilon_j(t)e_j/2} \tag{3.29}$$

with even ϵ_1 and odd ϵ_2 and ϵ_3 functions. As we will see, the oddness of ϵ_2 and ϵ_3 is crucial in showing that the spherically symmetric Nahm data are not invariant under global gauge transformations.

[1]The gauge symmetry is effectively SO(3) rather than SU(2) since under gauge transformations generated by $\boldsymbol{\alpha}$, roots $\boldsymbol{\beta}, \boldsymbol{\gamma}, \boldsymbol{\delta}$ form a triplet rather than doublet in the fundamental representation. Another way to see this is to notice that $\exp(2\pi i t^a(\boldsymbol{\alpha})) = \mathrm{diag}(-1,-1,-1,-1) \in \mathrm{Sp}(4)$ whose action is identical to I

Our monopole system is made of three monopoles, so the moduli space is twelve dimensional. We denote it as M^{12}. As mentioned before, M^{12} admits a gauge action $G_0 \cong \mathrm{U}(2)$. Since the U(1) center of G_0 is tri-holomorphic, we can construct a moment map (see appendix A for details)

$$\boldsymbol{\mu} = (\mathrm{tr}T_1, \mathrm{tr}T_2, \mathrm{tr}T_3). \tag{3.30}$$

Since $\boldsymbol{\mu}$ is invariant under the U(1) center, it leads to a hyperKähler quotient $\boldsymbol{\mu}^{-1}(0)/\mathrm{U}(1)$ that gives an eight dimensional hyperKähler space representing centered Nahm data[2]. This is called the relative moduli space and is denoted as M^8. Performing an ordinary group quotient on this manifold by the internal gauge symmetry SO(3) leads to a five dimensional manifold $N^5 = M^8/\mathrm{SO}(3)$. The coordinates for N^5 are chosen as the following gauge-invariant t-independent quantities [15, 16]:

$$\begin{aligned}
\lambda_1 &= \langle T_1, T_1\rangle - \langle T_2, T_2\rangle, \\
\lambda_2 &= \langle T_1, T_1\rangle - \langle T_3, T_3\rangle, \\
\lambda_3 &= \langle T_1, T_2\rangle, \\
\lambda_4 &= \langle T_1, T_3\rangle, \\
\lambda_5 &= \langle T_2, T_3\rangle,
\end{aligned} \tag{3.31}$$

[2]More generally, $\boldsymbol{\mu}^{-1}(\mathbf{x})/\mathrm{U}(1)$ represents the space of solution with center of mass at x.

where the inner product of Nahm data is defined by

$$< T, T' >= \int_{-1}^{1} dt \, \mathrm{tr}(TT'). \tag{3.32}$$

A further quotient of N^5 by the spatial rotation group SO(3) leads to a two dimensional surface $N^5/\mathrm{SO}(3)$, eight copies of which, as will be described in section 3.4, form a geodesically complete manifold $\mathcal{Y}^2$. We will also discuss some two-dimensional surfaces of revolution that describe axially symmetric configurations. The Nahm data (3.28) are the data on $\mathcal{Y}^2$ which lead to the coordinates

$$\begin{aligned} \lambda_1 &= -(1-k^2)D^2, \\ \lambda_2 &= -D^2, \\ \lambda_3 &= \lambda_4 = \lambda_5 = 0. \end{aligned} \tag{3.33}$$

Since the gauge group SO(3) is tri-holomorphic, instead of performing the ordinary group quotient there is another hyperKähler quotient of M^8 based on a U(1) subgroup of the gauge symmetry. With our choice of the boundary condition (3.14) and quaternion units (3.22), a convenient choice of this U(1) subgroup is the one generated by σ_3 (other choices are gauge equivalent to this choice). This U(1) group acts on M^8 freely (namely the isotropy group only contains the identity) because the corresponding gauge parameter ϵ_2 (since

σ_3 corresponds to e_2) in Eq. (3.29) is an odd function[3]. The corresponding moment map is (the coefficient 1/2 is chosen for convenience)

$$\begin{aligned} \boldsymbol{\mu} &= \frac{1}{2}\{\mathrm{tr}[T_1(1)\sigma_3], \mathrm{tr}[T_2(1)\sigma_3], \mathrm{tr}[T_3(1)\sigma_3]\} \\ &= (\zeta_1, \zeta_2, \zeta_3), \end{aligned} \tag{3.34}$$

ence (since T_i's are traceless),

$$\zeta_i = -[T_i(1)]_{22}, \tag{3.35}$$

and can be interpreted as the position of the massless monopole (the minus sign reflects the fact that it is $\mathbf{x} + \mathbf{T}$ rather than $\mathbf{x} - \mathbf{T}$ that appears in $\triangle^\dagger$). Since $\boldsymbol{\mu}$ is invariant under the U(1) transformation generated by σ_3, the hyperKähler quotient space $M^4(\boldsymbol{\zeta}) = \boldsymbol{\mu}^{-1}(\boldsymbol{\zeta})/U(1)$ is a four-dimensional hyperKähler space. The rotational transformation SO(3)=$\{a_{ij}\}$ generates a homeomorphic mapping from $M^4(\zeta_i)$ to $M^4(a_{ij}\zeta_j)$. Later on, we will see this family of spaces interpolates from the flat space $M^4(0) = R^3 \times S^1$ with minimal cloud size to the Atiyah-Hitchin space $M^4(\infty)$ with infinite cloud size. Under a gauge transformation of the Nahm data, the moment map transforms nontrivially. The gauge orbit of the position $\boldsymbol{\zeta}$ of the massless monopole will be shown to be an ellipsoid.

The submanifolds of the moduli space are summerized in Figure 3.2.

[3]With odd function $\epsilon_2(t)$ (unless $\epsilon_2(t) \equiv 0$ which corresponds to identity) the $ig\partial_t g^\dagger$ term will not vanish. Therefore the transformation will not leave a point in M^8 invariant.

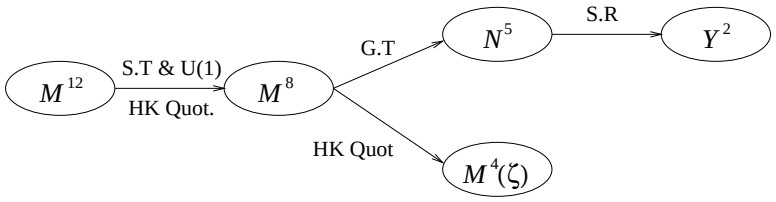

Figure 3.2: Submanifolds of the Sp(4) monopole moduli space. S.T means spatial translation, S.R means spatial rotation, G.T means gauge transformation and HK Quot means hyperKähler quotient.

3.3 Higgs Configurations

Having the explicit form of the Nahm data, we now use the ADHMN construction to compute the field configurations of the monopole system. Although the method itself is straightforward, due to the computational complexity our results will be limited to the cases with special symmetries. This exercise will not only give us some taste of how the ADHMN construction generates sensible results, but also provides a general understanding of the physical meaning of the parameters k and D appearing in the Nahm data.

Notice that in our case only one interval, namely the interval $[-1, 1]$, contributes to the field configuration. Let's denote a typical vector in the kernal of the construction operator $\triangle^\dagger$ as $v = (w_1, w_2, w_3, w_4)^T \in \mathrm{Ker}\triangle^\dagger$. Since the ADHMN construction is invariant under constant gauge transformations of the Nahm data, we can rotate e_1, e_2, e_3 to be e_2, e_3, e_1, respectively. Then, the equation $\triangle^\dagger v = 0$ can be written in the same form as those in Ref. [14, 17]

(except for a minus sign in coordinates):

$$\begin{aligned}
&\dot{w}_1 + x_1 w_1 + (x_3 - ix_2) w_3 + \frac{1}{2} f_1 w_1 + \frac{1}{2}(f_3 - f_2) w_4 = 0, \\
&\dot{w}_2 + x_1 w_2 + (x_3 - ix_2) w_4 - \frac{1}{2} f_1 w_2 + \frac{1}{2}(f_2 + f_3) w_3 = 0, \\
&\dot{w}_3 - x_1 w_3 + (x_3 + ix_2) w_1 - \frac{1}{2} f_1 w_3 + \frac{1}{2}(f_2 + f_3) w_2 = 0, \\
&\dot{w}_4 - x_1 w_4 + (x_3 + ix_2) w_2 + \frac{1}{2} f_1 w_4 + \frac{1}{2}(f_3 - f_2) w_1 = 0. \qquad (3.36)
\end{aligned}$$

Solving these equations with the constraint (2.78) and putting the result into (2.79) will give us Higgs configuration. In practice, however, it turns out that a slightly different method is computationally more convenient for many cases. The method is as follows: Let V be the matrix made from the kernal vectors v, doesn't have to satisfy normalization condition (2.78). If the commutator

$$\left[\int_{-1}^{1} t V^\dagger V dt, \int_{-1}^{1} V^\dagger V dt \right] = 0. \qquad (3.37)$$

Then the Higgs field can be computed as

$$\Phi = \left(\int_{-1}^{1} t V^\dagger V dt \right) \left(\int_{-1}^{1} V^\dagger V dt \right)^{-1}. \qquad (3.38)$$

This expression is gauge equivalent to (2.79) with constraint (2.78). The proof of this method is given in appendix A.3.

3.3.1 Spherically symmetric case

The first case we consider is the spherically symmetric solution which is given by $D = 0$ and so

$$f_1 = f_2 = f_3 = 0. \tag{3.39}$$

Clearly this Nahm data is invariant under the spatial SO(3) rotation (3.19). One may wonder whether these Nahm data are invariant under global gauge transformations (3.15) and (3.16). It is obvious that $T_i = 0$ is invariant under the global SO(3) gauge rotation (3.15). However, the initial $T_4 = 0$ is not necessarily invariant. The reason is that the gauge parameters ϵ_2, ϵ_3 of Eq. (3.29) are odd functions, so their t-derivatives don't vanish. But ϵ_1 is even, and so can be a constant leaving T_4 invariant. Thus, one expects a S^2 gauge orbit space for the spherically symmetric solution. This two sphere will appear in the metric of the moduli space as we will see in the next section. In Dancer's case, the spherically symmetric solution is not invariant for all three generators of SU(2) gauge rotations, therefore the gauge orbit is S^3.

The kernal equations (3.36) can be easily solved in the spherically symmetric case and give

$$V = \sqrt{\frac{r}{\sinh(2r)}} e^{-2tI \otimes (x_1\sigma_3 + x_2\sigma_2 + x_3\sigma_1)}, \tag{3.40}$$

which gives rise to the Higgs field

$$\Phi = 2\mathrm{H}(2r)\, \hat{\mathbf{r}} \cdot \mathbf{t}(\boldsymbol{\gamma}), \tag{3.41}$$

where $r = |\mathbf{x}|$, $\hat{\mathbf{r}} = \mathbf{x}/r$ and $\mathrm{H}(r)$ is given by Eq. (B.3). This is the well known single monopole solution with $\Phi_\infty \propto H_2$ along x_3 direction. This configuration is the SU(2) embedded solution associated with the composite root $\boldsymbol{\gamma}$. The energy density is maximized at the center. We have just argued that the corresponding Nahm data are not invariant under some of the global gauge transformations. To understand this in terms of the field configuration, one can verify from the root diagram given in Figure 3.1 that the generators $\mathbf{t}(\boldsymbol{\gamma})$ commute with $t^3(\boldsymbol{\alpha})$ but not with $t^{1,2}(\boldsymbol{\alpha})$. Thus the spherically symmetric field configuration is not invariant under two of the $t^i(\boldsymbol{\alpha})$, which is consistent with the previous argument.

3.3.2 Hyperbolic case

We now turn to axially symmetric cases. Just as in Dancer's case, we have two axially symmetric cases. The hyperbolic case appears when $k = 1$ and $0 \leq D < \infty$, so that

$$f_1 = f_2 = 0, \qquad f_3 = D. \tag{3.42}$$

These Nahm data are invariant under rotation around the x_3-axis. Although no hyperbolic function is involved here, we have used the same terminology as used in Ref. [14], because of the similarity in their qualitative behavior. The trigonometric case (to be discussed in the next subsection) appears when

$k = 0$ and $0 \leq D < \frac{\pi}{2}$, so that

$$f_1 = D\tan(Dt), \qquad f_2 = f_3 = -D\sec(Dt). \tag{3.43}$$

These data are invariant under rotation around the x_1-axis.

Our hyperbolic case is much simpler than the corresponding case in SU(3) theory. The kernal equation (3.36) leads to

$$V = \exp\left\{-t\left[\begin{pmatrix} x_3 & -\frac{1}{2}D \\ -\frac{1}{2}D & x_3 \end{pmatrix} \otimes \sigma_1 + x_2 I \otimes \sigma_2 + x_1 I \otimes \sigma_3\right]\right\}. \tag{3.44}$$

This expression is not normalized, but one can check that Eq. (3.37) is satisfied. Therefore we can apply Eq. (3.38) which (after a proper gauge transformation) gives the following Higgs configuration:

$$\Phi = 2\mathrm{H}(2r_-)\hat{\mathbf{r}}_- \cdot \mathbf{t}(\boldsymbol{\beta}) + 2\mathrm{H}(2r_+)\hat{\mathbf{r}}_+ \cdot \mathbf{t}(\boldsymbol{\delta}). \tag{3.45}$$

Here $\mathbf{r}_\pm = (x_1, x_2, x_3 \pm D/2)$. We recognize that this configuration describes $\boldsymbol{\beta}$ and $\boldsymbol{\delta}$ monopoles located at $x_3 = -D/2$ and $x_3 = D/2$, respectively. Since $[t^i(\boldsymbol{\beta}), t^j(\boldsymbol{\delta})] = 0$, there is no direct interaction between these two monopoles, and the field configuration (3.45) is a simple superposition of two corresponding configurations. In the SU(3) hyperbolic case, the two massive monopoles are interacting.

The above hyperbolic configuration is not invariant under global gauge rotations generated by $\mathbf{t}(\boldsymbol{\alpha})$ since $\mathbf{t}(\boldsymbol{\beta})$ and $\mathbf{t}(\boldsymbol{\delta})$ don't commute with $\mathbf{t}(\boldsymbol{\alpha})$.

Among the various dyonic excitations, the simplest one is given by a direct superposition of $\boldsymbol{\beta}$ and $\boldsymbol{\delta}$ dyons. Once the magnitudes of their electric charges are not identical, their relative charge (which is the relevant one in M^8) is nonzero. This corresponds to an excitation due to a $t^3(\boldsymbol{\alpha})$ rotation. Clearly this configuration would preserve the axial symmetry. In the next section, the motion which changes D and this relative charge will be described by a flat two dimensional surface of revolution.

3.3.3 Trigonometric case

In contrast to the simple hyperbolic case, our trigonometric case (3.43) is more complicated than the corresponding SU(3) case. Let's focus on the symmetry axis, Eq. (3.36) at $(z, 0, 0)$ becomes

$$\dot{w}_1 + z w_1 + \frac{1}{2} D \tan(Dt) w_1 = 0, \tag{3.46}$$

$$\dot{w}_2 + z w_2 - \frac{1}{2} D \tan(Dt) w_2 - D \sec(Dt) w_3 = 0, \tag{3.47}$$

$$\dot{w}_3 - z w_3 - \frac{1}{2} D \tan(Dt) w_3 - D \sec(Dt) w_2 = 0, \tag{3.48}$$

$$\dot{w}_4 - z w_4 + \frac{1}{2} D \tan(Dt) w_4 = 0. \tag{3.49}$$

Notice that the first and fourth equations are not coupled with anything else while the second and third equations are only coupled among themselves. Thus, after a proper SU(4) gauge transformation, the Higgs field can be

written as

$$\Phi = \begin{pmatrix} * & 0 & 0 & * \\ 0 & * & 0 & 0 \\ 0 & 0 & * & 0 \\ * & 0 & 0 & * \end{pmatrix}, \tag{3.50}$$

where "$*$" indicates non-vanishing entries. Since $\Phi^T J + J\Phi = 0$ with J given by Eq. (3.12), we get $\Phi_{33} = -\Phi_{22}$ and $\Phi_{44} = -\Phi_{11}$. From Eq. (3.46), we can easily obtain

$$\Phi_{22} = -\Phi_{33} = -\frac{f(z) - f(-z)}{g(z) + g(-z)}, \tag{3.51}$$

where

$$\begin{aligned} f(z) &= e^{2z}[(2z+1)D^2 + 4z^2(2z-1)]\cos D \\ &\quad + e^{2z}[D^3 + 4zD(z-1)]\sin D, \end{aligned} \tag{3.52}$$

$$g(z) = e^{2z}(D^2 + 4z^2)(2z\cos D + D\sin D). \tag{3.53}$$

We are not going to pursue the details for the corner 2×2 matrix part of Φ, which describes the non-Abelian structure. As the case of Ref. [15, 16], we believe that the general trigonometric data correspond to the situation where the energy density is maximized on a ring around the axis of symmetry, even though we have not done the numerical computation to check this. When $D = 0$, the configuration is spherically symmetric. When $D \to \pi/2$, we will see in a moment that our result approaches the well-known Atiyah-Hitchin case, which has a ring-like energy distribution. Thus, based on symmetry

and continuity, we believe the ring-like energy distribution is true for the general trigonometric case.

In the limit $D \to \pi/2$, Eq. (3.51) becomes

$$\Phi_{22} = -\left[\tanh(2z) - \frac{z}{z^2 + \left(\frac{\pi}{4}\right)^2}\right], \tag{3.54}$$

which is exactly equal to the known result of the Higgs field of two SU(2) monopoles on the symmetry axis [76]. In the same limit Eqs. (3.47) and (3.48) lead to $\Phi_{11} = -\Phi_{44} = -1$ and $\Phi_{14} = \Phi_{41} = 0$. Thus the Higgs field (3.50) along the symmetry axis becomes the Higgs field for a charge two SU(2) monopole configuration. This suggests that $D \to \pi/2$ is the Atiyah-Hitchin limit of the configuration.

As a general verification of the suggestion made above, let us check whether the three monopole Nahm data degenerate into the SU(2) result when $k = 0, D \to \pi/2$, or more generally when $D \to \mathrm{K}(k)$. In this limit, the Nahm data (3.28) approach

$$f_1, f_2, f_3 \approx -\frac{1}{1+t}, \tag{3.55}$$

near $t = -1$ and

$$-f_1, f_2, f_3 \approx -\frac{1}{1-t} \tag{3.56}$$

near $t = 1$. These are exactly the boundary conditions satisfied by the Nahm data for two identical monopoles in the SU(2) case [32]. This suggests that $D \to \mathrm{K}(k)$ gives the Atiyah-Hitchin limit.

3.3.4 Non-Abelian cloud and the physical meaning of moduli space parameters

Now we are at a good place to introduce a geometric picture of the non-Abelian cloud. As we mentioned, $\boldsymbol{\zeta}$ in Eq. (3.35) can be interpreted as the position of the massless monopole. $\boldsymbol{\zeta}$ changes under the gauge transformation (3.29). For a gauge transformation $g(t)$ we have $g^{-1}(1)e_i g(1) = \mathcal{R}_{ij}e_j$ which implies $\zeta_i = -[T_i]_{22} = -[\frac{i}{2}f_i\mathcal{R}_{ij}e_j]_{22} = \frac{1}{2}f_i\mathcal{R}_{i2}$. This means the position of the massless monopole is not a gauge invariant quantity. The gauge orbit of the position (3.35) is an ellipsoid defined by

$$\frac{\zeta_1^2}{[\frac{1}{2}f_1(1)]^2} + \frac{\zeta_2^2}{[\frac{1}{2}f_2(1)]^2} + \frac{\zeta_3^2}{[\frac{1}{2}f_3(1)]^2} = 1. \tag{3.57}$$

The size of this ellipsoid indicates the size of the non-Abelian cloud [50]. The ellipsoid for Dancer's case can be similarly given.

For the spherically symmetric solution with $D = 0$, this ellipsoid collapses to a point at the origin, indicating that the massless monopole is at the origin. It is consistent with this picture that all the three monopoles lie at the origin for this solution. The ellipsoid for the spherically symmetric solution in Dancer's case has a nonzero size.

For the hyperbolic solution with $k = 1$, this ellipsoid collapses into a line connecting two $\boldsymbol{\beta}$ monopoles. Especially when the $\boldsymbol{\alpha}$ monopole is in overlap with one of the $\boldsymbol{\beta}$ monopole, the configuration becomes a linear superposition

of a $\boldsymbol{\beta}$ and a $\boldsymbol{\delta}$ monopole. For the trigonometric case with $k = 0$, the ellipsoid becomes axially symmetric around the x_1 direction.

In the Atiyah-Hitchin limit, $D \to \mathrm{K}(k)$, the size of the ellipsoid becomes infinite, implying that the massless monopole has been sent to spatial infinity. The distance between the two massive Atiyah-Hitchin monopoles is known to be described by $\mathrm{K}(k)$.

From the above analysis of various limits, we can extract a rough meaning for the two parameters k and D. For a given k, D describes the size of the cloud such that large D corresponds to large cloud size, maximal D corresponds to infinite cloud size. For a given D, k (or $\mathrm{K}(k)$) describes the distance between the two massive monopoles. Large k corresponds to large distance and maximal k (namely $k = 1$) corresponds to the maximal distance that is allowed by the cloud size (namely D). Figure 3.3 shows the $k - D$ space. The spherically symmetric case corresponds to the line $D = 0$. The trigonometric case lies on the line $k = 0$ and $0 < D < \pi/2$, and the hyperbolic case does on the line $k = 1$. The Atiyah-Hitchin case corresponds to the curve $D = \mathrm{K}(k)$. When we examine the moduli space metric in the next section, we will see that a somewhat richer picture emerges.

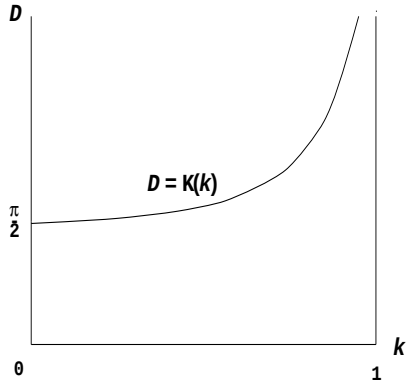

Figure 3.3: $k - D$ space of Sp(4) monopoles. The physical region is below the curve $D = \mathrm{K}(k)$ which describes the Atiyah-Hitchin limit. The vertical edge at $k = 0$ and $k = 1$ describe trigonometric and hyperbolic cases. The horizontal axis $D = 0$ describes the spherically symmetric case.

3.4 The Moduli Space Metric

3.4.1 The moduli space metric on M^8

Now let's turn our attention to the metric of the moduli space. By using centered Nahm data, we are working in the center of mass frame of the monopoles. The moduli space M^8 of centered Nahm data should isometrically correspond to the relative moduli space of the monopole dynamics. The metric for the center of mass motion is flat, so we expect that

$$M^{12} = R^3 \times \frac{S^1 \times M^8}{\Delta} \tag{3.58}$$

where Δ is a discrete subgroup, with which we will not be concerned here. Our work of finding the moduli space metric is greatly facilitated by the works done by Dancer [15, 16] and Irwin [38].

As discussed in chapter 2, a tangent vector Y_m in moduli space is defined by Eqs. (2.88) and (2.92). In general, the Y_m (which are traceless) can be expressed as $Y_m = y_{mi}(e_i/2)$. Substituting this expression into Eqs. (2.88) and (2.92), we will get twelve linear differential equations to determine the twelve coefficients y_{mi}. The non-singular solutions at a point in M^8 given by Nahm data (3.28) can be parametrized by eight real parameters $m_r,\ n_s$, as follows:

$$
\begin{aligned}
Y_1 &= \frac{i}{2}\left[\dot{f}_1 I_1 e_1 + \left(\dot{f}_2 I_2 + \frac{m_2}{f_2}\right) e_2 + \left(\dot{f}_3 I_3 + \frac{n_3}{f_3}\right) e_3\right], \\
Y_2 &= \frac{i}{2}\left[-\dot{f}_1 I_2 e_1 + \left(\dot{f}_2 I_1 + \frac{m_1}{f_2}\right) e_2 - \left(\dot{f}_3 I_4 + \frac{n_4}{f_3}\right) e_3\right], \\
Y_3 &= \frac{i}{2}\left[-\dot{f}_1 I_3 e_1 + \left(\dot{f}_2 I_4 + \frac{m_4}{f_2}\right) e_2 + \left(\dot{f}_3 I_1 + \frac{n_1}{f_3}\right) e_3\right], \\
Y_4 &= \frac{i}{2}\left[-\dot{f}_1 I_4 e_1 - \left(\dot{f}_2 I_3 + \frac{m_3}{f_2}\right) e_2 + \left(\dot{f}_3 I_2 + \frac{n_2}{f_3}\right) e_3\right],
\end{aligned}
\tag{3.59}
$$

where

$$
I_s(t) = \int_0^t dt' \left(\frac{m_s}{f_2(t')^2} + \frac{n_s}{f_3(t')^2}\right). \tag{3.60}
$$

The lower bound of $I_s(t)$ is chosen so that it is odd function of t, which makes the Y_s satisfy the compatibility condition $Y_m(-t)^T = CY_m(t)C^{-1}$, implied by Eq. (3.13).

The metric on the moduli space M^8 is induced from the flat metric (2.93). With solutions (3.59) and equation (3.32), the general results are

$$
\langle \mathbf{Y}, \mathbf{Y}' \rangle = [(g_1 + g_1^2 X) m_s m_s' + (g_2 + g_2^2 X) n_s n_s' + g_1 g_2 X (m_s n_s' + n_s m_s')], \tag{3.61}
$$

$$ds^2(\mathbf{Y},\mathbf{Y}) = \langle \mathbf{Y},\mathbf{Y} \rangle, \tag{3.62}$$

where

$$\begin{aligned} X(k,D) &= f_1(1)f_2(1)f_3(1), \\ g_1(k,D) &= \int_0^1 \frac{dt}{f_2(t)^2}, \\ g_2(k,D) &= \int_0^1 \frac{dt}{f_3(t)^2}. \end{aligned} \tag{3.63}$$

We can calculate the metric by finding the tangent vectors at a generic point of M^8, which can be obtained by applying SO(3)×SO(3) spatial and gauge rotations to the Nahm data (3.28). Due to the SO(3)×SO(3) symmetry of the metric, the general metric can be found once it is known near the identity of the symmetry group. To find the explicit metric in terms of the physical parameters, we need to relate the coordinates m_s, n_s of the tangent space at a specific point in M^8 to the infinitesimal changes of the physical parameters [38]. According to the similarity between the low energy monopole dynamics and mechanics introduced in chapter 2, the terms in moduli space metric corresponding to spatial and internal rotations are in analogue to the rotational energy of a rigid body. This analog means we can find the metric once we know the moment of inertia around each principal axis, which are the coordinate axes for our Nahm data (3.21) and (3.28) [15, 16]. The infinitesimal rotations of a rigid body are expressed in terms of the

left invariant 1-forms

$$\begin{aligned}\sigma_1 &= -\sin\psi d\theta + \cos\psi\sin\theta d\varphi,\\ \sigma_2 &= \cos\psi d\theta + \sin\psi\sin\theta d\varphi,\\ \sigma_3 &= d\psi + \cos\theta d\varphi,\end{aligned} \tag{3.64}$$

which correspond to infinitesimal spatial rotations around the three principal axes. The corresponding left-invariant 1-forms for the gauge rotations are similar and will be denoted as $\check{\sigma}_i$.

We will omit the lengthy computational details which basically follow the same routine as [15, 38]. The idea is to perform SO(3)×SO(3) transformation on the Nahm data, and express the physical parameters λ_i (five of which are introduced in (3.31)) in terms of the inner products of Nahm data. Noticing that $d\mathbf{T} = \mathbf{Y}$ (with infinitesimal parameters m_s, n_s introduced in Eqs. (3.59)), one can compute $d\lambda_i(\mathbf{Y})$ which establishes the relationship between $d\lambda_i$ and m_s, n_s. For our purpose, we can perform the computations in the vicinity of the Nahm data (3.28). The relations we seek are

$$\begin{aligned} m_1 &= -\frac{1}{2}d\lambda_1,\\ n_1 &= -\frac{1}{2}d\lambda_2,\\ m_2 &= \lambda_1\sigma_3,\\ n_2 &= -\frac{g_1\lambda_1}{1+g_2X}\sigma_3 + \frac{1}{\sqrt{g_2+g_2^2X}}\left\{b_3\sigma_3 - c_3(\frac{f_1(1)}{f_2(1)}\sigma_3 - \check{\sigma}_3)\right\},\end{aligned}$$

$$
\begin{aligned}
m_3 &= \frac{g_2\lambda_2}{1+g_1X}\sigma_2 - \frac{1}{\sqrt{g_1+g_1^2X}}\left\{b_2\sigma_2 - c_2(\frac{f_1(1)}{f_3(1)}\sigma_2 - \check{\sigma}_2)\right\}, \\
n_3 &= -\lambda_2\sigma_2, \\
m_4 &= -\frac{g_2(\lambda_1-\lambda_2)}{g_1+g_2}\sigma_1 \\
&\quad -\frac{1}{\sqrt{(g_1+g_2)(1+(g_1+g_2)X)}}\left\{b_1\sigma_1 - c_1(\frac{f_3(1)}{f_2(1)}\sigma_1 - \check{\sigma}_1)\right\}, \\
n_4 &= \frac{g_1(\lambda_1-\lambda_2)}{g_1+g_2}\sigma_1 \\
&\quad -\frac{1}{\sqrt{(g_1+g_2)(1+(g_1+g_2)X)}}\left\{b_1\sigma_1 - c_1(\frac{f_3(1)}{f_2(2)}\sigma_1 - \check{\sigma}_1)\right\}
\end{aligned}
\tag{3.65}
$$

where λ_1, λ_2 are given in Eq. (3.34),

$$
\begin{aligned}
b_1 &= k^2D^2\sqrt{\frac{g_1^2}{(g_1+g_2)(1+(g_1+g_2)X)}}, \\
b_2 &= \frac{g_2D^2}{\sqrt{g_1+g_1^2X}}, \\
b_3 &= \frac{g_1(1-k^2)D^2}{\sqrt{g_2+g_2^2X}},
\end{aligned}
\tag{3.66}
$$

and

$$
\begin{aligned}
c_1 &= f_2(1)f_3(1)\sqrt{\frac{g_1+g_2}{1+(g_1+g_2)X}}, \\
c_2 &= \frac{\sqrt{g_1+g_1^2X}}{f_2(1)g_1}, \\
c_3 &= \frac{\sqrt{g_2+g_2^2X}}{f_3(1)g_2}.
\end{aligned}
\tag{3.67}
$$

From Eqs. (3.61) (3.62) and (3.65), we can get the full metric on the relative moduli space M^8 of the two massive and one massless Sp(4) monopole system, which is

$$\begin{aligned} ds^2_{M^8}(\mathbf{Y},\mathbf{Y}) = \quad & \frac{1}{4}\Big\{X(g_1 d\lambda_1 + g_2 d\lambda_2)^2 + g_1 d\lambda_1^2 + g_2 d\lambda_2^2\Big\} \\ & + \left\{b_1\sigma_1 - c_1\left(\frac{f_3(1)}{f_2(1)}\sigma_1 - \check{\sigma}_1\right)\right\}^2 \\ & + \left\{b_2\sigma_2 - c_2\left(\frac{f_1(1)}{f_3(1)}\sigma_2 - \check{\sigma}_2\right)\right\}^2 \\ & + \left\{b_3\sigma_3 - c_3\left(\frac{f_1(1)}{f_2(1)}\sigma_3 - \check{\sigma}_3\right)\right\}^2 \\ & + a_1\sigma_1^2 + a_2\sigma_2^2 + a_3\sigma_3^2. \end{aligned} \tag{3.68}$$

This metric is hyperKähler. The isometric group is SO(3)$\times$ SO(3). The SO(3) global gauge transformations are tri-holomorphic and the SO(3) spatial rotations rotate the three complex structures of the manifold.

3.4.2 Submanifolds of moduli space and special limits of the metric

In this subsection, we will look at the following special cases of the general metric (3.68):

- The metric on $\mathcal{Y}^2 = N^5/\mathrm{SO}(3)$.
- The metric on N^5.
- The metric for the axially symmetric cases.

- The metric on a two-dimensional surface of revolution.
- The metric in the large cloud limit.
- The asymptotic metric of widely seperated monopoles.
- The metric on quotient manifold $M^4(0)$ (minimal cloud).

1. The two dimensional space $\mathcal{Y}^2$ is a geodesically complete space made of eight copies of the $k-D$ space. This space describes the motion of the monopoles with the rotational and internal degrees of freedom fixed, and therefore with vanishing SU(2) electric charge and zero angular momentum. The metric of this space obtained from Eq. (3.68), is

$$ds^2_{\mathcal{Y}^2} = \frac{1}{4}\Big\{X(g_1 d\lambda_1 + g_2 d\lambda_2)^2 + g_1 d\lambda_1^2 + g_2 d\lambda_2^2\Big\}. \tag{3.69}$$

Figure 3.3 shows this space in terms of two coordinates, which in the shaded region are $D = \sqrt{-\lambda_2}$ and $E \equiv \sqrt{1-k^2}D = \sqrt{-\lambda_1}$. Near the origin of the $D-E$ space, the above metric becomes

$$ds^2_{\mathcal{Y}^2}(D \to 0) \approx dD^2 + dE^2 \tag{3.70}$$

which is smooth and flat with D, E being the Cartesian coordinates. Figure 3.4 is an extended version of Figure 3.3. The origin of the D, E space corresponds to the spherically symmetric configuration. The two coordinate axes

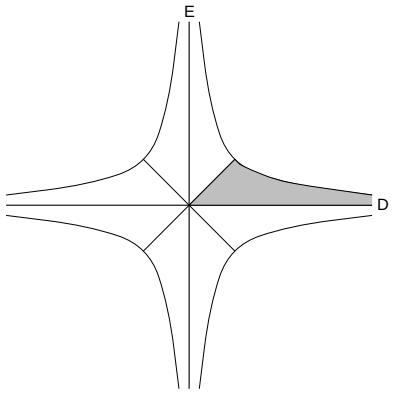

Figure 3.4: Sketch of the geodesically complete space in $D - E$ coordinates. The shaded region corresponds to the $N^5/\mathrm{SO}(3)$ space.

in Figure 3.4 correspond to two hyperbolic configurations symmetric with respect to two orthogonal spatial directions. The diagonal lines correspond to the trigonometric configurations symmetric with respect to two orthogonal spatial directions. The boundary curves correspond to the Atiyah-Hitchin limit, where the massless monopole has been moved to spatial infinity.

Although we will not study in detail the geodesic motions in this space, one can see from the symmetry that trigonometric configurations with velocity pointing to the origin will remain trigonometric after passing through the origin. With similar velocity, the hyperbolic configurations will remain hyperbolic. This contrasts to the SU(3) case where the trigonometric configuration changes to the hyperbolic one, and vice versa. When the cloud size becomes large, the configurations approach the Atiyah-Hitchin limit and the boundary

curve shows the expected rectangular scattering of these monopoles.

2. The metric on $N^5 = M^8/\mathrm{SO}(3)$ with the $\mathrm{Z}_2 \times \mathrm{Z}_2$ isotropy group can be found as

$$ds^2_{N^5} = ds^2_{\mathcal{Y}^2} + a_1\sigma_1^2 + a_2\sigma_2^2 + a_3\sigma_3^2 \tag{3.71}$$

with

$$\begin{aligned} a_1 &= k^4 D^4 \frac{g_1 g_2}{g_1 + g_2}, \\ a_2 &= D^4 \left\{ g_2 + \frac{g_2^2 X}{1 + g_1 X} \right\}, \\ a_3 &= (1-k^2)^2 D^4 \left\{ g_1 + \frac{g_1^2 X}{1 + g_2 X} \right\}, \end{aligned} \tag{3.72}$$

where the g's are defined in Eqs.(3.63). Here one uses the orthogonality condition for the tangential vectors of N^5 to that of gauge rotation [15, 16, 38], which can be found from Eq. (3.65) by dropping terms depending on b_i and c_i. There is no cross term for the invariant 1-forms, which is consistent with the $\mathrm{Z}_2 \times \mathrm{Z}_2$ isotropy group of N^5. This metric describes the monopole dynamics with fixed gauge degree of freedom. Figure 3.5 shows two massive monopoles (two half doughnuts on the x_3 axis) with generic cloud size and three principal axes.

In minimal cloud size, namely $k = 1$, the metric is symmetric under rotations around the x_3 axis so we expect $a_1 = a_2$ and $a_3 = 0$. This is indeed

the case since for $k = 1$, the metric (3.71) becomes

$$ds^2_{N^5}(k=1) = dD^2 + D^2\sigma_1^2 + D^2\sigma_2^2. \tag{3.73}$$

Similarly, in the trigonometric case $k = 0$, the metric is symmetric under rotation around the x_1 axis, so we expect $a_1 = 0$ and $a_2 = a_3$. This is also true since for $k = 0$, the metric (3.71) becomes

$$\begin{aligned} ds^2_{N^5}(k=0) &= \sec^2 D(1 + D\tan D)\left[1 + \frac{\sin(2D)}{2D}\right] dD^2 \\ &\quad + \left\{1 + \frac{\frac{D}{2}\sec^2 D\tan D\left[1 + \frac{\sin(2D)}{2D}\right]}{1 + \frac{D}{2}\sec^2 D\tan D\left[1 + \frac{\sin(2D)}{2D}\right]}\right\} \\ &\quad \times \frac{D^2}{4}\left[1 + \frac{\sin(2D)}{2D}\right](\sigma_2^2 + \sigma_3^2) \end{aligned} \tag{3.74}$$

The distance between two massive monopoles can be defined up to the monopole core size. We guess this distance as $r \approx \sqrt{a_1} \approx \sqrt{a_2}$, because the moment of inertia for a point particle would be its mass times the square of its distance from the origin. We will see later that the above approximation is true at least for the cases when the cloud size is very small or very large.

3. Now let's look at the hyperbolic and trigonometric cases of the metric (3.68). For the hyperbolic case (3.42), in which the cloud size is minimal, the metric (3.68) becomes

$$ds^2_{\text{hyper}} = dD^2 + D^2\sigma_1^2 + D^2\sigma_2^2 + D\tanh D\,\check{\sigma}_1^2 + D\coth D\,\check{\sigma}_2^2 + \check{\sigma}_3^2. \tag{3.75}$$

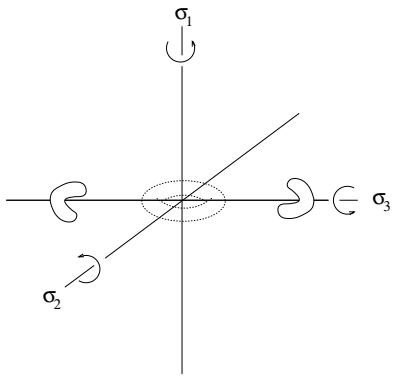

Figure 3.5: Principal axes and the configurations of Sp(4) monopoles. The central doughnut represents trigonometric case, the two half doughnuts on x_3 axis represents two separated massive monopoles with generic cloud size.

The moments of inertia for internal gauge transformations are nonzero, just as we argued in the subsection 3.3.2 (namely the hyperbolic configuration is not invariant under gauge transformations). For the spherically symmetric case, namely $D = 0$, the coefficient of $\check{\sigma}_1$ vanishes (which is consistent with the fact that the spherically symmetric configuration is invariant under gauge rotation ϵ_1), but those of $\check{\sigma}_2$ and $\check{\sigma}_3$ are non-vanishing and become identical, implying the S^2 gauge orbit space. For large separation, $D \gg 1$, the inertia for $\check{\sigma}_1$ and $\check{\sigma}_2$ become identical. We also see that $\sqrt{a_1} = \sqrt{a_2} = D$ is indeed the distance between the two massive monopoles.

For the trigonometric case, the metric (3.75) takes a rather complicated form. Although the explicit formula can be obtained straightforwardly, we will not bother writing it down here. We simply note that the moments

of inertia along the x_2 and x_3 axes are identical, because the trigonometric configurations are symmetric under rotation around the x_1-axis.

4. There are two types of surfaces of revolution, corresponding to the hyperbolic and trigonometric cases. When we include internal global gauge rotations which preserve the axial symmetry, we obtain two dimensional surfaces of revolution. The two dimensional metric for the trigonometric case with $k = 0$ is

$$ds^2_{\rm trig2} = \sec^2 D(1 + D\tan D)(1 + \frac{\sin 2D}{2D}) \left[dD^2 + \frac{D^2(\sigma_1 - \check{\sigma}_1)^2}{(1 + D\tan D)^2}\right], \quad (3.76)$$

where $\sigma_1 - \check{\sigma}_1$ can be put into a rotation $d\alpha$. As $D \to \pi/2$, the metric (3.76) becomes

$$ds^2_{\rm trig2}(D \approx \frac{\pi}{2}) \approx d\rho^2 + \frac{1}{4}\rho^2 d\alpha^2 \quad (3.77)$$

where $\rho = 2\sqrt{\pi/(\pi - 2D)}$. In this limit the massless monopole moves away from the massive monopoles, so the non-Abelian cloud is expected to become more spherical with a flat moduli space R^4 [50]. As we will see in a moment, the above metric is indeed a section of R^4 with a radial variable ρ. In physical space, the size of the massless cloud is characterized by ρ^2. The non-Abelian components of the gauge potential will change their behavior from $1/r$ to $1/r^2$ as one crosses this radius ρ^2. Another axially symmetric case is the hyperbolic case with $k = 1,\ 0 < D < \infty$, whose metric on the two dimensional surface

of evolution is

$$ds^2_{\rm hyper2} = dD^2 + \check{\sigma}_3^2 \tag{3.78}$$

Clearly this flat metric is a part of the metric (3.75).

5. The complete limit of the metric at large cloud size limit (or equivalently the case when the massless monopole is far away from the massive monopoles) can be found in the region where $\mathrm{K}(k) - D \ll 1$. Physically, it is clear that the two massive monopoles should form an Atiyah-Hitchin configuration, and the cloud should have a flat moduli space. In section 3.3, we argued that the Nahm data in this case approach those for the Atiyah-Hitchin case. Now we can show this from the point of view of the moduli space metric. The metric (3.68) becomes

$$\begin{aligned} ds^2_{M^8}(D \to \mathrm{K}(k)) &= d\rho^2 + \frac{\rho^2}{4}\left\{(\sigma_1 - \check{\sigma}_1)^2 + (\sigma_2 + \check{\sigma}_2)^2 + (\sigma_3 + \check{\sigma}_3)^2\right\} \\ &\quad + \frac{b^2}{\mathrm{K}^2} d\mathrm{K}^2 + a^2\sigma_1^2 + b^2\sigma_2^2 + c^2\sigma_3^2 + \mathcal{O}(\rho^{-1}) \end{aligned} \tag{3.79}$$

where $\rho = 2\sqrt{D/(\mathrm{K} - D)}$, and

$$\begin{aligned} a^2 &= \frac{\mathrm{K}(\mathrm{K} - \mathrm{E})(\mathrm{E} - (1-k^2)\mathrm{K})}{\mathrm{E}}, \\ b^2 &= \frac{\mathrm{EK}(\mathrm{K} - \mathrm{E})}{\mathrm{E} - (1-k^2)\mathrm{K}}, \\ c^2 &= \frac{\mathrm{EK}(\mathrm{E} - (1-k^2)\mathrm{K})}{\mathrm{K} - \mathrm{E}}, \end{aligned} \tag{3.80}$$

with the second complete elliptic integral $\mathrm{E}(k) = \int_0^{\pi/2} d\theta \sqrt{1 - k^2 \sin^2\theta}$. It can be verified that the coefficients defined here are equal to those defined by

Eq. (3.3). This means that the asymptotic space is a direct product of the Atiyah-Hitchin and R^4 (A combination of orbital and gauge angular variables needs to be introduced to make this R^4 explicit [38]). It can also be seen that Eq. (3.77) is a section of the R^4 part. We note that $\sqrt{a_1} = a \approx \sqrt{a_2} = b$. The distance between two massive monopoles is given approximately as $r \approx a \approx b \approx -\ln\sqrt{1-k^2}$ [4].

6. When all the three monopoles are far away from each other, we are in the asymptotic region of the moduli space. The moduli space metric in this case can be calculate by studying the interaction between dyons at large separation [25, 49] and taking the massless limit. The metric is in the Gibbons-Manton form. In the center of mass frame, the relative positions between the massive $\boldsymbol{\beta}$ monopoles and the massless $\boldsymbol{\alpha}$ monopole are denoted as $\mathbf{r}_1$ and $\mathbf{r}_2$ as shown in Figure 3.6. The relative position between two massive monopoles is $\mathbf{r} = \mathbf{r}_1 + \mathbf{r}_2$.

In terms of these relative positions $\mathbf{r}_a$ and the relative angles $\psi_a, a = 1, 2$, the asymptotic form of the metric for the relative moduli space M^8 can be obtained from the general Gibbons-Manton metric (3.4):

$$ds^2 = \sum_{a,b}^{2} \left[G_{ab} d\mathbf{r}_a \cdot d\mathbf{r}_b + (G^{-1})_{ab} D\psi_a D\psi_b \right], \tag{3.81}$$

where

$$G_{ab} = \begin{pmatrix} \frac{1+2\epsilon}{1+\epsilon} + \frac{1}{r_1} - \frac{1}{r} & \frac{1}{1+\epsilon} - \frac{1}{r} \\ \frac{1}{1+\epsilon} - \frac{1}{r} & \frac{1+2\epsilon}{1+\epsilon} + \frac{1}{r_2} - \frac{1}{r} \end{pmatrix}, \tag{3.82}$$

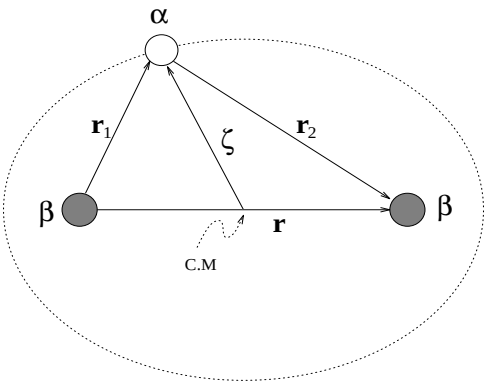

Figure 3.6: Parameters of the asymptotic metric. The center of mass is at the middle of the line connecting two massive $\boldsymbol{\beta}$ monopoles

$$D\psi_a = d\psi_a + \mathbf{w}(\mathbf{r}_a) \cdot d\mathbf{r}_a - \mathbf{w}(\mathbf{r}) \cdot d\mathbf{r}, \tag{3.83}$$

with the Dirac potential $\mathbf{w}$ satisfying $\nabla \times \mathbf{w}(\mathbf{r}) = \nabla(1/r)$. The parameter ϵ represents the ratio of the masses of the $\boldsymbol{\alpha}$ monopole and the $\boldsymbol{\beta}$ monopole. The limit where the $\boldsymbol{\alpha}$ monopole becomes massless is given by $\epsilon \to 0^+$. If we omit the direct interaction between the two identical massive monopoles, the above metric is identical to the Taubian-Calabi metric of the SU(4)→U(1)×SU(2)×U(1) case in which the shape of the non-Abelian cloud is known to be the three-dimensional ellipsoid defined by $r_1 + r_2 =$ constant. This shape of the non-Abelian cloud is also true for the Sp(4) case since the limit of the ellipsoid (3.57) becomes symmetric around the x_3 axis. In the large cloud size limit, one can compare the metric (3.79) and the above one. We see that $D/(\mathrm{K} - D) \approx \mathrm{K}/(\mathrm{K} - D) \sim r_1 + r_2$ and $r \approx \mathrm{K}(k) \approx -\ln\sqrt{1-k^2}$. The condition $r_1 + r_2 \gg r$ for large cloud size

becomes the condition $\mathrm{K}(k) - D \ll 1$ introduced previously.

7. Now we are in a position to learn more about the four-dimensional space $M^4(\boldsymbol{\zeta})$ defined by the moment map (3.34) corresponding to the U(1) symmetry generated by σ_3. For the Nahm data (3.21), (3.28) and Eq. (3.35) we get $\boldsymbol{\zeta} = (0, \zeta, 0)$ with

$$\zeta = D\sqrt{1-k^2}\frac{1}{\mathrm{cn}_k(D)}. \tag{3.84}$$

The general Nahm data is obtained from those in Eq. (3.28) by spatial and gauge rotations. Thus the general $\boldsymbol{\zeta}$ would be a function of rotational and gauge parameters. It is easy to see from Eq. (3.84) that $M^4(0) = \boldsymbol{\mu}^{-1}(0)/\mathrm{U}(1)$, which corresponds to $\boldsymbol{\zeta} = 0$, is realized by the hyperbolic case $k = 1$. The moduli space metric is given by (3.75). Notice that the gauge rotations generated by σ_1 are the only transformations that change $\boldsymbol{\zeta}$ away from zero, therefore the corresponding $\check{\sigma}_1$ part must be dropped in order to fix $\boldsymbol{\zeta} = 0$. Since $T_2 \propto \sigma_3$, dividing by the U(1) group of σ_3 implies dropping the $\check{\sigma}_2$ term from the metric. The resulting four dimensional space is the flat space $R^3 \times S^1$ with the metric

$$ds^2 = dD^2 + D^2(\sigma_1^2 + \sigma_2^2) + \check{\sigma}_3^2. \tag{3.85}$$

On the other hand, when $\zeta = \infty$, we have $D = \mathrm{K}(k)$, which means that the massless monopole has been removed, resulting in the Atiyah-Hitchin

metric. Thus we see that the family of spaces $M^4(\boldsymbol{\zeta})$ interpolates between $M^4(0) = R^3 \times S^1$ and the Atiyah-Hitchin space $M^4(\infty)$.

We can give another argument for the above result (3.85) by considering the asymptotic form of the metric (3.81). In terms of the parameters used in Eq. (3.81), the U(1) symmetry under consideration corresponds to the transformations $\psi_1 \to \psi_1 + \delta, \psi_2 \to \psi_2 - \delta$ whose moment map is [24]

$$\boldsymbol{\mu} = \boldsymbol{\zeta} = \frac{\mathbf{r}_1 - \mathbf{r}_2}{2}. \tag{3.86}$$

This is exactly the position of the massless monopole as shown in Figure 3.5. (Even in the maximally broken case, this moment map is correct.) As $\boldsymbol{\zeta}$ increases from zero to infinity, the size of the non-Abelian cloud increases from zero to infinity, consistent with the picture discussed in the previous paragraph. We can easily obtain the asymptotic form of the metric for $M^4(\boldsymbol{\zeta})$ from Eq. (3.81):

$$ds^2 = G\, d\mathbf{r}^2 + G^{-1}(d\psi + \mathbf{W} \cdot d\mathbf{r})^2, \tag{3.87}$$

where

$$G = 1 + \frac{1}{2|\mathbf{r} + 2\boldsymbol{\zeta}|} + \frac{1}{2|\mathbf{r} - 2\boldsymbol{\zeta}|} - \frac{1}{|\mathbf{r}|}, \tag{3.88}$$

and the Dirac potential function $\mathbf{W}$ is determined by the relation $\nabla G = \nabla \times \mathbf{W}$. Clearly this asymptotic form is hyperKählerian, as it satisfies the condition for the toric hyperKähler space [25]. This metric is correct whether

or not $\boldsymbol{\alpha}$ monopole is massless[4]. When $\boldsymbol{\zeta} = 0$, the metric (3.87) becomes the flat metric (3.85).

[4]A somewhat different approach has been taken in Ref. [34]. There the quotient space for Dancer's case is obtained by taking the infinite mass limit of the corresponding $\boldsymbol{\alpha}$ monopole. This fixes the absolute position of $\boldsymbol{\alpha}$ monopole rather than $\boldsymbol{\zeta}$, which is its position relative to the center of mass of two massive $\boldsymbol{\beta}$ monopoles. The resulting quotient metric seems not to be hyperKähler, as it does not conform to the generic metric for toric hyperKähler spaces.

Chapter 4

Two-Monopole Systems and the Formation of Non-Abelian Clouds

4.1 Introduction

As we discussed in chapter 2, when the unbroken gauge symmetry is non-Abelian, certain fundamental monopoles become massless. We need to distinguish between the cases where the total magnetic charge carried by the monopole system is non-Abelian and where it is purely Abelian. It turns out that the situation is free of topological pathologies only if the total magnetic charge is purely Abelian. The majority of the papers on monopoles in the presence of non-Abelian unbroken symmetry focus on this case. The modern picture of such systems is described by the so-called non-Abelian

cloud arising from the interaction between massless monopoles and massive monopoles.

In spite of the progress in understanding the field configurations and the moduli space metrics, the detailed behavior of the interaction that accounts for the formation of the non-Abelian cloud is still unclear. When one approaches the massless limit, an isolated monopole will spread out and eventually disappear. This trivial behavior can be significantly changed in the presence of massive monopoles. In the case when the system carries Abelian total charge, a would-be massless monopole will lose its identity as an isolated soliton once its core region overlaps with massive monopoles. Its size will cease to expand, and its internal structure will change in a way that reflects the restored non-Abelian symmetry. This picture must be distinguished from the case when the system carries non-Abelian total charge. Having a detailed description of the two situations will be helpful in understanding the formation of the non-Abelian cloud. In this chapter we will try to address some of these issues using Nahm's formalism. The models we are going to consider are the two monopole systems in SU(3) and Sp(4) theories with the gauge symmetries broken to $SU(2)\times U(1)$ They are the two simplest models with the features we want. We will compute the energy densities of the two systems using the formalism described in subsection 2.3.4, analyze their properties, compare our result with known results at various limits,

and finally consider and compare the interacting energy densities of the two systems when approaching the massless limit.

4.2 Two Fundamental Monopoles in SU(3) Theory

The root diagram of SU(3) is shown in Figure 4.1:

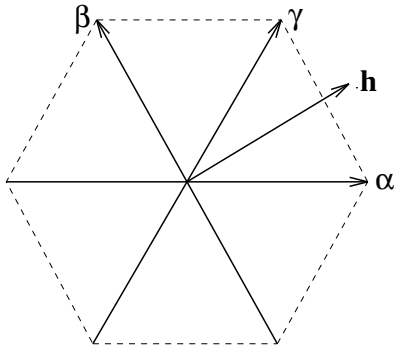

Figure 4.1: Root diagram of SU(3) theory.

We will consider the monopole system made of one $\boldsymbol{\alpha}$ and one $\boldsymbol{\beta}$ monopole, $\mathbf{h}$ denotes the asymptotic Higgs direction that makes $\boldsymbol{\beta}$ monopole massless.

4.2.1 Energy density

We choose Φ_∞ (along the z-direction) to be $\mathrm{diag}(-1-\mu, 2\mu, 1-\mu)$, with $-1/3 \leq \mu \leq 1/3$, so the masses of the two fundamental monopoles are

$$m_{\boldsymbol{\alpha}} = 1 + 3\mu, \quad m_{\boldsymbol{\beta}} = 1 - 3\mu. \tag{4.1}$$

The $\mathbf{h}$ direction in Figure 4.1 corresponds to $\mu = 1/3$. Without losing generality, we can place the $\boldsymbol{\alpha}$ monopole on the origin and $\boldsymbol{\beta}$ monopole on $(0, 0, \mathcal{D})$ which is equivalent to choosing $\mathbf{T}(t) = (0, 0, 0)$ in $t \in (-1-\mu, 2\mu)$ and $\mathbf{T}(t) = (0, 0, -\mathcal{D})$ in $t \in (2\mu, 1-\mu)$. The method to compute energy density in Nahm's formalism was introduced in chapter 2. We will first define a Green function using Eqs. (2.95) and (2.96), and then compute the energy density ρ using Eqs. (2.97) and (2.101). Applying Eqs. (2.95) and (2.96) to the current case we have

$$\left[-\frac{d^2}{dt^2} + |\mathbf{x} + \mathbf{T}(t)|^2 + \mathcal{D}\delta(t - 2\mu)\right] f(t, t') = \delta(t - t'), \tag{4.2}$$

$$f(-1-\mu, t') = f(1-\mu, t') = 0. \tag{4.3}$$

It's easy to see from these equations that the Green's function $f(t, t')$ has the following form:

- Case A: $-1 - \mu < t' < 2\mu$

$$f(t, t') = \begin{cases} A\sinh[r(t+1+\mu)] & (-1-\mu < t < t'), \\ B\sinh(rt) + C\cosh(rt) & (t' < t < 2\mu), \\ D\sinh[r'(1-\mu-t)] & (2\mu < t < 1-\mu). \end{cases} \tag{4.4}$$

- Case B: $2\mu < t' < 1 - \mu$

$$f(t, t') = \begin{cases} A'\sinh[r(t+1+\mu)] & (-1-\mu < t < 2\mu), \\ B'\sinh(r't) + C'\cosh(r't) & (2\mu < t < t'), \\ D'\sinh[r'(1-\mu-t)] & (t' < t < 1-\mu), \end{cases} \tag{4.5}$$

where $r = |\mathbf{x}|$ and $r' = |\mathbf{x} + \mathbf{T}|$ are the distances from two monopoles to the field point, and the coefficients $A, \cdots, C'$ are all functions of t'.

In each case Eq. (4.2) also implies the usual boundary conditions (which we won't bother writing down) concerning the continuity of $f(t,t')$ and the jumps of $\partial_t f(t,t')$ at each point where the arguments of the δ-functions become zero. All the coefficients can be computed from these boundary conditions. It's helpful to notice that Eq. (2.101) makes use of $f(t,t')$ only in the form of $\int dt' f(t',t')$, which is equal to

$$\begin{aligned} \int dt' f(t',t') &= \int_{-1-\mu}^{2\mu} dt' A(t') \sinh[r(t'+1+\mu)] \\ &+ \int_{2\mu}^{1-\mu} dt' D'(t') \sinh[r'(1-\mu-t')]. \end{aligned} \tag{4.6}$$

So we only need A and D'. Computing them using the boundary conditions and substituting into Eqs. (4.6) and (2.101) one obtains

$$\begin{aligned} \partial_i(\log\det f) &= -\frac{rp\sinh p\sinh q + A_1(p\cosh p - \sinh p)}{rM}\hat{r}_i \\ &- \frac{r'q\sinh q\sinh p + A_2(q\cosh q - \sinh q)}{r'M}\hat{r}'_i, \end{aligned} \tag{4.7}$$

where p, q, A_1, A_2, M are defined as

$$p = m_{\boldsymbol{\alpha}} r, \qquad q = m_{\boldsymbol{\beta}} r', \tag{4.8}$$

$$A_1 = \mathcal{D}\sinh q + r'\cosh q, \qquad A_2 = \mathcal{D}\sinh p + r\cosh p, \tag{4.9}$$

$$M = \mathcal{D}\sinh p\sinh q + r\cosh p\sinh q + r'\sinh p\cosh q. \tag{4.10}$$

Notice that nowhere in the computation do we need to compute $\det f$ directly. It turns out that $\det f$ itself is divergent. It contains an infinite factor that is independent of $\mathbf{x}$. This is why such a factor doesn't contribute to Eq. (4.7). From Eq. (4.7) one can verify that the regularized determinant of Green's function [44]

$$(\det f)_{\rm reg} = \frac{rr'}{M}, \tag{4.11}$$

which is defined so that it is finite and gives the same $\partial_i(\log\det f)$ and energy density ρ through

$$\partial_i(\log\det f) = \partial_i[\log(\det f)_{\rm reg}], \tag{4.12}$$

$$\rho = \triangle\triangle\log(\det f)_{\rm reg}. \tag{4.13}$$

An irrelevant infinite factor in the original $\det f$ has been dropped in $(\det f)_{\rm reg}$. Three typical configurations are shown in Figure 4.2 (plotted on the $x-z$ plane since the configurations are axially symmetric). From top to bottom, the three graphs correspond to $m_{\boldsymbol{\alpha}} : m_{\boldsymbol{\beta}}$ equals 1, 1.35 and 3. As expected, as the mass ratio increases, the heavier monopole has a much more significant peak in energy density than the lighter monopole. This is not merely reflecting the mass difference, but the fact that heavier monopole has a smaller core size and therefore a much denser energy distribution.

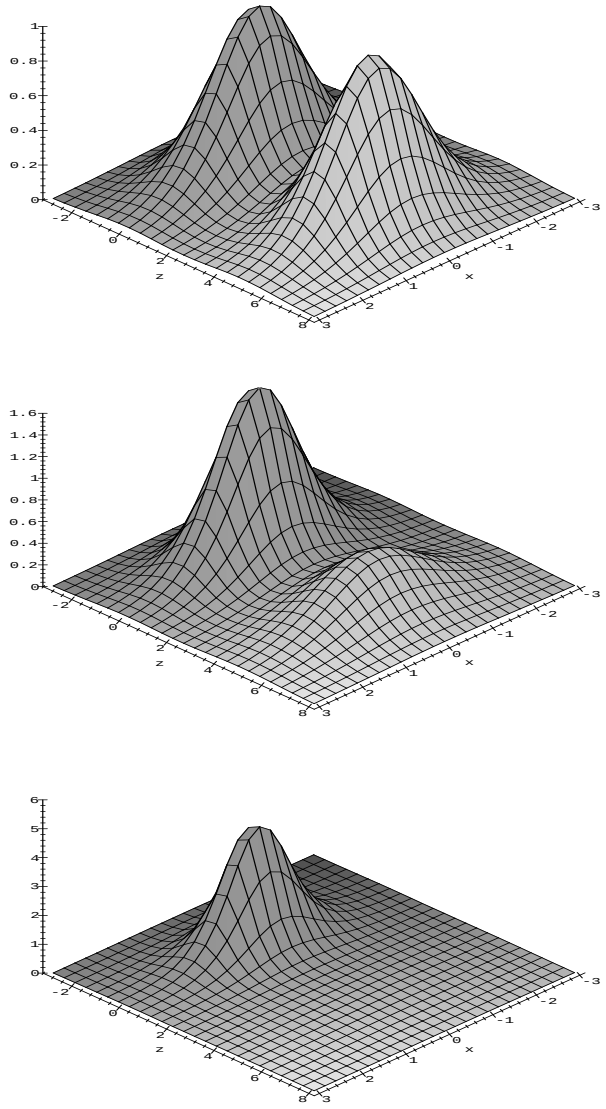

Figure 4.2: Energy density of two fundamental monopoles on the $x-z$ plane in SU(3) theory. $\boldsymbol{\alpha}$ and $\boldsymbol{\beta}$ monopoles are located at $(0,0)$ and $(0,5)$. The mass ratio $m_{\boldsymbol{\alpha}}/m_{\boldsymbol{\beta}}$ (from top to bottom) is chosen to be 1, 1.35 and 3

4.2.2 Various limits of the energy density

In this subsection let's look at several limits of the general form of the energy density. This serves as a partial verification of the result obtained in the last subsection.

1. $\mathcal{D} = 0$ case (the two monopoles are on top of each other):

   It is easy to see that $\boldsymbol{\alpha} + \boldsymbol{\beta} = \boldsymbol{\gamma}$, namely the total magnetic charge of the system is identical to that of a single $\boldsymbol{\gamma}$ monopole. When the two monopoles are on top of each other, we expect that the energy density is the same as that of the SU(2)-embedded $\boldsymbol{\gamma}$ monopole with mass $m = m_{\boldsymbol{\alpha}} + m_{\boldsymbol{\beta}} = 2$. Since two monopoles are overlapping, $r = r'$, $M = r\sinh(2r)$. Using Eqs. (4.11) and (4.12), one obtains

   $$\partial_i(\log\det f) = -2\hat{r}_i \mathrm{H}(2r), \tag{4.14}$$

   where $\mathrm{H}(2r)$ is the $m = 2$ (m is the mass parameter) case of the single monopole function defined by (B.3). From Eq. (4.14), one can further obtain

   $$\triangle(\log\det f) = \partial_i\partial_i(\log\det f) = 4\mathrm{H}^2(2r) - 4, \tag{4.15}$$

   which implies

   $$\rho = \triangle\,\triangle\,(\log\det f) = \triangle[4\mathrm{H}^2(2r)]. \tag{4.16}$$

This is fully compatible (with a suitable normalization convention) with a well known formula [76]

$$\rho = \triangle(\mathrm{tr}\Phi^2), \tag{4.17}$$

since the Higgs field of a single SU(2)-embedded monopole with mass $m = 2$ is $\Phi \propto 2\mathrm{H}(2r)$.

2. Massless limit:

   This is the case when one of the monopoles becomes massless (we will study this limit in more detail in section 4.4). With our conventions this happens when $\mu = \pm 1/3$. Without losing generality, we choose $\mu = 1/3$ (so the $\boldsymbol{\beta}$ monopole is massless) so $q = 0$, which leads to

$$\partial_i(\log\det f) = -2\hat{r}_i\mathrm{H}(2r). \tag{4.18}$$

   This is exactly the same result as the $\mathcal{D} = 0$ case which leads to the same energy density (4.16). Notice in this case $m_{\boldsymbol{\alpha}} = 2$, so such a result means that the $\boldsymbol{\beta}$ monopole doesn't contribute to the energy density at all which, as we will see, is very different from the Sp(4) case.

3. Move one monopole to spatial infinity (at arbitrary mass ratio):

   Again, without losing generality, let's remove the $\boldsymbol{\beta}$ monopole, namely let $r' \to \infty$, $\mathcal{D} \to \infty$ but keep r finite. The dominant term in M is

$$M \sim r'\exp(m_{\boldsymbol{\beta}}r')\sinh(m_{\boldsymbol{\alpha}}r), \tag{4.19}$$

which leads to

$$\partial_i(\log\det f) = -m_{\boldsymbol{\alpha}}\hat{r}_i \mathrm{H}(m_{\boldsymbol{\alpha}} r) - m_{\boldsymbol{\beta}}\hat{r}'_i. \tag{4.20}$$

Since $\hat{r}'_i$ are components of the constant unit vector $\hat{\mathbf{r}}'$ in this limit, only the first term in Eq. (4.20) contributes to the energy density, which leads to

$$\rho = \triangle[m^2_{\boldsymbol{\alpha}}\mathrm{H}^2(m_{\boldsymbol{\alpha}} r)]. \tag{4.21}$$

This is exactly what one expects for a single monopole with mass $m_{\boldsymbol{\alpha}}$.

4.3 Two Fundamental Monopoles in Sp(4) Theory

Another system we are going to study and compare with the SU(3) case is the two monopole system carrying Abelian total magnetic charge in Sp(4) ($\cong$ SO(5)) theory, which is the simplest theory for studying the non-Abelian cloud. The root diagram of the theory is shown in Figure 4.3.

Unlike what was considered in chapter 3, we are now interested in the case when the asymptotic Higgs field eventually approaches the $\mathbf{h}$ direction - the long root $\boldsymbol{\delta}$. The Abelian configuration in this case is made of one massive $\boldsymbol{\alpha}$ monopole and one massless $\boldsymbol{\beta}$ monopole [50]. In this section we will consider the energy density of this monopole system with arbitrary mass ratio, and then look at its behavior when approaching the massless limit.

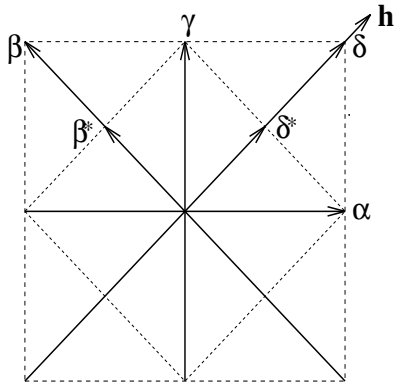

Figure 4.3: Root diagram of Sp(4) theory. $\boldsymbol{\beta}^*$ and $\boldsymbol{\delta}^*$ are co-roots, $\boldsymbol{\alpha}$ and $\boldsymbol{\gamma}$ are identical to their co-roots.

4.3.1 Energy density

We choose Φ_∞ (along the z-direction) to be diag$(-1, -\mu, \mu, 1)$ (with $0 \leq \mu \leq 1$), so the masses of the fundamental monopoles are:

$$m_{\boldsymbol{\alpha}} = 2 - 2\mu, \quad m_{\boldsymbol{\beta}} = 2\mu. \tag{4.22}$$

The $\mathbf{h}$ direction in Figure 4.3 corresponds to $\mu = 0$. The monopole locations are chosen to be the same as in the SU(3) case. As described in chapter 2, in Nahm's formalism the Sp(4) theory is embedded into the SU(4) theory. In our convention the SU(4) Nahm data are given by $\mathbf{T}(t) = (0, 0, 0)$ in $t \in (-1, -\mu) \cup (\mu, 1)$ and $\mathbf{T}(t) = (0, 0, \mathcal{D})$ in $t \in (-\mu, \mu)$. Applying Eqs. (2.95) and (2.96) to this case we have

$$\left[-\frac{d^2}{dt^2} + |\mathbf{x} - \mathbf{T}(t)|^2 + \mathcal{D}\delta(t + \mu) + \mathcal{D}\delta(t - \mu) \right] f(t, t') = \delta(t - t'), \tag{4.23}$$

$$f(-1,t') = f(1,t') = 0. \tag{4.24}$$

The Green's function $f(t,t')$ satisfying these equations has the following form:

- Case A: $-1 < t' < -\mu$

$$f(t,t') = \begin{cases} A\sinh[r(t+1)] & (-1 < t < t'), \\ B\sinh(rt) + C\cosh(rt) & (t' < t < -\mu), \\ D\sinh(r't) + E\cosh(r't) & (-\mu < t < \mu), \\ F\sinh[r(1-t)] & (\mu < t < 1). \end{cases} \tag{4.25}$$

- Case B: $-\mu < t' < \mu$

$$f(t,t') = \begin{cases} A'\sinh[r(t+1)] & (-1 < t < -\mu), \\ B'\sinh(r't) + C'\cosh(r't) & (-\mu < t < t'), \\ D'\sinh(r't) + E'\cosh(r't) & (t' < t < \mu), \\ F'\sinh[r(1-t)] & (\mu < t < 1). \end{cases} \tag{4.26}$$

- Case C: $\mu < t' < 1$

$$f(t,t') = \begin{cases} A''\sinh[r(t+1)] & (-1 < t < -\mu), \\ B''\sinh(r't) + C''\cosh(r't) & (-\mu < t < \mu), \\ D''\sinh(rt) + E''\cosh(rt) & (\mu < t < t'), \\ F''\sinh[r(1-t)] & (t' < t < 1), \end{cases} \tag{4.27}$$

where r and r' have the same meaning as before, and $A, ..., F''$ are all functions of t'.

As in the SU(3) case, we only need some of the coefficients (A, B', C', D'') which (as well as all other coefficients) can be determined by the boundary conditions regarding the continuity of f and discontinuity of f'_t coming from the δ-functions in Eq. (4.23). Computing them and substituting into Eq. (2.101) one obtains

$$\partial_i(\log\det f) = -\frac{PA_1 + QA_2}{\cosh r P + \sinh r Q}\hat{r}_i - \left(\frac{MB_1}{L} + \frac{LB_2}{M}\right)\hat{r}'_i, \tag{4.28}$$

where the following auxiliary functions are introduced:

$$u = (1-\mu)r, \quad v = \mu r, \quad w = \mu r', \tag{4.29}$$

$$A_1 = \frac{-\cosh r + \cosh(u-v)}{r} + 2(1-\mu)\sinh r, \tag{4.30}$$

$$A_2 = \frac{-\sinh r - \sinh(u-v)}{r} + 2(1-\mu)\cosh r, \tag{4.31}$$

$$B_1 = \mu + \frac{\sinh(2\mu r')}{2r'}, \quad B_2 = \mu - \frac{\sinh(2\mu r')}{2r'}, \tag{4.32}$$

$$L = \mathcal{D}\sinh u\cosh w + r\cosh u\cosh w + r'\sinh u\sinh w, \tag{4.33}$$

$$M = \mathcal{D}\sinh u\sinh w + r\cosh u\sinh w + r'\sinh u\cosh w, \tag{4.34}$$

$$N_1 = \mathcal{D}\sinh v\sinh w - r\cosh v\sinh w + r'\sinh v\cosh w, \tag{4.35}$$

$$N_2 = \mathcal{D}\cosh v\sinh w - r\sinh v\sinh w + r'\cosh v\cosh w, \tag{4.36}$$

$$N_3 = \mathcal{D}\sinh u\sinh(2w) + r\cosh u\sinh(2w) + r'\sinh u\cosh(2w) \tag{4.37}$$

$$P = r'\sinh vM - N_1N_3, \quad Q = -r'\cosh vM + N_2N_3. \tag{4.38}$$

It can be verified that the reguralized determinant of the Green's function is given by

$$(\det f)_{\rm reg} = \frac{r^2r'}{LM}. \tag{4.39}$$

The asymmetry between r and r' in the regularized Green's function reflects the asymmetric role of $\boldsymbol{\alpha}$ and $\boldsymbol{\beta}$ monopoles in the embedding procedure ($\boldsymbol{\alpha}$ monopole is a superposition of two SU(4) monopoles). Three typical

configurations are shown in Figure 4.4. The mass ratios of the $\boldsymbol{\alpha}$ and $\boldsymbol{\beta}$ monopoles (from top to bottom) are 1, 2 and 4 respectively.

One can see that the energy density in Sp(4) theory is not symmetric between the two monopoles. This is because $\boldsymbol{\alpha}$ and $\boldsymbol{\beta}$ monopoles have different energy distributions. As we know from Eqs. (2.24) and (2.25), the mass of an SU(2)-embedded $\boldsymbol{\gamma}$ monopole in an arbitrary gauge theory is given by $\mathbf{h} \cdot \boldsymbol{\gamma}^*$, while the scale of such a monopole is determined by $1/(\mathbf{h} \cdot \boldsymbol{\gamma})$. As a consequence, in Sp(4) theory when $\boldsymbol{\alpha}$ and $\boldsymbol{\beta}$ monopoles have the same mass, the scale of the $\boldsymbol{\beta}$ monopole is only half of the scale of the $\boldsymbol{\alpha}$ monopole. Therefore the maximal energy density is eight times that of the $\boldsymbol{\alpha}$ monopole. This is why in the plotting with $m_{\boldsymbol{\alpha}} : m_{\boldsymbol{\beta}} = 1$ the $\boldsymbol{\alpha}$ monopole is almost invisible.

4.3.2 Various limits of the energy density

The expression (4.28)of the Sp(4) theory is much more complicated than the corresponding one in the SU(3) case, to check our results, let's look at several special cases.

1. $\mathcal{D} = 0$ case (the two monopoles are on top of each other):

   Since $\boldsymbol{\alpha} + \boldsymbol{\beta} = \boldsymbol{\delta}$, when the two monopoles are on top of each other, we expect the energy density to be identical to that of a single SU(2)-

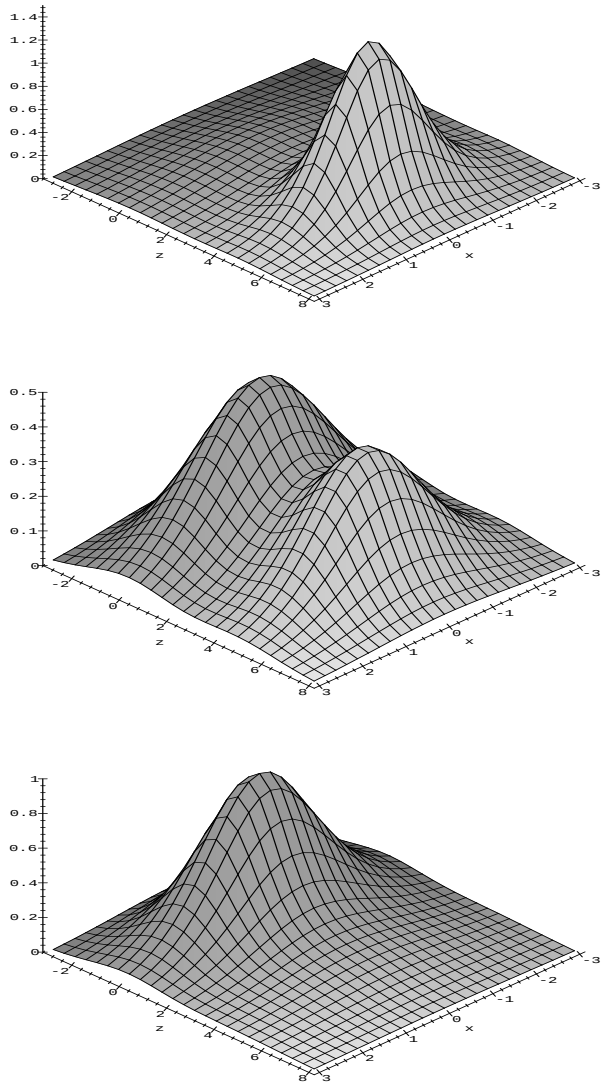

Figure 4.4: Energy density of two fundamental monopoles on the $x - z$ plane in Sp(4) theory. $\boldsymbol{\alpha}$ and $\boldsymbol{\beta}$ monopoles are located at $(0, 0)$ and $(0, 5)$. Mass ratio $m_{\boldsymbol{\alpha}}/m_{\boldsymbol{\beta}}$ (from top to bottom) is chosen to be 1, 2 and 4

embedded $\boldsymbol{\delta}$ monopole with mass $m = m_{\boldsymbol{\alpha}} + m_{\boldsymbol{\beta}} = 2$. This can easily be verified since

$$\partial_i(\log\det f) = -2\hat{r}_i \mathrm{H}(2r) \tag{4.40}$$

is the same result as Eq. (4.14) which leads to the same energy density (4.16) of a mass 2 monopole.

2. Massless limit:

   The massless limit of this monopole system carrying Abelian total magnetic charge is realized by $\mu \to 0$ (when the $\boldsymbol{\beta}$ monopole becomes massless), so $v = 0$, $w = 0$. This limit is very interesting since it is known to contain a non-Abelian cloud. It is not hard to verify that

$$\partial_i(\log\det f) = -\hat{r}_i \frac{2\cosh(2r)(r^2-\mathcal{D}) + r\sinh(2r)(2\mathcal{D}-1) + 2\mathcal{D}}{r^2\sinh(2r) + \mathcal{D}r\cosh(2r) - \mathcal{D}r}. \tag{4.41}$$

   On the other hand, the Higgs configuration in this limit is obtained in [78, 80]. In those papers, the Higgs configuration of $N-1$ fundamental monopoles is calculated for the symmetry breaking pattern SU(N)→U(1)×SU(N-2)×U(1). The relevant Sp(4) Higgs configuration can be obtained by taking the $N = 4$ case and putting two massive monopoles on top of each other. With a proper normalization the

result in those papers can be simplified and expressed as

$$\Phi = \frac{1}{\sqrt{2}} \begin{pmatrix} 2\mathrm{H}(2r)\sigma_r & \sqrt{\frac{8\mathcal{D}\tanh^2 r}{\sinh(2r)(r+\mathcal{D}\tanh r)}} \\ \sqrt{\frac{8\mathcal{D}\tanh^2 r}{\sinh(2r)(r+\mathcal{D}\tanh r)}} & \frac{4\mathcal{D}r-2\mathcal{D}\sinh(2r)}{2r\cosh^2 r(r+\mathcal{D}\tanh r)}\sigma_r \end{pmatrix}, \tag{4.42}$$

(where $\sigma_r = \boldsymbol{\sigma}\cdot\hat{\mathbf{r}}$) which leads to

$$\begin{aligned} \mathrm{tr}\Phi^2 &= 4\mathrm{H}^2(2r) + \frac{16\mathcal{D}\tanh^2 r}{\sinh(2r)(r+\mathcal{D}\tanh r)} \\ &\quad + \left[\frac{4\mathcal{D}r - 2\mathcal{D}\sinh(2r)}{2r\cosh^2 r(r+\mathcal{D}\tanh r)}\right]^2. \end{aligned} \tag{4.43}$$

Obviously, in order to show that Eqs. (2.97), (4.41) and (4.17), (4.43) give the same result it is sufficient to show that the difference between $\partial_i\partial_i(\log\det f)$ and $\mathrm{tr}\Phi^2$ is a constant. This turns out to be true since

$$\partial_i\partial_i(\log\det f) = \mathrm{tr}\Phi^2 - 4. \tag{4.44}$$

So the massless limit works out correctly. Unlike the SU(3) case, the massless limit of Sp(4) case is rather non-trivial because of the presence of non-Abelian cloud.

From Eq. (4.41), we can examine the role of non-Abelian cloud by looking at the energy density inside and outside the cloud. To simplify computation, we restrict our consideration to the case $r \gg 1$ (namely outside the core of the massive monopole). It's easy to see that

$$\partial_i(\log\det f) = -2\hat{r}_i + \hat{r}_i\frac{2\mathcal{D}+r}{r(\mathcal{D}+r)} + \mathcal{O}\left(e^{-2r}\right). \tag{4.45}$$

The $-2\hat{r}_i$ term, which leads to a δ-function in energy density, doesn't contribute in the region $r \gg 1$, so the dominant contribution comes from the 2nd term. It is easy to see that when $r \ll \mathcal{D}$,

$$\partial_i(\log\det f) \sim \begin{cases} \frac{2}{r}\hat{r}_i & (r \ll \mathcal{D}) \\ \frac{1}{r}\hat{r}_i & (r \gg \mathcal{D}) \end{cases} \tag{4.46}$$

The factor of 2 difference comes from the fact that outside the cloud the non-Abelian components of the magnetic charge are neutralized by the cloud.

One can easily show that when the $\boldsymbol{\alpha}$ monopole becomes massless (so that the total magnetic charge is non-Abelian), the situation is similar to the SU(3) case, and the energy density is equal to the energy density of a single $\boldsymbol{\beta}$ monopole.

3. Move the $\boldsymbol{\alpha}$ monopole to spatial infinity (at arbitrary mass ratio):

Now let's look at what happens when one monopole is removed. As discussed in last subsection, the two monopoles are not symmetric in the Sp(4) case so we need to check them separately. When $\mathcal{D} \to \infty, r \to \infty$ and r' is kept finite, the $\boldsymbol{\alpha}$ monopole is removed. The leading contributions to L, M are:

$$L \sim r\exp[(1-\mu)r]\cosh(\mu r'), \tag{4.47}$$

$$M \sim r\exp[(1-\mu)r]\sinh(\mu r'). \tag{4.48}$$

Plugging into Eqs. (4.39) and (4.12) gives

$$\partial_i(\log\det f) = -2\mu\hat{r}'_i \mathrm{H}(2\mu r') - m_{\boldsymbol{\alpha}}\hat{r}_i, \tag{4.49}$$

which leads to an energy density

$$\rho = \triangle[4\mu^2\mathrm{H}^2(2\mu r')]. \tag{4.50}$$

This represents an SU(2)-embedded monopole with mass $m = m_{\boldsymbol{\beta}} = 2\mu$, which is what we expect.

4. Move the $\boldsymbol{\beta}$ monopole to spatial infinity (at arbitrary mass ratio):

When $\mathcal{D} \to \infty, r' \to \infty$ and r is kept finite, the $\boldsymbol{\beta}$ monopole is removed. The leading contributions to L, M are

$$L \sim M \sim r' \exp(\mu r') \sinh[(1-\mu)r], \tag{4.51}$$

which lead to

$$\partial_i(\log\det f) = -2(1-\mu)\hat{r}\mathrm{H}[(1-\mu)r] - m_{\boldsymbol{\beta}}\hat{r}'_i. \tag{4.52}$$

The energy density coming from this expression is

$$\rho = 2\triangle\left\{(1-\mu)^2\mathrm{H}^2\left[(1-\mu)r'\right)\right\}, \tag{4.53}$$

which is the same as that from two directly superposed SU(2) monopoles with mass $m = 1-\mu = m_{\boldsymbol{\alpha}}/2$. This is consistent with the SU(4) embedded picture since the $\boldsymbol{\alpha}$ monopole in Sp(4) theory is considered as

two overlapping SU(4) monopoles. This also gives a direct demonstration of our discussion at the end of subsection 4.3.1.

4.3.3 From the moment of inertia to the moduli space metric at massless limit

Since we have the analytic form of the energy density, we are now able to compute the internal part of the moduli space metric using a nice "mechanical" interpretation. The idea of using a mechanical interpretation for the moduli space metric can be traced to Manton's original work [55] (where the concept of the moduli space metric itself was introduced by comparing the action of the monopole system and a mechanical system, see chapter 2 for details). In this subsection we will consider the massless limit of the moduli space metric of the Sp(4) system. The metric in this case (changed into our convention) is known to be [50]:

$$ds^2 = m d\mathbf{x}^2 + \frac{16\pi^2}{m} d\chi^2 + \frac{4\pi}{\mathcal{D}} d\mathcal{D}^2 + 4\pi\mathcal{D}(\sigma_1^2 + \sigma_2^2 + \sigma_3^2), \tag{4.54}$$

where m is the total mass (which is just the mass of the $\boldsymbol{\alpha}$ monopole in this case) of the system, and σ_1, σ_2 and σ_3 are 1-forms given by (3.64) with the Euler angles θ, ϕ and ψ having periodicities $\pi, 2\pi$ and 4π, respectively. It's interesting to notice that the last term in Eq. (4.54) has a "mechanical interpretation" as the rotational energy in internal (gauge) space associated

with the massless cloud, with the coefficient $4\pi\mathcal{D}$ being the moment of inertia of the cloud. To see this let's calculate the moment of inertia of the non-Abelian cloud. As we know, for a spherically symmetric system the moment of inertia tensor has the form $I_{ij} = I\delta_{ij}$ with

$$I = \frac{2}{3}\int dV r^2 \rho. \tag{4.55}$$

Since rotation of the cloud is actually a gauge rotation in internal space, we should remove the gauge invariant part $\rho(\mathcal{D} = 0)$ which represents a gauge invariant SU(2)-embedded $\boldsymbol{\gamma}$ monopole. The effective energy density relevant for the internal rotation is $\rho(\mathcal{D}) - \rho(0)$. Using the result obtained in the last subsection, one can verify that

$$\begin{aligned} I &= \frac{2}{3}\int dV\ r^2[\rho(\mathcal{D}) - \rho(0)] \\ &= \frac{8\pi}{3}\int dr\ r^4[\rho(\mathcal{D}) - \rho(0)] \\ &= 16\pi\mathcal{D}, \end{aligned} \tag{4.56}$$

which leads to a term $16\pi\mathcal{D}(d\omega_1^2 + d\omega_2^2 + d\omega_3^2)$ in the moduli space metric. Here the 1-forms $d\omega_1, d\omega_2$ and $d\omega_3$ are defined in the group space of SU(2) (namely S^3). In order to see why the coefficient 16 is compatible with the previously known coefficient 4 in Eq. (4.54), one notices that

$$\sigma_1^2 + \sigma_2^2 + \sigma_3^2 = d\theta^2 + d\phi^2 + d\psi^2 + 2\cos\theta d\phi d\psi, \tag{4.57}$$

so that the volume of the (θ, ϕ, ψ) space is

$$\mathcal{V} = \int \sqrt{|g|} d\theta d\phi d\psi = 16\pi^2, \tag{4.58}$$

where $g = \det(g_{ij})$ is the determinant of the metric matrix coming from Eq. (4.57). Since the volume of group space S^3 is $2\pi^2$, the two sets of 1-forms are related by $\sigma_i = 2d\omega_i$ $(i = 1, 2, 3)$. Taking this into account we see that $16\pi\mathcal{D}(d\omega_1^2 + d\omega_2^2 + d\omega_3^2)$ computed from the moment of inertia is in accordance with the last term in the moduli space metric (4.54).

4.4 Interaction Energy Density and the Formation of Non-Abelian Clouds

In previous sections we have calculated the energy density of two-monopole systems in the SU(3) and Sp(4) theories. We already know that in the massless limit the situations are very different, depending on the total magnetic charge. If the total magnetic charge is non-Abelian, the resulting energy density is simply the same as the energy density of the remaining massive monopole. When the total magnetic charge is purely Abelian, however, the energy density distribution is deeply affected by the existence of the massless monopole. In the latter case, there is a non-Abelian cloud surrounding the massive monopole, neutralizing the non-Abelian components of the magnetic charge. In this section we want to have a closer look at the evolution of the

energy density when one approaches the massless limit.

There's no unique choice of variable to describe the formation of the non-Abelian cloud, nor is there any unambiguous definition of the non-Abelian cloud itself. But physically there is no doubt that it is the interaction between the massive and massless monopoles that determines the formation of the non-Abelian cloud. Our strategy is to study the interaction energy density defined as

$$\rho_{\rm int} = \rho_{\rm total} - \rho_{\boldsymbol{\alpha}} - \rho_{\boldsymbol{\beta}}, \tag{4.59}$$

where $\rho_{\boldsymbol{\alpha}}$ and $\rho_{\boldsymbol{\beta}}$ are the energy densities of isolated $\boldsymbol{\alpha}$ and $\boldsymbol{\beta}$ monopoles. $\rho_{\rm int}$ describes the change of energy distribution caused by the interaction between the two monopoles. In particular we will look at the contour of zero interaction energy density, which gives the information on where interaction gathers energy and from where it extracts energy.

We have used MAPLE to generate numerical data and plotted several typical contours (shown in Figures 4.5 and 4.6) for the SU(3) and Sp(4) theories.

From the contour diagrams one can see the major difference between the two theories when approaching the massless limit. In both cases we start with a simply connected contour for a small mass ratio $m_{\boldsymbol{\alpha}} : m_{\boldsymbol{\beta}}$ ($\boldsymbol{\beta}$ is the would-be massless monopole). The contour deforms and grows

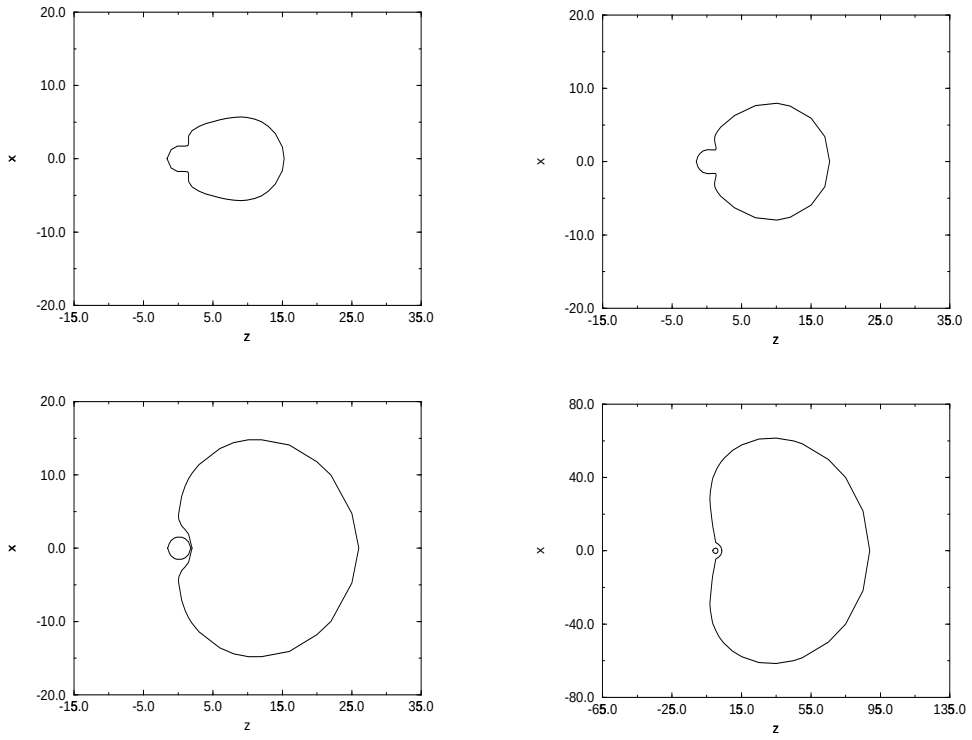

Figure 4.5: Contour diagrams of $\rho_{\rm int} = 0$ on the $x - z$ plane for the SU(3) theory. The $\boldsymbol{\alpha}$ and $\boldsymbol{\beta}$ monopoles are located at $(0, 0)$ and $(0, 10)$. The mass ratios $m_{\boldsymbol{\alpha}} : m_{\boldsymbol{\beta}}$ are chosen to be (from top to bottom) 4 (top left), 7 (top right), 19 (bottom left), 199 (bottom right). The region enclosed by the contour has a positive $\rho_{\rm int}$. As the mass ratio increases, the magnitude of $\rho_{\rm int}$ approaches zero everywhere.

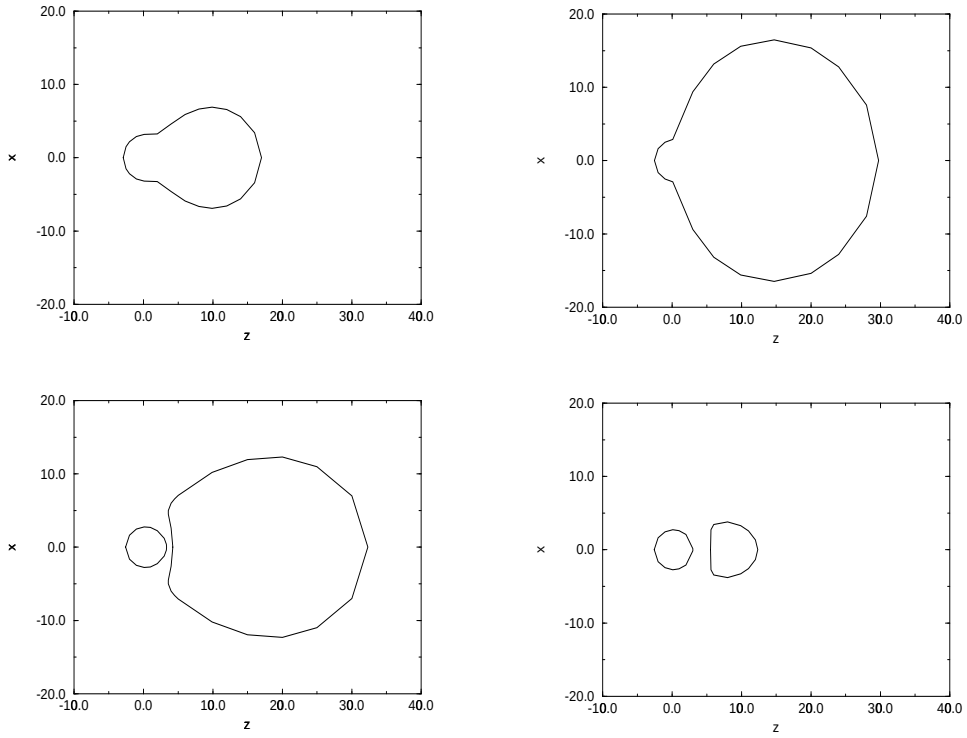

Figure 4.6: Contour diagrams of $\rho_{\rm int} = 0$ on the $x - z$ plane for the Sp(4) theory. The $\boldsymbol{\alpha}$ and $\boldsymbol{\beta}$ monopoles are located at $(0, 0)$ and $(0, 10)$. The mass ratios $m_{\boldsymbol{\alpha}} : m_{\boldsymbol{\beta}}$ are chosen to be (from top to bottom) 4 (top left), 19 (top right), 66 (bottom left), 99 (bottom right). The region enclosed by the contour has a positive $\rho_{\rm int}$. As the mass ratio increases, the right blob disappears. $\rho_{\rm int}$ is nonzero and is negative outside the monopole core, which reflects the fact that it neutralizes the non-Abelian components of the magnetic field.

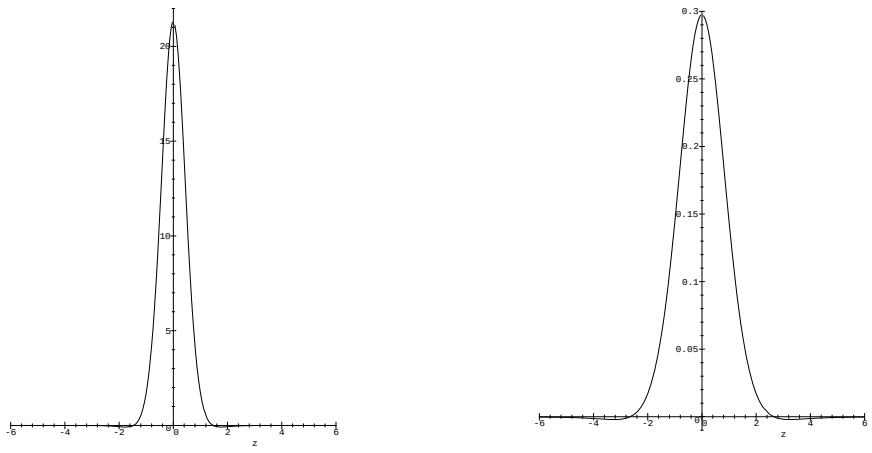

Figure 4.7: $\rho_{\rm int}$ for the SU(3) (left) and the Sp(4) (right) theories at massless limit. The vertical axis of the SU(3) curve is actually $\rho_{\rm int}/m_{\boldsymbol{\beta}}$. This curve is independent of $\mathcal{D}$. The Sp(4) curve has a weak dependence on $\mathcal{D}$ and is plotted for $\mathcal{D} = 10$.

when the mass ratio increases. In both cases it breaks into two disjoint pieces when the mass ratio is sufficiently large. The reason it breaks can be understood by directly analyzing the massless limit of $\rho_{\rm int}$ (in the SU(3) case $\rho_{\rm int}$ itself vanishes but one can use $\rho_{\rm int}/m_{\boldsymbol{\beta}}$, which is finite and independent of $\mathcal{D}$, to determine the sign of $\rho_{\rm int}$). Figures 4.7 shows those limits: In both cases the interaction energy density becomes negative outside the core of the $\boldsymbol{\alpha}$ monopole. This means that the contour (for the $\mathcal{D} = 10$ case) can't keep growing and remain simply connected as one increases the mass

ratio. After the breaking point, the part of the contour that surrounds the $\boldsymbol{\alpha}$ monopole is stabilized, but the other part, which is associated with the (would-be massless) $\boldsymbol{\beta}$ monopole undergoes a very different evolution in the two cases: In the SU(3) case that part of the contour grows unbounded and its magnitude decreases as one approaches the massless limit. This behavior of the $\boldsymbol{\beta}$ monopole is qualitatively similar to that of an isolated monopole. It grows into an infinite volume and its energy density approaches zero everywhere, all its dynamic effects diminish. In the Sp(4) case, however, the situation is the opposite. The other part of the contour eventually shrinks and finally disappears. This phenomenon reflects the fact that the would-be massless monopole eventually loses its own identity as an independent object. The interaction energy density is nonzero in the massless limit for the Sp(4) case, and the density is negative outside the core of the $\boldsymbol{\alpha}$ monopole. This phenomenon comes from the fact that the massless monopole, which forms a non-Abelian cloud, tends to neutralize the non-Abelian components of the magnetic fields generated by the $\boldsymbol{\alpha}$ monopole. Such a neutralization leads to a negtive interaction energy density.

It should be mentioned for the Sp(4) case that, if the $\boldsymbol{\beta}$ monopole is inside the core of the $\boldsymbol{\alpha}$ monopole, as the mass ratio increases, the contour of zero interaction energy density could shrink and be stabilized without first breaking into two pieces.

The difference in the contour diagrams of the two cases provides a picture for the formation of the non-Abelian cloud. Although in both cases, the interaction alters the energy distribution by accumulating energy in certain regions, in the case of SU(3) that region is expanding as one approaches the massless limit and the effect of the interaction is smeared out over an unbounded area, this leaves the final energy density completely dominated by the remaining massive monopole. On the other hand, in the Sp(4) case, the interaction extracts energy and deposits it into a small region (in some sense one can say that the interaction is more "localized" in this case). Physically, such an interaction changes the magnetic field and only allows the Abelian field components to penetrate the non-Abelian cloud and exist as long range fields. As a result the interaction significantly affects the energy density distribution. Because of the interaction the massless monopole doesn't grow in size as it would if it was isolated. At large mass ratio, the location of the $\boldsymbol{\beta}$ monopole gradually loses its meaning (the contour associated to it disappears). In this process, the $\boldsymbol{\beta}$ monopole evolves into a non-Abelian cloud.

Chapter 5

SU(2) Calorons and Magnetic Monopoles

5.1 Introduction

As explained in chapter 1, it is interesting to explore the relation between instantons and magnetic monopoles. Recently such a relation was considered on a more general background, namely at finite temperature and with symmetry breaking. The relevant objects are calorons and magnetic monopoles on $R^3 \times S^1$. The gauge symmetry is broken maximally by the Wilson loop, which is nothing but the Higgs expectation value if one treats the fourth component of the gauge field as the Higgs field. Among the self-dual configurations of a theory with a simple gauge group G of rank r, the configurations that are independent of the S^1 coordinate satisfy the ordinary BPS equations

for magnetic monopoles on R^3. As discussed in chapter 2, on R^3 there exist r types of fundamental BPS monopoles each of which is associated with a simple root [77]. On $R^3 \times S^1$, however, it was shown in [46, 52] that there exists an additional type of fundamental monopole associated with the lowest negative root. It was argued in these papers that a single caloron is made of a unique combination of the $r+1$ different fundamental monopoles such that the net magnetic charge is zero. The explicit moduli space metric of a single caloron was found in the SU(N) theory up to normalization factor [52]. In this chapter, we are going to construct the explicit field configuration of an SU(2) caloron and explore in a quantitative way the constituent monopole picture.

The usual caloron solutions were found in the late seventies [27, 29, 72]. The difference between those works and ours lies in the Wilson loop $W(\mathbf{x}) = P\exp(\int dx_4 A_4)$. In all the cases studied before, the Wilson loop is trivial and magnetic monopoles appear only when the scale of the instanton is taken to be infinity (see [72] or chapter 2 for details). In our case, however, the Wilson loop is nontrivial. In a chosen gauge the value of A_4 at spatial infinity

$$(A_4)_\infty = v\frac{\sigma_3}{2} \tag{5.1}$$

plays the role of the asymptotic Higgs value (as usual, we will often simply call v the Higgs value).

In this chapter we will construct the explicit field configuration for a single SU(2) caloron on $R^3 \times S^1$ with nontrivial Wilson loop by using Nahm's formalism and give an explicit demonstration that a single caloron is made of two distinct fundamental monopoles. We will examine various limits of the configuration, especially the trivial Wilson loop limit (which should give rise to the usual caloron) and the zero temperature limit. Another interesting question is to find the moduli space metric (including the normalization). The relative moduli space for a single caloron was argued to be Taub $-$ NUT with Z_2 singularity [52]. We will derive the exact moduli space metric using the constituent monopole picture.

5.2 ADHMN Construction of a Single SU(2) Caloron

5.2.1 Fundamental SU(2) monopoles on $R^3 \times S^1$

In finite temperature field theory, it is well known that only the gauge field configurations periodic in $x_4 \in [0, \beta]$ contribute to the path integral. The allowed local gauge transformations are those that leave the gauge field single-valued. For the gauge group SU(2), there is a group of topologically nontrivial (large) gauge transformations, for instance,

$$g(x_4) = \exp(-i\frac{\pi x_4}{\beta}\sigma_3), \tag{5.2}$$

that are not single-valued but is still acceptable since they preserve the single-valuedness of the gauge fields. Using the large gauge transformation given by (5.2) which shifts v by $-\frac{2\pi}{\beta}$, we can always choose the range of v to be

$$0 \leq v \leq \frac{2\pi}{\beta}. \tag{5.3}$$

When v is not equal to 0 or $2\pi/\beta$, the gauge symmetry is spontaneously broken from SU(2) to U(1). The theory also has an additional global U(1) symmetry corresponding to the translational symmetry on S^1 [52].

In the normalization where the coupling constant $e^2 = 1$, the action, or the four dimensional energy, is bounded from below, $S \geq 8\pi^2|n|$, by the topological index (2.48) which we re-write as

$$\begin{aligned} n &= \frac{1}{64\pi^2}\int d^4x\, \epsilon_{mnrs} F^a_{mn} F^a_{rs} \\ &= \frac{1}{16\pi^2}\int d^3S_i\, \epsilon_{ijk}(F^a_{ij}A^a_4 - A^a_j \partial_4 A^a_k). \end{aligned} \tag{5.4}$$

The surface integral is over both the spatial infinity (of $R^3 \times S^1$) and the small spheres surrounding the singularities. When $n > 0$, the bound is saturated by the field configurations satisfying the self-dual equations (2.50) which we re-write as

$$F_{ij} = \epsilon_{ijk}(D_k A_4 - \partial_4 A_k). \tag{5.5}$$

When the asymptotic value of A_4 lies in the interval (5.3), it was shown that there exist self-dual configurations for two kinds of fundamental magnetic monopoles with four zero modes each [46, 52]. One configuration is

the ordinary BPS solution (with $\Phi \equiv A_4$), which is independent of x_4. It describes monopoles of positive magnetic charge 4π and asymptotic Higgs value v. Another solution is an ordinary monopole with asymptotic Higgs value $2\pi/\beta - v$. We need to apply a large gauge transformation (5.2) and a Weyl reflection $e^{i(\pi/4)\sigma_2}$ to this solution to get the boundary condition (5.1). After these transformations the Higgs value of the second monopole is $2\pi/\beta$ at the center and v at spatial infinity[1]. It describes monopoles of negative magnetic charge -4π. Notice that topological charge is invariant under gauge transformations. For ordinary monopole with asymptotic value v, Eq. (5.4) gives

$$n = \frac{1}{8\pi^2}\int_0^\beta dx_4 \int d^2S_i \; B_i^a A_4^a = \frac{\beta v}{2\pi}. \tag{5.6}$$

So the topological charges of both type of monopoles are positive and are given, respectively, by

$$n_1 = \frac{\beta v}{2\pi}, \qquad n_2 = 1 - \frac{\beta v}{2\pi}. \tag{5.7}$$

It can be noticed immediately that the total topological charge of the two fundamental monopoles is one, which an evidence that an instanton might be thought as the superposition of these two monopoles. The masses of the magnetic monopoles in the conventional sense are the magnetic charge times

[1]The transformation (5.2) shifts the Higgs value to be $-2\pi/\beta$ at origin and $-v$ at spatial infinity, Weyl reflection flips the Higgs value, thus it becomes $2\pi/\beta$ at origin and v at spatial infinity.

the length scale, and so

$$m_1 = 4\pi v, \quad m_2 = 4\pi(\frac{2\pi}{\beta} - v). \tag{5.8}$$

Each type of monopole can carry electric charge q_i, which is quantized as they arise from W boson excitations.

The reason for the opposite magnetic charges of these two monopoles can be seen easily in the unitary gauge. For the first monopole, A_4 increases from zero to v as one moves from the monopole core to spatial infinity. For the second monopole, the value of A_4 decreases from $2\pi/\beta$ to v as one moves from the monopole core to spatial infinity. The magnetic field is proportional to the spatial derivative of A_4 and so the two monopoles carry opposite charges. However, there is no static force between them because the dilatonic interaction is now repulsive, as the monopoles with negative magnetic charges carry opposite dilatonic charges. The dilatonic force cancels the magnetic attraction exactly. This is why in principle the two monopole solutions can be superposed. The configurations for two superposed distinct fundamental monopoles satisfy the self-dual equations and have zero total magnetic charge, unit topological charge, and eight zero modes. Those are exactly the field configurations expected for a single instanton.

5.2.2 ADHMN construction

For an SU(2) gauge theory on $R^3 \times S^1$ with asymptotic Higgs value given by Eq. (5.1), there are three relevant intervals for Nahm's equations,

$$-\frac{\pi}{\beta} < t < -\frac{v}{2}, \quad -\frac{v}{2} < t < \frac{v}{2}, \quad \frac{v}{2} < t < \frac{\pi}{\beta}. \tag{5.9}$$

Since we are considering calorons, we require the Nahm data to be periodic with respect to the time variable t in Nahm's equations [20, 60]. The first and last intervals correspond to a monopole of topological charge n_2 and the middle interval corresponds to a monopole of topological charge n_1.

Since the caloron is made of two distinct fundamental monopoles, the Nahm data representing an SU(2) caloron are constant triplets in each interval. Without losing generality, we can choose coordinates so that the two massive monopoles lie on the z-axis. The corresponding Nahm data are

$$\begin{aligned} \mathbf{T}_0 &= \mathbf{T}_2 = -\mathbf{x}_2 = -(0, 0, (\mathbf{x}_2)_3), \\ \mathbf{T}_1 &= -\mathbf{x}_1 = -(0, 0, (\mathbf{x}_1)_3), \end{aligned} \tag{5.10}$$

where $\mathbf{x}_1, \mathbf{x}_2$ are the positions of two massive monopoles. With our choice, the distance between two monopoles is $D = (\mathbf{x}_2 - \mathbf{x}_1)_3 > 0$. For a given field point $\mathbf{x}$, it is convenient to introduce the relative positions with respect to two monopoles, as shown in Figure 5.1,

$$\mathbf{y}_1 = \mathbf{x} - \mathbf{x}_1, \quad \mathbf{y}_2 = \mathbf{x} - \mathbf{x}_2, \tag{5.11}$$

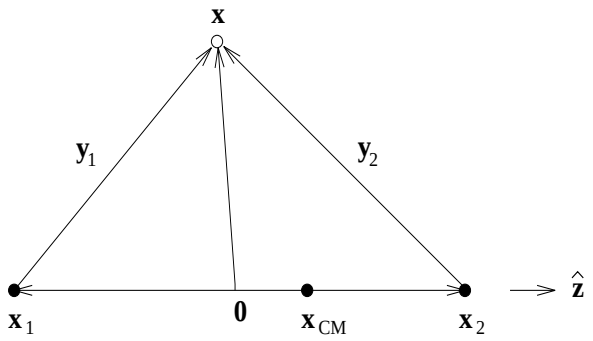

Figure 5.1: Positions of the two constituent monopoles of an SU(2) caloron

and the weighted relative positions

$$\mathbf{s}_1 = v\mathbf{y}_1, \quad \mathbf{s}_2 = (\frac{2\pi}{\beta} - v)\mathbf{y}_2. \tag{5.12}$$

The center-of-mass position of the two monopoles is at

$$\mathbf{x}_{\rm cm} = n_1\mathbf{x}_1 + n_2\mathbf{x}_2. \tag{5.13}$$

From our choice of Nahm data, the discontinuities of the Nahm data at $t = -v/2$ and $t = v/2$ are $\Delta^1 T_i = D\delta_{i3}$ and $\Delta^2 T_i = -D\delta_{i3}$ respectively. The corresponding row vectors defined by Eq. (2.83) are then

$$a_1 = (\sqrt{2D}, 0), \ a_2 = (0, \sqrt{2D}). \tag{5.14}$$

The solutions of the ADHMN equation (2.77) can be expressed as

$$V_0(t) = \frac{1}{\sqrt{N_2}} \exp\left[(ix_4 + \boldsymbol{\sigma}\cdot\mathbf{y}_2)\left(t + \frac{\pi}{\beta}\right)\right] C_2 \quad \text{for } t \in [-\frac{\pi}{\beta}, -\frac{v}{2}),$$
$$V_1(t) = \frac{1}{\sqrt{N_1}} \exp\left[(ix_4 + \boldsymbol{\sigma}\cdot\mathbf{y}_1)t\right] C_1 \quad \text{for } t \in (-\frac{v}{2}, \frac{v}{2}),$$

$$V_2(t) = \frac{1}{\sqrt{N_2}} \exp\left[(ix_4 + \boldsymbol{\sigma}\cdot\mathbf{y}_2)\left(t - \frac{\pi}{\beta}\right)\right] C_2 \quad \text{for } t \in (\frac{v}{2}, \frac{\pi}{\beta}], \quad (5.15)$$

where C_i are 2×2 matrices and

$$N_i = \frac{1}{y_i}\sinh s_i \ (i = 1, 2). \quad (5.16)$$

The periodicity condition $V_0(-\pi/\beta) = V_2(\pi/\beta)$ is automatically satisfied. The normalization condition (2.85) becomes

$$C_1^\dagger C_1 + C_2^\dagger C_2 + S_1^\dagger S_1 + S_2^\dagger S_2 = I, \quad (5.17)$$

where S_1 and S_2 are defined by Eq.(2.84). To find C_1, C_2 and S_1, S_2, we take into account the discontinuity equations (2.84). In addition, we require the gauge field (2.86) to be single-valued, which is physically obvious. Then, C_i and S_i are determined uniquely up to an allowed gauge transformation. The row vectors S_1 and S_2 can be combined into a 2×2 matrix S,

$$S = \frac{1}{\sqrt{\mathcal{N}}} e^{-i\frac{vx_4}{2}\sigma_3} \quad (5.18)$$

with

$$\mathcal{N} = 1 + \frac{2D}{\mathcal{M}}\Big\{N_1[\cosh s_2 - (\hat{\mathbf{y}}_2)_3 \sinh s_2] + N_2[\cosh s_1 + (\hat{\mathbf{y}}_1)_3 \sinh s_1]\Big\}. \quad (5.19)$$

The two matrices C_i are much more complicated. To express them it is useful first to introduce two 2×2 matrices,

$$B_1 \;=\; \exp\left(i\frac{\pi}{\beta}x_4\right)\exp\left(-\frac{\boldsymbol{\sigma}\cdot\mathbf{s}_1}{2}\right)\exp\left(-\frac{\boldsymbol{\sigma}\cdot\mathbf{s}_2}{2}\right)$$

$$
\begin{aligned}
& - \exp\left(-i\frac{\pi}{\beta}x_4\right)\exp\left(\frac{\boldsymbol{\sigma}\cdot\mathbf{s}_1}{2}\right)\exp\left(\frac{\boldsymbol{\sigma}\cdot\mathbf{s}_2}{2}\right), \\
B_2 \;=\; & \exp\left(i\frac{\pi}{\beta}x_4\right)\exp\left(-\frac{\boldsymbol{\sigma}\cdot\mathbf{s}_2}{2}\right)\exp\left(-\frac{\boldsymbol{\sigma}\cdot\mathbf{s}_1}{2}\right) \\
& - \exp\left(-i\frac{\pi}{\beta}x_4\right)\exp\left(\frac{\boldsymbol{\sigma}\cdot\mathbf{s}_2}{2}\right)\exp\left(\frac{\boldsymbol{\sigma}\cdot\mathbf{s}_1}{2}\right), \qquad (5.20)
\end{aligned}
$$

and a scalar quantity

$$
\mathcal{M} = 2\Big\{\cosh s_1\cosh s_2 + \hat{\mathbf{y}}_1\cdot\hat{\mathbf{y}}_2\sinh s_1\sinh s_2 - \cos(\frac{2\pi}{\beta}x_4)\Big\}. \qquad (5.21)
$$

It can be verified that $\mathcal{M} = B_1B_1^\dagger = B_2B_2^\dagger$. C_1 and C_3 can be expressed as

$$
\begin{aligned}
C_1 \;&=\; \sqrt{\frac{2DN_1}{\mathcal{N}}}\frac{B_1^\dagger}{\mathcal{M}}\Big[\exp\left(-\frac{\sigma\cdot\mathbf{s}_2}{2}\right)Q_+ + \exp\left(\frac{\sigma\cdot\mathbf{s}_2}{2}\right)Q_-\Big]e^{-i\frac{\pi x_4}{\beta}\sigma_3}, \\
C_2 \;&=\; \sqrt{\frac{2DN_2}{\mathcal{N}}}\frac{B_2^\dagger}{\mathcal{M}}\Big[\exp\left(\frac{\sigma\cdot\mathbf{s}_1}{2}\right)Q_+ + \exp\left(-\frac{\sigma\cdot\mathbf{s}_1}{2}\right)Q_-\Big], \qquad (5.22)
\end{aligned}
$$

where the projection operators $Q_\pm$ are defined as

$$
Q_\pm = \frac{1\pm\sigma_3}{2}. \qquad (5.23)
$$

Using all these auxiliary variables, the gauge field given by (2.86) can be expressed as

$$
\begin{aligned}
A_m(\mathbf{x},x_4) \;=\;& C_1^\dagger W_m(\mathbf{y}_1;v)C_1 + C_2^\dagger W_m(\mathbf{y}_2;\frac{2\pi}{\beta}-v)C_2 \\
& + iC_1^\dagger\partial_m C_1 + iC_2^\dagger\partial_m C_2 + iS^\dagger\partial_m S, \qquad (5.24)
\end{aligned}
$$

where $W_m(\mathbf{x};v)$ represent the ordinary BPS monopole solution (B.1)–(B.4),

$$
\begin{aligned}
W_4(\mathbf{x};v) \;&=\; \Big[\frac{1}{|\mathbf{x}|} - \frac{v}{\coth(v|\mathbf{x}|)}\Big]\hat{x}_a\frac{\sigma_a}{2}, \\
W_i(\mathbf{x};v) \;&=\; \epsilon_{aij}\Big[\frac{1}{|\mathbf{x}|} - \frac{v}{\sinh(v|\mathbf{x}|)}\Big]\hat{x}_j\frac{\sigma_a}{2}. \qquad (5.25)
\end{aligned}
$$

The field configuration (5.24) is the desired expression for a single SU(2) caloron. Under the gauge transformation $A_m \to gA_m g^\dagger + ig\partial_m g^\dagger$, we see $C_i \to C_i g^\dagger$ and $S \to Sg^\dagger$.

Notice from equation Eq. (5.21) that $\mathcal{M}$ vanishes only at one point

$$x_{\text{singular}} = (\mathbf{x}_{\text{cm}}, x_4 = 0), \tag{5.26}$$

which is the center of mass of the constituent monopoles. We will see later on that the gauge field (5.24) turns out to have a gauge singularity at this point.

5.3 Various Limits of the Configuration

In this section, we will look at several special cases of the general caloron solution (5.24). A general picture of the relation between our solution and various special configurations is described by Figure 5.2.

The general caloron solution contains three parameters: $\mathcal{D}, v$ and β. When $v = 2\pi/\beta$ (or equivalently $v = 0$), it becomes the simple caloron solution known from [29] with two parameters $\rho = (\beta\mathcal{D}/\pi)^{1/2}$ and β. In the zero temperature limit ($\beta \to \infty$) with $\beta\mathcal{D}$ finite, the solutions of both the general and the simple caloron degenerate into the usual instanton solution with a single parameter $\rho = (\beta\mathcal{D}/\pi)^{1/2}$. When $\mathcal{D}$ gets large, a general caloron becomes two widely seperated constituent monopoles. Depending on which

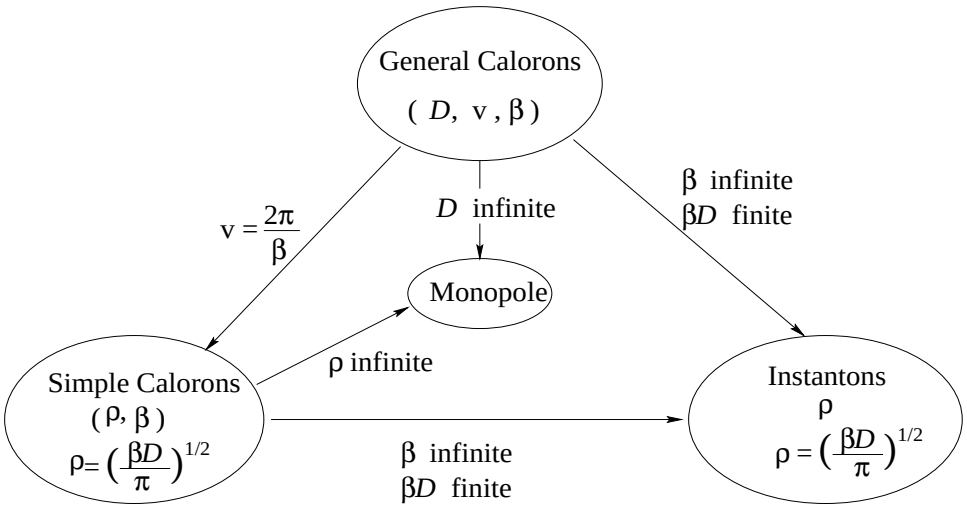

Figure 5.2: General calorons and their relation with other solutions.

monopole one is approaching, one can directly verify this monopole configuration. If one starts from the simple caloron solution and takes the large $\mathcal{D}$ limit (which means large ρ for a simple caloron), the limit will describe a single monopole as was mentioned in subsection 2.2.2. The reason for this is easy to understand in the constituent monopole picture, since in the case of a simple caloron, the other monopole is massless and large $\mathcal{D}$ limit separates the massless monopole which makes it trivial. We will see all these explicitly in the following subsections.

5.3.1 Near each monopole

To explicitly see that the configuration given by Eq. (5.24) describes two magnetic monopoles of opposite charge, let us consider the limit when the

distance D between the two monopoles is much greater than the core size of the monopoles, namely $D \gg 1/v$ and $D \gg (2\pi/\beta - v)^{-1}$. We expect the configuration to approach that of a single monopole near $\mathbf{x}_1$ or $\mathbf{x}_2$. If we are near the first monopole, $|\mathbf{y}_1| \ll D$, it's easy to see that

$$C_2, S_1, S_2 \sim \mathcal{O}(\frac{1}{\sqrt{D}}), \tag{5.27}$$

and

$$C_1 = \frac{\sigma_3 \cosh\frac{s_1}{2} - \boldsymbol{\sigma}\cdot\hat{\mathbf{y}}_1 \sinh\frac{s_1}{2}}{\sqrt{\cosh s_1 - (\hat{\mathbf{y}}_1)_3 \sinh s_1}} + \mathcal{O}(\frac{1}{D}). \tag{5.28}$$

Since C_1 is a single-valued unitary matrix, the whole gauge configuration (5.24) is gauge equivalent to the single monopole configuration $W_m(\mathbf{y}_1; v)$.

Similarly, if we are near the second monopole, $|\mathbf{y}_2| \ll D$, we see that

$$C_1, S_1, S_2 \sim \mathcal{O}(\frac{1}{\sqrt{D}}), \tag{5.29}$$

and

$$C_2 = \frac{-\sigma_3 \cosh\frac{s_2}{2} - \boldsymbol{\sigma}\cdot\hat{\mathbf{y}}_2 \sinh\frac{s_2}{2}}{\sqrt{\cosh s_2 + (\hat{\mathbf{y}}_2)_3 \sinh s_2}} e^{-i\frac{\pi x_4}{\beta}\sigma_3} + \mathcal{O}(\frac{1}{D}), \tag{5.30}$$

which is also a unitary matrix. Thus, the field configuration (5.24) becomes a gauge transformation of the second monopole configuration. The above discussion shows that the constituent monopoles can be identified when their cores are not overlapping.

5.3.2 Near singularity

To consider the singularity at point (5.26), let's choose the origin of the coordinates to be the center of mass of the two constituent monopoles. In this coordinate system, $(\mathbf{x}_1)_3 = -n_2 D$ and $(\mathbf{x}_2)_3 = n_1 D$. By expanding C_1, C_2 and S around $x_m = 0$, we get

$$C_1 \approx C_2 \approx \frac{i}{\sqrt{2}} g(x)_s, \quad S \approx \mathcal{O}(1), \tag{5.31}$$

where

$$g(x)_s = \frac{x_4 + i\sigma_3 x_3 + i(\sigma_1 x_1 + \sigma_2 x_2)q}{\sqrt{x_4^2 + x_3^2 + (x_1^2 + x_2^2)q^2}} \tag{5.32}$$

is a singular gauge transformation with $q = \sinh(2\pi n_1 n_2 D/\beta)/(2\pi n_1 n_2 D/\beta)$.

Thus the gauge field near the singularity $x_m = 0$ becomes

$$A_m = i g_s \partial_m g_s^\dagger + \mathcal{O}(1) \tag{5.33}$$

showing that it is a pure gauge singularity. Comparing Eqs. (5.32) and (5.33) with Eqs. (2.59) and (2.60), one can see that the nontrivial contribution at this gauge singularity to the topological charge (5.4) is one, as expected for a single instanton.

5.3.3 Massless monopole limit

When one of the constituent monopole becomes massless, the Wilson loop becomes trivial. The gauge symmetry is restored to the original SU(2) [29].

This is the situation in which the caloron solution was first derived. Without losing generality, we choose $v = 2\pi/\beta$. In this case the single monopole solution $W_m(y_2, 2\pi/\beta - v)$ disappears. The size of that monopole becomes infinite and its topological charge $1 - \beta v/2\pi$ vanishes. It loses its meaning as an isolated object.

It is convenient to put the massive monopole at the origin so that $\mathbf{y}_1 = \mathbf{x}$ and $\mathbf{y}_2 = D\hat{\mathbf{z}}$. In this limit, $N_2 = C_2 = 0$. After a large gauge transformation, $e^{-i\frac{\pi x_4}{\beta}\sigma_3}$, one can verify that the solution (5.24) becomes

$$A_m = -\bar{\Sigma}_{mn}\partial_n \ln \mathcal{N}, \tag{5.34}$$

with $\bar{\Sigma}_{mn}$ given by Eq. (2.63) and $\mathcal{N}$ given by

$$\mathcal{N} = 1 + \frac{D}{|\mathbf{x}|}\frac{\sinh(\frac{2\pi}{\beta}|\mathbf{x}|)}{\cosh(\frac{2\pi}{\beta}|\mathbf{x}|) - \cos(\frac{2\pi}{\beta}x_4)}. \tag{5.35}$$

This is exactly the periodic instanton solution (2.66) once we introduce a relation

$$D = \frac{\pi\rho^2}{\beta} \tag{5.36}$$

between the inter-monopole distance D and the instanton scale parameter ρ. At the zero temperature limit, $\beta \to \infty$, one can see from Eq. (5.36) that the finite size instanton solution can be obtained only if the distance between two magnetic monopoles approaches zero.

The caloron solution with massless constituent monopoles can be interpreted consistently with the previous picture of massless monopoles. When

we remove the massless monopole, $D \to \infty$, the configuration becomes that of a pure magnetic monopole [72]. When the massless monopole is at finite distance, the non-Abelian cloud shields the magnetic charge of the massive monopole at a distance scale D and the field configuration at $r \gg D$ falls off like a dipole field configuration which is the normal falloff behavior of an instanton [27].

5.3.4 Zero temperature limit

Another interesting limit to consider is the zero temperature limit $\beta \to \infty$, which implies $v \to 0$ by Eq. (5.3). Choosing the origin of the coordinates at the center-of-mass, we see that for finite $x = (\mathbf{x}, x_4)$,

$$\mathcal{M} \approx (2\pi/\beta)^2 x^2, \quad \mathcal{N} \approx 1 + \frac{\beta D}{\pi x^2}. \tag{5.37}$$

Thus the zero temperature limit of S in Eq. (5.18) is nontrivial only if βD remains finite. This is consistent with the argument after Eq. (5.36). After removing the singularity at the origin by a singular gauge transformation $g^\dagger = (x_4 + i\boldsymbol{\sigma} \cdot \mathbf{x})/\sqrt{x^2}$, the 2×2 matrix S of Eq. (5.18) becomes

$$S = \frac{x_4 + i\boldsymbol{\sigma} \cdot \mathbf{x}}{\sqrt{x^2 + \rho^2}} \tag{5.38}$$

with $\rho^2 = \beta D/\pi$ as shown in Eq. (5.36). The two matrices V_1, V_2 of Eq. (5.15) are simply

$$V_1 \approx V_2 \approx -\frac{\beta}{2\pi}\sqrt{\frac{2D}{x^2}} \tag{5.39}$$

From Eq. (2.87), it can be seen that the only contribution of the gauge field comes from the S terms, which lead to

$$A_m = \frac{2\Sigma_{mn}x_\nu}{x^2+\rho^2} \tag{5.40}$$

where Σ_{mn} is defined by Eq. (2.58). This is exactly the standard expression (2.57) for a single instanton on R^4.

5.4 Moduli Space Metric

Up to a normalization factor, the relative moduli space of the two constituent monopoles for a single instanton is known to be the Taub-NUT space with Z_2 division [52]. In this section, we will fix the normalization and provide a global picture of the moduli space. This also shed light on the zero temperature limit and the trivial Wilson loop limit.

To fix the normalization, we consider the additional real time direction x^0, which makes our theory five dimensional. Instantons and magnetic monopoles appear as self-dual solitons in the theory. The number of zero modes of a single instanton is eight and is the sum of the zero modes of the constituent monopoles. Each monopole carries four zero modes for its position and internal U(1) phase. We can interpret the eight instanton zero modes as four for the center of mass motion and four for the relative motions of the constituent monopoles. With the constituent monopole picture

in mind, defining the moduli space is quite similar to what people did for monopole cases [21]. For the infinitesimal change of the moduli parameters λ^α, $\alpha = 1, ..., 8$, the corresponding infinitesimal change $\delta_\alpha A_m$ should satisfy the background gauge (2.37) and the linearized self-dual equations (2.38). Then the moduli space metric is given by

$$g_{\alpha\beta} = \int d^4x \ \mathrm{tr}\,(\delta_\alpha A_m \delta_\beta A_m) \tag{5.41}$$

One can show this space to be hyperKähler by generalizing the argument in Ref. [21].

Since the two constituent monopoles are distinct and both are fundamental, the Lee-Weinberg-Yi metric can be applied. The only modification for the case at hand is that we have to integrate over x_4. This leads to an overall multiplicative factor β on the low energy effective Lagrangian. The center of mass moduli space is just $R^3 \times S^1$. Since $\beta(m_1 + m_2) = 8\pi^2$, the metric for the center-of-mass moduli space becomes

$$ds^2_{\mathrm{cm}} = 8\pi^2(d\mathbf{R}^2 + \frac{\beta^2}{4\pi^2} d\chi^2), \tag{5.42}$$

where $\mathbf{R}$ is the center-of-mass position and χ is the conjugate variable for the total electric charge. The overall coefficient $8\pi^2$ is the mass of the instanton.

The relative mass $m_1 m_2/(m_1 + m_2)$ of the two-monopole system is equal to $8\pi^2 n_1 n_2/\beta$, where n_1 and n_2 are introduced in Eq. (5.7). We introduce

$\mathbf{r} = \mathbf{x}_1 - \mathbf{x}_2$ to be the relative position between two monopoles. Applying the Lee-Weinberg-Yi metric to this case, one can obtain the metric for the relative moduli space (by multiplying β to Eq. (5.8) in Ref. [49]) as

$$ds^2_{\rm rel} = 8\pi^2 n_1 n_2 \Big[(1 + r_0/r)d\mathbf{r}^2 + r_0^2(1 + r_0/r)^{-1}(d\psi + \mathbf{w} \cdot d\mathbf{r})^2\Big], \qquad (5.43)$$

where $r_0 = \beta/(2\pi n_1 n_2)$ and $\mathbf{w}$ is the Dirac potential satisfying $\nabla \times \mathbf{w}(\mathbf{r}) = \nabla(1/r)$. This is the Taub-NUT space with length parameter $r_0/2$.

In the zero temperature limit $\beta \to \infty$, or in the limit where symmetry is restored, say, $n_2 \to 0$, the relative metric becomes flat. This is similar to the massless limit of the relative moduli space metric in SO(5) theory [50]. Using the instanton scale parameter ρ defined by Eq. (5.36), the metric (5.43) becomes

$$ds^2 = 16\pi^2(d\rho^2 + \rho^2 d\Omega_3^2) \qquad (5.44)$$

where $d\Omega_3^2$ is the metric of a unit three sphere. The overall coefficient $16\pi^2$ comes directly from calculating $\int d^4x(\delta_\rho A_m^a)^2$, which is straightforward because $\partial A_m^a/\partial\rho$ of Eq. (5.40) automatically satisfies the background gauge $D_m \delta A_m = 0$.

Chapter 6

Conclusion

In previous chapters, we have discussed several topics about topological objects in gauge theories. These discussions can be generalized along various directions. In this chapter, we would like to have a prospective look on these topics.

In chapter 3, we studied a purely Abelian BPS monopole configuration made of two identical massive monopoles and one massless monopole in an Sp(4) theory with symmetry breaking pattern $\mathrm{Sp}(4) \to \mathrm{SU}(2) \times \mathrm{U}(1)$.

As we mentioned in section 3.1, there are three gauge theories (based on SU(3), Sp(4) and G_2 gauge groups) that contain similar monopole systems to what we studied. Among these theories, the G_2 case has not been studied yet. From the previous experiences, we can see how in principle one might find the moduli space metric for two identical massive and one massless

monopoles in the theory with $G_2 \rightarrow SU(2)\times U(1)$. To get this, one may start from the theory with $SO(8) \rightarrow SU(2)^3\times U(1)$ with two identical massive and three distinct (and non-interacting) massless monopoles. If one identifies all three massless monopoles, then the configuration would be the demanded two massive and one massless monopoles in G_2. The boundary conditions in this case will be much more complicated than those in SU(3) and Sp(4) cases since one has to not only consider the identification of three SO(8) monopoles but also to embed the SO(8) group itself into the SU(8) group.

Although we don't have quantitative results for the G_2 case, we can still make a few conjectures. We think the four dimensional hyperKähler quotient spaces $M^4(\boldsymbol{\zeta} = 0)$ corresponding to SU(3), Sp(4) and G_2 are Atiyah-Hitchin (a double covering of it), $R^3 \times S^1$ and Taub-NUT, respectively. This conjecture is known to be true for SU(3) and Sp(4) cases, and we believe that for both the Sp(4) and G_2 cases, $\boldsymbol{\zeta} = 0$ corresponds to minimal cloud size, namely the massless monopole is on the line connecting the two massive monopoles. Since the position of the massless monopole can be changed by gauge transformations, one can make it overlap with one of the massive monopoles. In doing this, $M^4(\boldsymbol{\zeta} = 0)$ can be thought of describing the moduli space of one $\boldsymbol{\beta}$ and one $\boldsymbol{\alpha} + \boldsymbol{\beta}$ monopoles. It's easy to verify from the G_2 root diagram that $\boldsymbol{\beta}$ and $\boldsymbol{\alpha} + \boldsymbol{\beta}$ are equivalent roots with relative angle $4\pi/3$ and therefore are equivalent to the two distinct simple roots of SU(3) group. The moduli

space of such a monopole system is known to be Taub-NUT[1].

It's quite amusing to notice that the $D-E$ space of the Sp(4) case is made of eight copies of the $k-D$ spaces as if the $D-E$ space is divided by the *root diagram* of the gauge group Sp(4) (see Figure 3.3). Similarly in the SU(3) case, the $D-E$ space is made of six copies of the $k-D$ spaces [16] as if the $D-E$ space is divided by the root diagram of SU(3). One might guess that the $D-E$ space of G_2 theory is divided by the G_2 root diagram, namely made of twelve copies of $k-D$ spaces.

Another direction to explore is to find the moduli space in the case when the $\boldsymbol{\alpha}$ monopole becomes massive so that there are two identical massive monopoles and one distinct massive monopole. For the SU(3) case, this problem has already been solved [35]. A similar consideration for Sp(4) is possible. Finally it would be very interesting to find out the structure of the moduli space of three massive and three massless monopoles in the theory where SU(4)$\rightarrow$SU(3)$\times$U(1). As argued in section 3.1, these configurations can be regarded as a kind of magnetic dual of baryons. Studying such configurations might be helpful to understand the structure of baryons.

In chapter 4, we analyzed the energy density of two monopole systems in SU(3) and Sp(4) theories and obtained some idea of how the massless cloud

[1]This argument also works for the Sp(4) case when $\boldsymbol{\beta}$ and $\boldsymbol{\alpha}+\boldsymbol{\beta}$ are equivalent roots with relative angle $\pi/2$ and therefore describe two non-interacting monopoles. The moduli space is thus $R^3 \times S^1$.

forms. Based on these results one can make some qualitative conjectures on what might happen in the general case where the interaction energy can be defined as

$$\rho_{\rm int} = \rho_{\rm total} - \rho_{\rm massive} - \rho_{\rm massless} \tag{6.1}$$

The basic property of $\rho_{\rm int}$ that we learned from the previous observation is that when the total magnetic charge is purely Abelian, the interaction is more "localized" in contrast to the opposite case. Such an interaction extracts energy from distant regions, accumulates it in the vicinity of the massive monopoles and gradually builds up the structure of the non-Abelian cloud. This is fairly similar to the Sp(4) case.

When the total magnetic charge is non-Abelian, however, qualitatively different situations could arise in general. To see this, let's look at the case with the symmetry breaking pattern SU(N)→U(1)×SU(N-2)×U(1) ($N >$ 4). Let $\boldsymbol{\alpha}_1, ..., \boldsymbol{\alpha}_{N-1}$ denote simple roots. When the system contains massive $\boldsymbol{\alpha}_1$, $\boldsymbol{\alpha}_{N-1}$ and would-be massless $\boldsymbol{\alpha}_i$ ($i = 2, ..., N-3$) monopoles (notice that the $\boldsymbol{\alpha}_{N-2}$ monopole is absent and so the total magnetic charge of the system is non-Abelian), only massive monopoles survive at the massless limit. This can be seen by noticing that the system under consideration is equivalent to the system studied in [80] (which contains the $\boldsymbol{\alpha}_{N-2}$ monopole as well and so the total magnetic charge is Abelian) with the $\boldsymbol{\alpha}_{N-2}$ monopole removed.

From [80] we know that the only cloud parameter of the system is given by

$$\mathcal{D} = \sum_{i=2}^{N-1} |\mathbf{x}_i - \mathbf{x}_{i-1}| \tag{6.2}$$

So removing any massless monopole is equivalent to removing the whole cloud (since it makes the cloud size infinity) therefore only massive monopoles survive. This situation is similar to the SU(3) case we have studied. But there are other systems which don't show such a direct analogue with SU(3) case. As an example we can go back to our Sp(4) theory, and consider a system with N massive $\boldsymbol{\alpha}$ monopoles and $N-1$ would-be massless $\boldsymbol{\beta}$ monopoles (so the total magnetic charge is non-Abelian). In the massless limit, the massless monopoles in this system will form a non-Abelian cloud rather than disappearing. This is because such system can be obtained by removing one $\boldsymbol{\beta}$ monopole from a system containing N ($N > 1$) $\boldsymbol{\alpha}-\boldsymbol{\beta}$ pairs. At the massless limit the latter system contains a non-Abelian cloud with many independent size parameters. Removing one $\boldsymbol{\beta}$ monopole will not make all these parameters infinite and therefore will not destroy the whole cloud. Another way to understand this is to notice that when the extra $\boldsymbol{\alpha}$ monopole is removed, we are left with a system made of $N-1$ $\boldsymbol{\alpha}-\boldsymbol{\beta}$ pairs (it can be called an Abelian sub-system) which certainly contains a non-Abelian cloud. Since removing the $\boldsymbol{\alpha}$ monopole won't create a cloud, the cloud must exist in the original system. This argument can be generalized.

These examples reveal the complexity of the general cases. It seems that in the massless limit a system with a non-Abelian total magnetic charge can still contain massless monopoles (in the form of a non-Abelian cloud) in a "maximal Abelian sub-system". Further considerations on such situations will be interesting.

In chapter 5, by using ADHMN construction, we found the field configuration for a single instanton in the SU(2) gauge theory on $R^3 \times S^1$. When the gauge group is spontaneously broken by the Wilson loop, a single instanton is shown to be composed of two fundamental monopoles of opposite magnetic charge. By taking various limits, our solution is shown to be consistent with previously known ideas about periodic instantons, massless monopoles and zero temperature instantons.

Parallel to what we introduced in chapter 5, a different method was adopted in Ref. [41, 42, 43]. In these works, the usual ADHM method for instanton was used. The existence of these two methods itself can be thought of as a good explanation of the fact that instantons are made of constituent monopoles.

As we mentioned in chapter 1, understanding the relationship between instantons and magnetic monopoles is crucial in order to have a consistent picture of QCD vacuum. The constituent monopole picture of instantons might be a good start point to pursue this problem [8, 63].

There are several interesting implications from our work as mentioned in Ref. [46, 52]. Here we want to point out that the zero temperature limit may be interesting. In the zero temperature limit of a single caloron, the positions of both monopoles should come together to the center in order to get a finite size instanton, which makes the monopole picture somewhat trivial. However the story cannot be that simple for the two-caloron case. Even in the zero temperature limit of two close-by calorons, there are no identifiable instanton positions [10, 39]. Thus, it is not clear where the four constituent monopoles for the two calorons will end up at the zero temperature limit. Thus, we hope that the picture of the composite instantons and their constituent monopoles survives nontrivially, and leads to new insight on understanding the chiral symmetry and confinement in zero temperature QCD.

It will also be interesting to explore the relation between the constituent monopole picture and the previously conjectured picture based on Abelian projection [75].

The structure of non-Abelian gauge theories was established almost half a century ago. Regardless of the breakthrough physicists have made since then, we are still far away from fully understanding the implications of those theories. The past 20 years have seen a burst of new ideas, concepts and techniques in related to topological objects in gauge theories. We believe that this is only the beginning of the story. What we have probed is only a

tip of the iceberg. Topological objects of the gauge theories are like windows through which we will be able to reveal the tremendously rich structures hidden in the those theories.

Appendix A

Mathematics Appendix

A.1 Simple Facts about Lie Algebras

It is known that associated to any n-parameter Lie group there are n infinitesimal operators defined by their commutation properties. These operators form a mathematical structure called a Lie algebra. More precisely, one has the following definition:

Definition 1: A vector space $\mathcal{G}$ over a field K is said to constitute a *Lie algebra* if for any pair of vectors $X, Y \in \mathcal{G}$ there corresponds a vector $Z = [X, Y] \in \mathcal{G}$ such that

$$[\kappa X + \lambda Y, Z] = \kappa[X, Z] + \lambda[Y, Z] \tag{A.1}$$

$$[X, Y] + [Y, X] = 0 \tag{A.2}$$

$$[X, [Y, Z]] + [Y, [Z, X]] + [Z, [X, Y]] = 0 \tag{A.3}$$

hold for all $\kappa, \lambda \in K$ and all $X, Y, Z \in \mathcal{G}$. $Z = [X, Y]$ is called the *Lie bracket* or *commutator* of X and Y.

The following concepts about subalgebras will be used in other definitions:

Definition 2: A subset $\mathcal{G}'$ of a Lie algebra $\mathcal{G}$ is called a *subalgebra* of $\mathcal{G}$ if $\mathcal{G}'$ itself forms a Lie algebra. The subalgebra $\mathcal{G}'$ is said to be *Abelian* if $[X, Y] = 0$ $(\forall X, Y \in \mathcal{G}')$. The subalgebra $\mathcal{G}'$ is said to be *proper* if it is not the whole algebra but contains elements other than 0. The subalgebra $\mathcal{G}'$ is called an *invariant subalgebra* if $[X, Y] \in \mathcal{G}'$ $(\forall X \in \mathcal{G}', Y \in \mathcal{G})$.

Now we can define the important concepts of simple and semi-simple algebras:

Definition 3: A Lie algebra is said to be *simple* if it is not Abelian and contains no proper invariant subalgebras. A Lie algebra is said to be *semi-simple* if it is not Abelian and contains no proper Abelian invariant subalgebras.

Any simple or semi-simple algebra must be more than one dimensional. A simple algebra is always semi-simple. All these concepts of Lie algebras can be similarly defined for Lie groups. Simple (semi-simple) Lie algebras correspond to simple (semi-simple) Lie groups. All the classical Lie groups, namely SO(N) ($N \geq 3$), SU(N) ($N \geq 2$), Sp($2N$) ($N \geq 1$) and exceptional Lie groups, namely G_2, F_4, E_6, E_7, E_8 are semi-simple groups. Among them, all except SO(4)$\cong$ SO(3)$\oplus$SO(3) are simple groups.

Since Lie algebras are all vector spaces, we can always choose a proper

set of base vectors as we can do for any other vector spaces. For physicists, the so-called Cartan-Weyl basis is particularly useful.

Definition 4: A *Cartan-Weyl basis* of an n-dimensional Lie algebra contains r elements $H_1, ..., H_r$ that form a maximal mutually commutative set (the number of elements r of this set is called the rank of the Lie algebra. This set of elements span a subalgebra called the *Cartan subalgebra*) and $n-r$ other elements $E_{\boldsymbol{\alpha}}, E_{\boldsymbol{\beta}}, ...$ satisfying the following commutative relations:

$$[H_i, H_j] = 0 \tag{A.4}$$

$$[H_i, E_{\boldsymbol{\alpha}}] = \alpha_i E_{\boldsymbol{\alpha}} \tag{A.5}$$

$$[E_{\boldsymbol{\alpha}}, E_{-\boldsymbol{\alpha}}] = \boldsymbol{\alpha} \cdot \mathbf{H} \tag{A.6}$$

$$[E_{\boldsymbol{\alpha}}, E_{\boldsymbol{\beta}}] = N_{\boldsymbol{\alpha}\boldsymbol{\beta}} E_{\boldsymbol{\alpha}+\boldsymbol{\beta}} \quad (\boldsymbol{\alpha} + \boldsymbol{\beta} \neq 0) \tag{A.7}$$

The choice of Cartan-Weyl basis is not unique. In particular, one can choose the Cartan subalgebra to contain any given set of mutually commutative elements of the Lie algebra. We have used this fact in subsection 2.1.4 to choose both Φ_∞ and $G(\hat{\mathbf{z}})$ to be in the Cartan subalgebra.

From Eq. (A.5) we notice that any element $E_{\boldsymbol{\alpha}} \in \mathcal{G}$ can be represented by an r-dimensional vector $\boldsymbol{\alpha}$ whose components are the α_i appearing in Eq. (A.5). These vectors $\boldsymbol{\alpha}, \boldsymbol{\beta}, ...$ are called root vectors. A diagram containing all those roots is called a root diagram.

Definition 5: A set of linearly independent roots are called *simple roots* if any other root can be expressed as a linear combinations of these roots with coefficients either all positive integers (the corresponding root is called a *positive root*) or all negative integers (the corresponding root is called a *negative root*).

For any Lie algebra, it is always possible to find a set of simple roots, and usually there is more than one set of simple roots.

Definition 6: There is associated to any root $\boldsymbol{\alpha}$ a *co-root* (or *dual root*) $\boldsymbol{\alpha}^*$ which is defined as $\boldsymbol{\alpha}^* = \boldsymbol{\alpha}/|\boldsymbol{\alpha}|^2$.

It turns out that, as in the case of roots, any co-root can be expressed as a linear combination of the co-roots of simple roots with coefficients either all positive integers or all negative integers.

A.2 HyperKähler Quotient

This section gives a brief description of the concepts of moment map and hyperKählar quotient which are used in chapter 3. For more details, see [28, 33]. The hyperKähler quotient is a powerful tool to construct new hyperKähler spaces based on the symmetries of known hyperKähler spaces.

Let M be a symplectic manifold[1] with symplectic form ω. Let $G : M \rightarrow$

[1]Briefly speaking, a symplectic manifold is an even dimensional manifold equipped with a non-singular, closed 2-form.

M be a transformation group acting on M which leaves the symplectic structure ω invariant, namely $L_\xi \omega = 0$, for all the left invariant vector field ξ corresponding to the Lie algebra g of the group G.

Notice that $L_\xi = d \cdot i_\xi + i_\xi \cdot d$, where i_ξ acting on any form gives the inner product of the vector field ξ and that form. Since the simplectic form ω is closed, $d\omega = 0$, we have

$$L_\xi \omega = d(i_\xi \omega) + i_\xi \cdot d\omega = d(i_\xi \omega) = 0 \tag{A.8}$$

which means $i_\xi \omega$ is a closed 1-form.

Under certain mild topological conditions (namely that the first cohomology group $H_1(M, R)$ vanishes – which we assume to be satisfied) any closed 1-form is exact. So for each $i_\xi \omega$ there exists a function $f_\xi(x)$ (the subscript ξ reminds us that f depends on ξ) such that

$$i_\xi \omega \equiv \langle \xi, \omega \rangle = df_\xi(x). \tag{A.9}$$

For any given x, this relation defines a linear function that maps a Lie algebra element ξ into a real number $f_\xi(x)$, Such linear functions on g are (by definition) elements in the dual space g^* of the Lie algebra g. We use $\mu(x)$ to denote these element (x reminds us that different x correspond to different elements). They satisfy:

$$(\mu(x), \xi) \equiv f_\xi(x). \tag{A.10}$$

Since $\mu(x)$ is an element in g^*, one can treat μ as a map from the manifold M to the dual of the Lie algebra g^*, namely $\mu : M \to g^*$.

The map μ defined in this way is called the *moment map* on the symplectic manifold. Since Kähler and hyperKähler manifolds are special kinds of symplectic manifolds[2], the definition of moment map remains the same for those manifolds.

The moment map has an important property: $\forall a \in G : \mu(ax) = a\mu(x)$, where the a at right hand side is actually in the co-adjoint representation of G which takes the vector space g^* as its base space (see [28] for a proof of this statement). So far the only pre-requisite we used is a symmetry group that leaves the symplectic form invariant.

What makes the moment map useful is that it helps us to construct new symplectic (or Kähler and hyperKähler) manifolds from known symplectic (or Kähler and hyperKähler) manifolds. We will use the *symplectic quotient* as an example to show how it works.

Let $\lambda \in g^*$ be an element of g^*. $N_\lambda = \mu^{-1}(\lambda) \subset M$ is a submanifold of M. It can be proved that $\dim N_\lambda = 2n - \dim G$,[3] which is not always an even

[2]A Kähler manifold is a symplectic manifold equipped with a complex structure. A hyperKähler manifold is a symplectic manifold equipped with three complex structures satisfying the quaternion algebra.

[3]To see this, first notice that for all $x \in N$ and $\xi \in g$, $f_\xi(x) \equiv (\mu(x), \xi) = (\lambda, \xi)$ is independent of x. So $df_\xi(x)|_{x \in N_\lambda} = 0$, which means $df_\xi \in T^*M$ vanishes when acting on $\eta \in TN_\lambda$. We then remember $df_\xi \equiv i_\xi \omega$, so $df_\xi(\eta) = 0$ is equivalent to $i_\xi \omega(\eta) = \omega(\xi, \eta) = 0$.

number. Therefore N_λ is usually not a symplectic space. But fortunately it turns out that in case λ is invariant under G (in its co-adjoint representation), N_λ admits a symmetry G,[4] which means the quotient manifold N_λ/G is well defined. This quotient manifold has dimension $2n-2\dim G$ and has a natural symplectic form derived from N_λ [33] and therefore is always a symplectic manifold. Such a manifold is called the symplectic quotient manifold of M.

In the above construction the group G is assumed to act on M *freely* (namely the isotropy subgroup [5] is the identity) which ensures that each orbit has dimension $\dim G$.

Let's summarize the logic briefly. To construct the symplectic quotient, we need to do two things: The first is to find a group action that leaves the symplectic structure of the manifold invariant. Such a group defines a moment map μ. The second is to find a G-invariant point λ in the range of μ, this ensures that $\mu^{-1}(\lambda)$ is invariant under G, therefore one can construct the symplectic quotient manifold $\mu^{-1}(\lambda)/G$. The whole point of the symplectic quotient is based on the symmetries of the manifold and it gives a powerful tool to construct new symplectic space from the known ones.

Now notice that ξ is an arbitrary element of g, so $\dim\{\xi\} = \dim G$. Let $\dim M = 2n$, since ω is non-singular so $\dim N_\lambda = \dim T_x N_\lambda = \dim\{\eta\} = \dim M - \dim\{\xi\} = 2n - \dim G$.

[4] To see this, notice that $G\lambda = \lambda$ implies $\mu(Gx) = G\mu(x) = G\lambda = \lambda$, therefore $Gx \in N_\lambda$ $(\forall x \in N_\lambda)$.

[5] At each point of M, the isotropy subgroup is a subgroup of G that leaves that point invariant.

For a Kähler manifold M, if G preserves the metric and the Kähler form and acts on M freely, then the same construction (now called the Kähler quotient) leads to a manifold admitting a natural Kähler structure. Similarly, for a hyperKähler manifold M, if a group G preserves the metric and all three Kähler forms (such group action is said to be *tri-holomorphic*) and acts on M freely then we would have three moment maps (corresponding to three Kähler forms) which can be combined into a single moment map $\boldsymbol{\mu} : M \to g^* \times R^3$ (since the element in $g^* \times R^3$ has form $(\lambda_1, \lambda_2, \lambda_3)$). The same construction (now called the hyperKähler quotient) leads to a new hyperKähler mainfold.

The dimension of the Kähler quotient manifold is $\dim M - 2\dim G$, the same as the dimension of the symplectic quotient manifold, but the dimension of hyperKähler quotient manifold is $\dim M - 4\dim G$ since instead of $\omega(\xi, \eta) = 0$ we now have two more such constraints.

As an example, let's derive Eq. (3.30). Let

$$\mathbf{T} = e_i T_i + T_4. \tag{A.11}$$

The metric of the quaternion space is defined as

$$ds^2(\mathbf{T}, \mathbf{T}) = \int_{-1}^{1} dt \ \mathrm{tr}\,(T_m T_m). \tag{A.12}$$

It is easy to see that the three Kähler forms are

$$\omega_1 \equiv ds^2(e_1\mathbf{T}, \mathbf{T}) = \int_{-1}^{1} dt \ \mathrm{tr}\,(dT_4 \wedge dT_1 + dT_2 \wedge dT_3)$$

$$\omega_2 \equiv ds^2(e_2\mathbf{T},\mathbf{T}) = \int_{-1}^{1} dt\ \mathrm{tr}\,(dT_4 \wedge dT_2 + dT_3 \wedge dT_1) \tag{A.13}$$
$$\omega_3 \equiv ds^2(e_3\mathbf{T},\mathbf{T}) = \int_{-1}^{1} dt\ \mathrm{tr}\,(dT_4 \wedge dT_3 + dT_1 \wedge dT_2)$$

The U(1) center of the U(2) transformation is generated by $g = e^{i\delta\theta\cdot t}$ which leads to $\delta T_4 = \delta\theta,\ \ \delta T_i = 0$. The corresponding tangent vector field is:

$$\xi = \delta\theta \frac{\partial}{\partial T_4}, \tag{A.14}$$

which leads to

$$\langle \xi, \omega_i \rangle = \delta\theta \mathrm{tr}\, dT_i = d(\delta\theta \mathrm{tr}\, T_i). \tag{A.15}$$

Comparing with Eq. (A.9), we obtains the following vector function (since we now have three components):

$$\mathbf{f}_\xi = \delta\theta(\mathrm{tr}\, T_1, \mathrm{tr}\, T_2, \mathrm{tr}\, T_3). \tag{A.16}$$

Since $\mathbf{f}_\xi = \langle \boldsymbol{\mu}, \xi \rangle = \delta\theta\boldsymbol{\mu}$, so the moment map is

$$\boldsymbol{\mu} = (\mathrm{tr}\, T_1, \mathrm{tr}\, T_2, \mathrm{tr}\, T_3), \tag{A.17}$$

which is just Eq. (3.30).

A.3 Derivation of (3.38)

We are considering the case with a single interval. To distinguish the normalized kernal matrix (made of kernal vectors) from the non-normalized kernal

matrix, we denote the former as V_0, namely

$$\int V_0^\dagger V_0 dt = I. \tag{A.18}$$

The Higgs field given by (2.79) can be written as

$$\Phi = \int t V_0^\dagger V_0 dt. \tag{A.19}$$

To prove that (A.19) and (3.38) give gauge equivalent results (of course under the condition (3.37)), it is sufficient to prove that both expressions can be diagonized (through unitary transformations with same winding number) into a common diagonal matric (since Φ is Hermitian, it is always diagonalizable). We will prove this in this section.

Notice that both $\int V^\dagger V dt$ and $\int tV^\dagger V dt$ are Hermitian matrices, and because of condition (3.37), they can be diagonized by a common unitary matrix U:

$$\int V^\dagger V dt = U\Lambda_1 U^\dagger, \tag{A.20}$$

$$\int tV^\dagger V dt = U\Lambda_2 U^\dagger, \tag{A.21}$$

where Λ_1 and Λ_2 are diagonal matrices. It is easy to see from (A.18) and (A.20) that

$$\int V^\dagger V dt = U\Lambda_1^{\frac{1}{2}} \left(\int V_0^\dagger V_0 dt \right) \Lambda_1^{\frac{1}{2}} U^\dagger, \tag{A.22}$$

which means that one can choose V_0 to be

$$V_0 = VU\Lambda_1^{-\frac{1}{2}} U'^\dagger \tag{A.23}$$

in order to satisfy normalization condition. Here the unitary transformation U' has the same winding number as U, it is introduced to cancel any possible winding effect caused by U.

Now let's diagonize the Higgs field given by (A.19) and (3.38). Using relation (A.23), (A.19) can be written as

$$\begin{aligned}
\Phi &= \int t V_0^\dagger V_0 dt \\
&= U' \Lambda_1^{-\frac{1}{2}} U^\dagger \left(\int t V^\dagger V dt \right) U \Lambda_1^{-\frac{1}{2}} U'^\dagger \\
&= U' \Lambda_1^{-\frac{1}{2}} \Lambda_2 \Lambda_1^{-\frac{1}{2}} U'^\dagger \\
&= U' \Lambda_1^{-1} \Lambda_2 U'^\dagger . \qquad \text{(A.24)}
\end{aligned}$$

On the other hand it's easy to see that (3.38) leads to

$$\Phi = U \Lambda_1^{-1} \Lambda_2 U^\dagger . \qquad \text{(A.25)}$$

Eqs. (A.24) and (A.25) means the two methods are gauge equivalent (since U and U' have same winding number).

Appendix B

Single SU(2) Monopole

B.1 Field Configuration

In this subsection of the appendix, let's construct the field configuration of a single static SU(2) monopole. We adopt the following ansatz ($r = |\mathbf{x}|, \hat{r}^j = x^j/r$):

$$\Phi^a(\mathbf{x}, v) = v\hat{r}^a \mathrm{H}(evr), \tag{B.1}$$

$$A_i^a(\mathbf{x}, v) = -\epsilon_{ij}^a \frac{\hat{r}^j}{er}[1 - \mathrm{J}(evr)], \quad A_0^a = 0. \tag{B.2}$$

Here we have stressed the v dependence of the solution. This ansatz ensures a unit winding number for the Higgs configuration and the transversality of gauge potential. The rest of the conventions are for convenience of computation. We want our monopole solution to satisfy the proper asymptotic behavior at spatial infinity and to be non-singular at the origin. This leads

to the boundary conditions: $\mathrm{H}(\infty) = 1,\ \mathrm{J}(\infty) = 0,\ \mathrm{H}(0) = 0$ and $\mathrm{J}(0) = 1$. Plugging ansatz (B.1) and (B.2) into the equations of motion we will get a set of differential equations for $\mathrm{H}(x)$ and $\mathrm{J}(x)$. Although it is known that well-behaviored solutions exist for this set of differential equations and boundary conditions, so far no analytical solution has been found for $\lambda \neq 0$. The case with $\lambda = 0$ was first considered by M. K. Prasad and C. M. Sommerfeld [69] and is now called the Prasad-Sommerfeld limit. In this limit the solution for $\mathrm{H}(x)$ and $\mathrm{J}(x)$ can be found as

$$\mathrm{H}(x) = \coth x - \frac{1}{x}, \tag{B.3}$$

$$\mathrm{J}(x) = \frac{x}{\sinh x}. \tag{B.4}$$

Plugging Eqs. (B.3) and (B.4) into ansatz (B.1) and (B.2) one obtains the explicit configuration of a single SU(2) monopole.

In the Prasad-Sommerfeld limit, the Higgs potential vanishes but $\Phi^a\Phi^a = v^2$ is still imposed as a constraint. It is this parameter v that generates the mass scale of the theory. In the Prasad-Sommerfeld limit the massless Higgs is often called the dilaton and the dilatonic field D is defined by the following expansion

$$\Phi^a = (v + D)\hat{r}^a + \mathcal{O}\left[\exp(-2evr)\right]. \tag{B.5}$$

Comparing with the explicit solution one can easily evaluate the dilatonic

charge:

$$Q_D = \int_{S_\infty} \nabla D \cdot d\vec{S} = g. \tag{B.6}$$

The fact that the dilatonic charge of a monopole is equal to its magnetic charge is crucial for the existence of multi-monopole solutions.

B.2 Moduli Space and Its Metric

It is known that a single SU(2) monopole has four collective coordinates (or zero modes). It is quite obvious that three of them are the spatial coordinates of the monopole. The fourth coordinate turns out to be the unbroken U(1) phase angle. To see this we notice that the fourth tangent vector satisfies Eqs. (2.52) and (2.53). It is not hard to check that the solution of these equations (modulo small gauge transformations) can be chosen as

$$\delta A_0 = 0, \tag{B.7}$$

$$\delta A_m = D_m(\chi\Phi). \tag{B.8}$$

This ansatz can be generated by a gauge transformation (of A_m) with $g = e^{i\chi\Phi}$. Since g does not approach unity at spatial infinity, this is a large transformation which means χ is a coordinate in the moduli space. Since χ is periodic this fourth coordinate is S^1 rather than R^1,

These collective coordinates of the monopole moduli space label degenerate monopole solutions. However, any motion in the moduli space will cause

an increase in energy. We are talking about slow motions in moduli space such that the Bogomol'nyi condition can be thought of as being satisfied at each instant. It is obvious that a translation of an single SU(2) monopole will generate a kinetic energy $\frac{1}{2}vg\dot{\mathbf{x}}^2$. How about the motion along the fourth coordinate? From Eqs. (B.7) and (B.8) one can see that any motion along the fourth coordinate will generate an electric field

$$E_i = D_0\delta A_i = \dot{\chi}D_i\Phi = \dot{\chi}B_i. \tag{B.9}$$

Thus, the motion along the fourth coordinates turns a monopole into a dyon. The kinetic energy due to the electric field is $\frac{1}{2}vg\dot{\chi}^2$.

The metric structure of the moduli space can be obtained without computation since from the conservation laws of energy, momentum and charge, any constant motion will remain constant. Therefore the metric is flat. So not only topologically, but also metrically, the moduli space of a single SU(2) monopole is

$$\mathcal{M} = R^3 \times S^1, \tag{B.10}$$

with flat metric

$$ds^2 = \frac{1}{2}vgd\mathbf{x}\cdot d\mathbf{x} + \frac{1}{2}vgd\chi d\chi. \tag{B.11}$$

The metric coefficients come directly from the kinetic energy of the monopole.

B.3 ADHMN Construction

As a demonstration of the ADHMN construction, let's compute the Higgs configuration of a single SU(2) monopole. The Nahm data in this case are a triplet of constants representing the center of the monopole. Without losing generality, we choose these to be zero. Therefore Eq. (2.77) becomes

$$\left(i\frac{d}{dt} - i\mathbf{x}\cdot\boldsymbol{\sigma}\right) V = 0. \tag{B.12}$$

We further choose the interval to be $[-\frac{1}{2}, \frac{1}{2}]$, namely $v = 1$ (mass $m = 4\pi$). By requiring

$$\int_{-\frac{1}{2}}^{\frac{1}{2}} dt\, V^\dagger V = 1 \tag{B.13}$$

we obtain the solution

$$V = \left(\frac{r}{\sinh r}\right)^{\frac{1}{2}} \exp(\mathbf{x}\cdot\boldsymbol{\sigma} t). \tag{B.14}$$

Plugging this into Eqs. (2.78)(2.80) yields the expected result:

$$\Phi = -\int_{-\frac{1}{2}}^{\frac{1}{2}} dt\, tV^\dagger V = \Phi^a t^a, \tag{B.15}$$

$$A_i = i\int_{-\frac{1}{2}}^{\frac{1}{2}} dt\, V^\dagger \partial_i V = A_i^a t^a, \tag{B.16}$$

where

$$t^a = -\frac{1}{2}\sigma^a, \tag{B.17}$$

$$\Phi^a = \mathrm{H}(r)\hat{r}^a, \tag{B.18}$$

$$A_i^a = -\epsilon_{ij}^a \frac{\hat{r}^j}{r}\left[1 - \frac{r}{\sinh r}\right]. \tag{B.19}$$

The minus sign for t^a comes from the fact that the interval is defined to be $[-\frac{1}{2}, \frac{1}{2}]$ therefore $\mathbf{h} \cdot \mathbf{H} \propto -\sigma_3$. If we choose the interval to be $[\frac{1}{2}, -\frac{1}{2}]$, the minus sign will disappear.

Appendix C

Quantization of Charges

C.1 Dirac's Monopole

Dirac considered the the quantum mechanics of a charged particle moving in the magnetic field generated by a point-like magnetic monopole. He assumed, in complete analogy with electricity, that the magnetic field of such a monopole is given by Coulomb's law:

$$\mathbf{B} = \frac{g\hat{\mathbf{r}}}{4\pi r^2} \tag{C.1}$$

To consider the quantum mechanics of electrically charged particles in a magnetic field, we notice that one of the remarkable features of quantum mechanics is that it is the vector potential (defined by $\mathbf{B} = \nabla \times \mathbf{A}$) rather than the magnetic field that enters wave equation. For our purpose, let's look at the vector potential on a sphere centered at the location of the monopole.

From Eq. (C.1), it is easy to see that in spherical coordinates (r, θ, ϕ),

$$\mathbf{A} = \frac{g}{4\pi} \frac{a - \cos\theta}{r \sin\theta} \hat{\boldsymbol{\phi}} + \nabla\chi, \tag{C.2}$$

where a is an arbitrary constant and χ is an arbitrary smooth function. Since the gradient term is smooth and won't affect any of our arguments, we will drop it in what follows. As for the first term we notice that it is impossible to choose any value of a such that $\mathbf{A}$ is non-singular on the whole sphere. This is not surprising since there is no non-singular vector field on the sphere. The standard method to handle this problem is to introduce two patches to cover the sphere and define a non-singular vector potential on each patch. Let's choose the first patch U_1 to cover the upper hemisphere and the equator, the second patch U_2 to cover the lower hemisphere and the equator. It is easy to see that a can be chosen as 1 in the first patch and –1 in the second to ensure a non-singular $\mathbf{A}$ in the corresponding patch, namely

$$\mathbf{A}_{U_1} = \frac{g}{4\pi} \frac{1 - \cos\theta}{r \sin\theta} \hat{\boldsymbol{\phi}}, \tag{C.3}$$

$$\mathbf{A}_{U_2} = -\frac{g}{4\pi} \frac{1 + \cos\theta}{r \sin\theta} \hat{\boldsymbol{\phi}}. \tag{C.4}$$

In the overlap of the patches $U_1 \cap U_2$ we have

$$\mathbf{A}_{U_1} - \mathbf{A}_{U_2} = \frac{g}{2\pi \sin\theta} \hat{\boldsymbol{\phi}} = \nabla \left(\frac{g\phi}{2\pi} \right), \tag{C.5}$$

which means that the two expressions of $\mathbf{A}$ differ by a gauge transformation. It is known that under such a gauge transformation the wave functions (in

$U_1 \cap U_2$) are related by

$$\psi_{U_1} = \exp\left(\frac{ieg\phi}{2\pi\hbar}\right)\psi_{U_2}. \tag{C.6}$$

This is valid in both the non-relativistic and the relativistic cases. Since both wave functions must be single-valued (namely $\phi = 2\pi$ must be identified with $\phi = 0$), therefore we have the following condition:

$$eg = 2\pi n\hbar. \tag{C.7}$$

This is the famous Dirac quantization condition.

Dirac quantization condition (C.7) is a very general result. As we can see from the derivation, we have only used the behavior of the gauge field on a sphere, therefore Coulomb's law (C.1) doesn't have to be satisfied everywhere. This is crucial when we apply the Dirac quantization condition to solitonic monopoles for which Coulomb's law is only asymptotically satisfied.

C.2 Quantization Conditions

Comparing the Dirac quantization condition (C.7) with the topological quantization condition (2.11), one notices that although they are quite similar, there are two major differences:

1. They differ by a factor of two.

2. The topological quantization condition doesn't contain $\hbar$.

As we have seen in appendix C.1, the Dirac quantization condition is derived from the very basic principles of quantum mechanics and the assumption that the asymptotic magnetic field obeys Coulomb's law, both of which are applicable to topological monopoles. Therefore we expect a consistency between the two quantization conditions. This section is devoted to this consistency problem.

The factor of two comes from the fact that the SU(2) model we are considering allows fermions in fundamental representations that carry electric charge $\pm e/2$. It is the Dirac quantization to these electrically charged states that leads to the extra factor of 2. It might look strange that a theory is aware of particles that are *not* present in the theory, but this is exactly what the consistency of the theory requires. Adding fermions in fundamental representations of SU(2) will *not* affect the (purely bosonic) structure of magnetic monopoles, therefore the topological quantization condition must accomandate the possible existence of such particles. In general magnetic monopoles in any gauge theory with gauge group G are always determined by the universal covering group $\overline{G}$ [81].

The reason for the missing $\hbar$ comes from the fact that what we have been dealing with is a *purely classical* field theory. We have introduced a coupling constant e, which is not necessarily equal to the electric charge carried by fundamental excitations of the quantized field (namely W bosons). Actually,

at this classical level, *no* electrically charged particle exists in the theory! To introduce the W boson one must quantize the theory. By doing that, $\hbar$ will naturally enter the theory.

To see where $\hbar$ should appear, we don't have to pursue the details of field quantization. Simple dimensional analysis will be sufficient for our purpose. Remember that

$$\left[\int \mathcal{L} d^4x\right] = [\hbar], \tag{C.8}$$

where we use [quantity] to denote the dimension of that quantity, M and L denote the dimensions of mass and spatial coordinate, and the speed of light is chosen to be dimensionless. From the $F_{\mu\nu}^2$ term in the Lagrangian, we can derive

$$[e] = \left[\hbar^{-1/2}\right], \tag{C.9}$$

$$[A_\mu] = \frac{\left[\hbar^{1/2}\right]}{L}. \tag{C.10}$$

From Eq. (C.9) and the topological quantization condition (2.11) one obtains

$$[g] = \frac{1}{[e]} = \left[\hbar^{1/2}\right], \tag{C.11}$$

which is compatible with Coulomb's law:

$$[F] \equiv ML^{-1} = \left[\frac{g^2}{4\pi r^2}\right]. \tag{C.12}$$

This is expected since even at the classical level, the magnetic monopole appears as localized object and its magnetic field satisfies Coulomb's law

asymptotically. On the other hand, e has a different dimension than g so the electric Coulomb's law with e being the electric charge is *not* dimensionally correct. This is not as unreasonable as it might look because in this classical theory there is no guarantee that e must be the electric charge. Since the only new parameter that enters the theory after quantization is $\hbar$, therefore from Eqs. (C.9) and (C.11) it is clear that electric charge of the quantized theory must be defined as[1]

$$q = e\hbar. \tag{C.13}$$

With Eq. (C.13) at hand and with the factor 2 taken into account, we now have a full consistency between the Dirac quantization condition and topological quantization.

[1]An alternative way to see this is to notice that after quantization the generalized momentum operator $\mathbf{p} - q\mathbf{A}$ requires $[q] = \left[\hbar^{1/2}\right] = [e\hbar]$.

Bibliography

[1] A. Abouelsaood, Phys. Lett. **125B**, 467 (1983).

[2] A. Abouelsaood, Nucl. Phys. **B226**, 309 (1983).

[3] M. F. Atiyah and N. J. Hitchin, V. G. Drinfeld, and Yu. I. Mannin, **65A**, 185 (1978).

[4] M. F. Atiyah, N. J. Hitchin, *The Geometry and Dynamics of Magnetic Monopoles* (Princeton University Press, Princeton, 1988).

[5] A. Balachandran, G. Marmo, M. Mukunda, J. Nilsson, E. Sudarshan, and F. Zaccaria, Phys. Rev. Lett. **50**, 1553 (1983).

[6] A. A. Belavin, A. M. Polyakov, A. S. Shvarts, and Yu. S. Tyupkin, Phys. Lett. **59B**, 85 (1975).

[7] E. B. Bogomol'nyi, Sov. J. Nucl. Phys. **24**, 449 (1976).

[8] R. C. Brower, D. Chen, J. Negele, K. Orginos and C. I. Tan, Nucl. Phys. Proc. Suppl. **73**, 557 (1999).

[9] G. Chalmers, "Multi-Monopole Moduli spaces for SU(N) gauge groups", hep-th/9605182.

[10] N. H. Christ, E. J. Weinberg, and N. K. Stanton, Phys. Rev. D **18**, 2013 (1978).

[11] S. Coleman, S. Parke, A. Neveu, and C. M. Sommerfield, Phys. Rev. D **15**, 544 (1977).

[12] S. A. Connell, "The Dynamics of the SU(3) Charge (1,1) Magnetic Monopole" (unpublished preprint, 1991).

[13] E. Corrigan and P Goddard, Ann. Phys. (N.Y.) **154**, 253 (1984).

[14] A. S. Dancer, Nonlinearity **5**, 1355 (1992).

[15] A. S. Dancer, Commun. Math. Phys. **158**, 545 (1993).

[16] A. S. Dancer and R. A. Leese, Proc. R. Soc. London **A440**, 421 (1993).

[17] A. S. Dancer adn R. A. Leese, Phys. Lett. **390B**, 252 (1997).

[18] P. A. M. Dirac, Proc. Roy. Soc. **A133**, 60 (1931).

[19] S. K. Donaldson, Commun. Math. Phys. **96**, 387 (1984).

[20] H. Garland and M. Murray, Commun. Math. Phys. **120**, 335 (1988).

[21] J. P. Gauntlett, Nucl. Phys. **B411**, 433 (1994).

[22] J. P. Gauntlett and D. A. Lowe, Nucl. Phys. **B472**, 194 (1996).

[23] H. Georgi, *Lie Algebras in Particle Physics* (Benjamin/Cummings PUblishing Company. Inc, U.S.A, 1982).

[24] G. W. Gibbons, P. Rychenkova, and R. Goto, Commun. Math. Phys. **186**, 581 (1997).

[25] G. W. Gibbons and N. S. Manton, Phys. Lett. **356B**, 32 (1995).

[26] P. Goddard, J. Nuyts, and D. Olive, Nucl. Phys. **B125**, 1 (1977).

[27] D. Gross, R. Pisarski, and L. G. Yaffe, Rev. Mod. Phys. **53**, 42 (1981).

[28] V. Guillemin and S. Sternberg, *Symplectic Techniques in Physics* (Cambridge University Press, Cambridge, 1984).

[29] B. J. Harrington and H. K. Shepard, Phys. Rev. D **17**, 2122 (1978).

[30] J. A. Harvey, "Magnetic Monopoles, Duality, and Supersymmetry", hep-th/9603086.

[31] N. J. Hitchin, *Monopoles, Minimal Surfaces and Algebraic Curves* (Les Presses de L'Université de Montréal, Montréal, 1987).

[32] N. J. Hitchin, Commun. Math. Phys. **89**, 145 (1983).

[33] N. J. Hitchin, A. Karlhede, U. Lindström, and M. Roček, Commun. Math. Phys. **108**, 535 (1987).

[34] C. J. Houghton, Phys. Rev. D **56**, 1220 (1997).

[35] C. J. Houghton, P. W. Irwin and A. J. Mountain, JHEP 9904:029 (1999).

[36] J. C. Hurtubise and M. K. Murray, Commun. Math. Phys. **122**, 35 (1989).

[37] J. C. Hurtubise, Commun. Math. Phys. **120**, 613 (1989).

[38] P. Irwin, Phys. Rev. D **56**, 5200 (1997).

[39] R. Jackiw, C. Nohl, and C. Rebbi, Phys. Rev. D **15**, 1642 (1977).

[40] S. V. Ketov, Fortsch. Phys. **45**, 237 (1997).

[41] T. C. Kraan and P. van Baal, Phys. Lett. **428B**, 268 (1998).

[42] T. C. Kraan and P. van Baal, Nucl. Phys. **B533**, 627 (1998).

[43] T. C. Kraan and P. van Baal, Phys. Lett. **435B**, 389 (1998).

[44] T. C. Kraan and P. van Baal, Nucl. Phys. Proc. Suppl. **73**, 554 (1999).

[45] K. Lee, "BPS Monopoles and Electromagnetic Duality", hep-th/9702200.

[46] K. Lee, Phys. Lett. **426B**, 323 (1998).

[47] K. Lee and C. Lu, Phys. Rev. D **57**, 5260 (1998).

[48] K. Lee and C. Lu, Phys. Rev. D **58**, 025011 (1998).

[49] K. Lee, E. J. Weinberg, and P. Yi, Phys. Rev. D **54**, 1633 (1996).

[50] K. Lee, E. J. Weinberg, and P. Yi, Phys. Rev. D **54**, 6351 (1996).

[51] K. Lee, E. J. Weinberg, and P. Yi, Phys. Lett. **376B**, 97 (1996).

[52] K. Lee and P. Yi, Phys. Rev. D **56**, 3711 (1997).

[53] K. Lee and P. Yi, Nucl. Phys. **B520**, 1571 (1998).

[54] C. Lu, Phys. Rev. D **58**, 125010 (1998).

[55] N. S. Manton, Phys. Lett. **110B**, 54 (1982).

[56] M. K. Murray, J. Geom. Phys. **23**, 31 (1997).

[57] W. Nahm, Phys. Lett. **90B**, 413 (1980).

[58] W. Nahm, in *Monopoles in Quantum Field Theory*, edited by N. S., Cragie *et al.* (World Scientific, Singapore, 1982).

[59] W. Nahm, in *Structural Elements in Particle Physics and Statistical Mechanics*, edited by J. Honerkamp *et al.* (Plenum, New York, 1983).

[60] W. Nahm, in *Group Theoretical Methods in Physcs*, edited by G. Denardo *et al.* (Springer-Verlag. Berlin, 1984).

[61] W. Nahm, in *Theory and Detection of Magnetic Monopoles in Gauge Theories*, edited by N. Craigie. (World Scientific, Singapore, 1986).

[62] H. Nakajima, in *Einstein Metrics and Yang-Mills Connections*, edited by T. Mabuch *et al.* (Dekker, New York, 1993).

[63] J. W. Negele, Nucl. Phys. Proc. Suppl. **73**, 92 (1999).

[64] P. Nelson, Phys. Rev. Lett. **50**, 939 (1983).

[65] P. Nelson and A. Manohar, Phys. Rev. Lett. **50**, 943 (1983).

[66] P. Nelson and S. Coleman, Nucl. Phys. **B237**, 1 (1984).

[67] H. Osborn, Ann. Phys. (N.Y.) **135**, 373 (1981).

[68] A. M. Polyakov, JETP Lett. **20**, 194 (1974).

[69] M. K. Prasad and C. M. Sommerfield, Phys. Rev. Lett. **35**, 760 (1975).

[70] R. Rajaraman, *Solitons and Instantons* (North-Holland Publishing Company, Amsterdam, 1982).

[71] M. Roček, Physica D **15**, 75 (1985).

[72] P. Rossi, Nucl. Phys. **B149**, 170 (1979).

[73] T. Schäfer and E. V. Shuryak, Rev. Mod. Phys **70**, 323 (1998).

[74] G. 't Hooft, Nucl. Phys. **B79**, 276 (1974).

[75] G. 't Hooft, Nucl. Phys. **B190**, 455 (1981).

[76] R. S. Ward, Commun. Math. Phys. **79**, 317 (1981).

[77] E. J. Weinberg, Nucl. Phys. **B167**, 500 (1980).

[78] E. J. Weinberg, Phys. Lett. **119B**, 151 (1982).

[79] E. J. Weinberg, Nucl. Phys. **B203**, 445 (1982).

[80] E. J. Weinberg and P. Yi, Phys. Rev. D **58**, 046001 (1998).

[81] S. Weinberg, *The Quantum Theory of Fields*, vol II (Cambridge University Press, 1996)

[82] B. G. Wybourne, *Classical Groups for Physicists* (John Wiley & Sons. Inc, New York, 1974).